Establishing the safe use of the Bridging Infix method for anterior pelvic fixation

Submitted by:

Jerolize van Schalkwyk

A thesis submitted to the Department of Anatomy, School of Medicine, Faculty of Health Sciences, University of Pretoria, in the fulfilment of the requirements for the degree
of
MSc in Anatomy

Pretoria
2022

Supervisor: Dr Nkhensani Mogale
Co-supervisor: Prof. Natalie Keough
Collaborators: Dr Sven Strydom
Dr Christian Hugo Snyckers

DECLARATION OF ORIGINALITY

The Department of Anatomy places great emphasis upon integrity and ethical conduct in the preparation of all written work submitted for academic evaluation.

While academic staff teaches you about referencing techniques and how to avoid plagiarism, you too have a responsibility in this regard. If you are at any stage uncertain as to what is required, you should speak to your lecturer before any written work is submitted.

You are guilty of plagiarism if you copy something from another author's work (e.g. a book, an article or a website) without acknowledging the source and pass it off as your own. In effect you are stealing something that belongs to someone else. This is not only the case when you copy work word-for-word (verbatim), but also when you submit someone else's work in a slightly altered form (paraphrase) or use a line of argument without acknowledging it. You are not allowed to use work previously produced by another student. You are also not allowed to let anybody copy your work with the intention of passing if off as his/her work.

Students who commit plagiarism will not be given any credit for plagiarised work. The matter may also be referred to the Disciplinary Committee (Students) for a ruling. Plagiarism is regarded as a serious contravention of the University's rules and can lead to expulsion from the University.

The declaration which follows must accompany all written work submitted while you are a student of the Department of Anatomy. No written work will be accepted unless the declaration has been completed and attached.

Full names of student: Jerolize van Schalkwyk

Student number: u17060461

Topic of work: Establishing the safe use of the Bridging Infix method for anterior pelvic fixation

Declaration

1. I understand what plagiarism is and am aware of the University's policy in this regard.
2. I declare that this MSc Dissertation (e.g. essay, report, project, assignment, dissertation, thesis, etc.) is my own original work. Where other people's work has been used (either from a printed source, internet or any other source), this has been properly acknowledged and referenced in accordance with departmental requirements.
3. I have not used work previously produced by another student or any other person to hand in as my own.
4. I have not allowed, and will not allow, anyone to copy my work with the intention of passing it off as his or her own work.

SIGNATURE ....

TABLE OF CONTENTS

LIST OF FIGURES

LIST OF TABLES

LIST OF ABBREVIATIONS

APEF	Anterior Pelvic External Fixation
APIF	Anterior Pelvic Internal Fixation
ASIS	Anterior Superior Iliac Spine
AIIS	Anterior Inferior Iliac Spine
B	Black
BMI	Body Mass Index
CI	Confidence Interval
CT	Computed Tomography scan
df	Degrees of Freedom
F	Female
FA	Femoral Artery
FN	Femoral Nerve
FV	Femoral Vein
I	Inferior
ICC	Interclass Correlation Coefficients
IQR	Interquartile Range
IHN	Iliohypogastric Nerve
IIN	Ilioinguinal Nerve
IRTR	Implant single screw of the rod-to-rod connector
L	Left
L	Lateral
LFCN	Lateral Femoral Cutaneous Nerve
M	Male
M	Medial
Max	Maximum value
Min	Minimum value
MR	Mean Rank
MRI	Magnetic Resonance Imaging
n	Sample Size
ORIF	Open Reduction with Internal Fixation
PS	Pubic Symphysis
PT	Pubic Tubercle
R	Right
S	Superior
SC	Spermatic Cord

SCIV	Superficial Circumflex Iliac Vessels
SD	Standard Deviation
SEPV	Superficial External Pudendal Vein
SEV	Superficial Epigastric Vessels
SFJ	Saphenofemoral junction
W	White

ACKNOWLEDGEMENTS

Dr Nkhensani Mogale, thank you for once again agreeing to be my supervisor even after you saw how exhausting I was last year. I appreciate all your patience, guidance, and encouragement throughout the project. Thank you for helping me with my interobserver error measurements before your departure and for all your editing of my dissertation.

Prof. Natalie Keough, thank you for always responding to my emails rapidly and all your valuable advice. Your input in this project has been irreplaceable. Thank you for agreeing to be my co-supervisor. Furthermore, thank you for securing the funds required to incorporate the fresh tissue specimens into the study.

Dr Chris Snyckers, thank you for entrusting me with your new ideas and allowing me to conduct your research. I am grateful for the multiple clinical simulations that you performed on weekends in between your busy schedule. Thank you for always trying to help me succeed and being willing to teach.

Dr Sven Strydom, thank you for always having the time to assist me with all the different aspects of this project. Thank you for giving up your time, weekdays, and weekends, to come in and implant the next cadavers. Thank you for all that you have done to make this study successful.

Mr Andries Masenge, for his statistical knowledge, analysis, interpretation and help usually on very short notice. I am thankful for your assistance, without your data analysis, I would still be trying to decide on what which statistical tests are appropriate.

My parents and love. Thank you for pushing me and encouraging me to continue my studies. Without your support, this study would not have been completed in such a short period. Thank you for attempting to help proof-read my drafts and help editing. My love, thank you for listening to my endless rants and helping me see the positives.

The anatomy department and specifically the head of department, Prof. Prashilla Soma, for allowing me to conduct my research. Thank you for always being welcoming in the department.

The departmental technical staff, namely Mr Moses, Mr Eric, Ms Johanna, and Ms Mavis for always being friendly in my time spent in the basement. Thank you for always being willing to help me move the cadavers back and forth, even when I open the cadaver just to find out that I had to exclude it and needed another.

We acknowledge the NRF for providing funding that was used to secure the fresh specimens used in the study. Without the funding, the important clinical simulation part of the study would not have been possible.

The University of Pretoria is acknowledged for awarding me the UP-Postgraduate Masters Research Bursary for the 2021 academic year which has made completing my studies less stressful.

The donors and their families are acknowledged for their donation to research. Thank you for your generous donation that will hopefully affect many other lives in the future.

DePuy syntheses, for the donation of the implant sets as well as the loan of the instrumentation required to accurately conduct this study. Without you, the study would not have been possible.

Without the swift assistance from every team member, we would not have been able to conclude this study in record time. Furthermore, we would not have been able to use the preliminary results for an abstract and poster for the South African Orthopaedic Association congress in August 2021. With the help we were able to win the clinical excellence award for best poster. The team effort has made it possible to get the study's important results out in a short period for which I will be forever grateful. Thank you.

CHAPTER 1: INTRODUCTION

Pelvic ring injuries account for approximately 8% of injuries in trauma cases (Mason *et al*., 2005; Moazzam *et al*., 2012; Hung *et al*., 2018), and between 0.3%-6% of all fractures (Court-Brown & Caesar, 2006; Cole *et al*., 2012; Küper *et al.,* 2019), with women showing a higher prevalence (70:30) (Court-Brown *& Caesar*, 2006). Although pelvic ring injuries are not as frequent as other traumatic fractures, these injuries are known to have high morbidity and mortality rates, in which pelvic haemorrhage accounts for approximately 6% - 42% of deaths (Mason *et al*., 2005; Moazzam *et al*., 2012). With modern medical accomplishments leading to an increasing life expectancy and aging population, insufficiency fractures of the pelvic ring have become more frequent, with 73% of pelvic fractures occurring in this elderly cohort (Oberkircher *et al*., 2018; Banierink *et al*., 2019). This can be a result of the increased prevalence of osteoporosis which increases the fragility of bone (Maier *et al*., 2016). In the elderly, pelvic fragility fractures most often result in immobility and impair their quality of life, which in turn increases the patient's dependency (Maier *et al*., 2016; Oberkircher *et al*., 2018).

Conservative treatment has been shown to work well for isolated pubic rami fractures with a swift return to mobility and minimal pain to prevent side-effects such as pulmonary infections or osteopenia (Oberkircher *et al*., 2018; Küper *et al*., 2019). However, the conservative treatment approach for complex pelvic fractures and insufficiency fractures is associated with significant morbidity (Maier *et al*., 2016). Maier *et al*. (2016) also concluded that conservative treatment results in the loss of independence, both physical and social, as well as autonomy for the patient. Furthermore, the morbidity rate is high, with the time for the improvement of symptoms ranging between 4 - 14 weeks (Maier *et al*., 2016). Pelvic insufficiency fractures are commonly misdiagnosed and as a result are often poorly treated (Oberkircher *et al*., 2018). Surgical options are considered as an alternative if the patient's pain intensity doesn't improve or mobilization is not improved (Rommens *et al*., 2017).

Early treatment for complex or unstable fractures is essential. For posterior stability, sacral screws or trans-iliac fixation for complex fractures has proven to be effective (Oberkircher *et al*., 2018). Cole *et al*. (2017) and Küper *et al.* (2019) highlighted posterior ring injuries and the need to address them first, prior to anterior fixation. In cases of posterior stability, retrograde pubic rami screw fixation, external fixation, and open reduction with internal fixation (ORIF) as well as subcutaneous techniques are available (Oberkircher *et al*., 2018).

Retrograde pelvic rami screws are a percutaneous, minimally invasive technique that requires the precise placement of medullary screws (Starr *et al*., 2008). This technique has shown a high rate of reduction loss and is not suitable for all fracture types or in obese patients (Mosheiff & Leibergall, 2002; Starr *et al*., 2008). However, percutaneous techniques are favoured if adequate stabilization can be reached (Rommens *et al*., 2017).

Cole *et al*. (2012) described external fixation as a moderately quick and easy procedure to stabilize the pelvis. However, this procedure has an exceptionally high complication rate (Cole *et al*., 2012; Viadya *et al*., 2012; Cole *et al*., 2017; Rommens *et al*., 2017; Küper *et al*., 2019; Steer *et al*., 2019). The fixator is also cumbersome, making nursing of these patients difficult and reducing the patient's quality of life. Quality of life difficulties include difficulty wearing clothing, public stigma, difficulty sitting at a table, and intercourse encroachment (Cole *et al*., 2012). When external fixation is compared to ORIF, it provides less stability of the anterior pelvic ring but a lower peri-operative risk (Küper *et al*., 2019). ORIF techniques with screw or plate osteosynthesis is widely used for anterior stabilization (Küper *et al*., 2019). Generally, in osteoporotic bones, plate osteosynthesis provides more stability. However, the ORIF techniques require a more invasive surgical approach, which often relates to a higher rate of complications (Küper *et al*., 2019).

Minimally invasive internal fixation techniques have become more popular for fracture fixation (Scheyerer *et al*., 2014; Rommens *et al*., 2017; Steer *et al*., 2019). These techniques have reduced complication rates and provide equivalent fixation when compared to external fixation (Scheyerer *et al*., 2014; Cole *et al*., 2017). There is a reduced risk of surgical site infection, nursing care demands, and interference with daily activities as a result of the subcutaneous location of internal fixation (Steer *et al*., 2019). Numerous internal fixation techniques have been established and include the INFIX and pelvic bridge. The INFIX requires the placement of a pedicle screw along with a connecting rod, extending between the anterior inferior iliac spines bilaterally (Reichel *et al*., 2018). The most significant known complication for the INFIX is injury of the lateral femoral cutaneous nerve (LFCN), which has been permanent in some cases (Dahill *et al*., 2017; Vaidya *et al*., 2018). The pelvic bridge involves the placement of a plate-rod construct that spans between the ipsilateral iliac crest and either the ipsilateral or contralateral pubic symphysis (Hiesterman *et al*., 2012). A merit of the pelvic bridge is that it has been said that it can be applied to any type of physique (Cole *et al*., 2017). However, Cole *et al*. (2017) emphasised the need for the pelvic bridge procedure to be performed by experienced surgeons, or surgeons immensely familiar with pelvic anatomy.

A modified technique using an internal bridge plate and rod technique has been proposed by Dr Strydom and Dr Snyckers (2021). This technique combines the benefits of the pelvic bridge and ORIF with the extra-pelvic fixation methods, with the aim of reducing known complications

(Strydom & Snyckers, 2021). As the Bridging Infix follows the same course as the pelvic bridge, it is suspected that the incidence of LFCN injury would be similar to that of the pelvic bridge thereby reducing a significant risk of the INFIX technique.

In the course of internal fixation surgery, several important anatomical structures that course in the vicinity of the anterior bony pelvis are at risk of injury. These structures include -but are not limited to- the LFCN, which innervates the anterior and lateral skin of the thigh, the femoral artery which supplies the majority of blood to the lower limb, the femoral nerve which innervates many muscles in the thigh and many more structures (Moore *et al*., 2014; Drake *et al*., 2015). As a result of the proposed technique being novel, the risk to surrounding structures are unknown at present. Therefore, this study aims to establish the safety of using the Bridging Infix for anterior pelvic fixation by determining the relationship to neighbouring anatomical structures. Doing so aims to locate a safe-zone that reduces the associated complications with anterior pelvic fixation.

1.1 PROBLEM STATEMENT

Both the pelvic bridge and INFIX have their advantages but also great disadvantages. The new modified, minimally invasive Bridging Infix aims to have the benefits of both established methods whilst reducing the risks associated with either. As this is a new modified procedure, the exact anatomical at-risk structures are not yet known. Anatomical studies are limited to the North American, European, Asian and Australian samples (Vaidya *et al*., 2018). It is the belief of the authors that no anatomical studies have been conducted on a South African sample for any anterior pelvic fixation technique. Thus, this study was conducted to accurately determine whether the Bridging Infix can reduce anatomically related complications in comparison to the currently established methods utilized within a South African sample.

CHAPTER 2: LITERATURE REVIEW

2.1 REGIONAL ANATOMY

2.1.1 Anterior pelvis

The pelvis is considered the transition area between the trunk and lower limbs and is surrounded by the pelvic girdle, which connects the axial skeleton to the appendicular skeleton (Moore *et al*., 2014). The pelvic girdle is a strong, rigid structure due to its main function of weight bearing (Moore *et al*., 2014). The left and right pelvic bones articulate with the sacrum posteriorly to form the pelvic girdle, while the anterior articulation is between the left and right pubic bones forming the pubic symphysis (Moore *et al*., 2014).

In children, the pelvic bones consist of three separate bones; the ilium, ischium and pubis, joined by the triradiate cartilage that later fuses to form the adult pelvic bone (Moore *et al*., 2014; Drake *et al*., 2015). The ilium is generally fan-shaped and directed superiorly (Moore *et al*., 2014; Drake *et al*., 2015). The iliac crest follows the contour of the wing of the ilium and is located between the anterior and posterior iliac spines (Moore *et al*., 2014). The ischium forms the inferior and posterior part of the pelvic bone consisting of two parts; the body and ramus (Drake *et al*., 2015). The body of the ischium forms part of the acetabulum while the ramus forms part of the obturator foramen (Moore *et al*., 2014). The pubis forms the anterior and inferior part of the pelvic bone and has both a body as well as two rami (Drake *et al*., 2015). The pubis has a thickening anteriorly on the body which is known as the pubic crest which extends laterally to a palpable structure known as the pubic tubercle (Moore *et al*., 2014). The pubic symphysis is comprised of a fibrocartilaginous inter-pubic disc as well as several surrounding ligaments that are thickened at their superior and inferior margins.

Male and female pelvic anatomy differs in numerous ways as the pelvis is the most sexually dimorphic skeletal part (Patriquin *et al*., 2003; Cox, 2021). The pelvic bone has also been said to overall be the most extensively studied bone (Karakas *et al*., 2013). Some examples of these sexual differences include the general structure of the male pelvis being thicker and heavier in comparison to that of the female pelvis which is thinner and lighter (Moore *et al*., 2014). The lesser pelvis appears deeper and narrower in males whereas in females it is wider and shallower (Moore *et al*., 2014). These differences have been said to occur mainly due to males' general heavier build with larger muscles in comparison to females whose lesser pelvis is adapted for childbearing (Moore *et al*., 2014). The subpubic angle is one of the most common and easily identifiable features that differ between males and females, with the angle being generally wider in females compared to males (Moore *et al*., 2014). Karakasr *et al*., (2013) reported the mean subpubic angle to be $65.9 \pm 7.2^{\circ}$ in males and $82.6 \pm 7.7^{\circ}$ in females. The presence of dimorphism has been related to childbirth (Karakas *et al*., 2013). More features that have shown differences between sexes include the shape of the greater sciatic notch, ischiopubic ramus roughness, orientation of the ischial tuberosity and the overall pubic bone shape (Patriquin *et al*., 2003). Interestingly, the shape of the greater sciatic notch was found to be the most variable, whereas iliac crest was the only element with barely any dimorphism in shape (Cox, 2021).

2.1.2 Inguinal ligament and canal

The inguinal ligament extends between the anterior superior iliac spine (ASIS) laterally and the pubic tubercle medially (Moore *et al*., 2014; Drake *et al*., 2015). Anatomically, this is the region where structures pass into or out of the abdomen. This ligament forms the most inferior part of the external oblique aponeurosis (Moore *et al*., 2014; Drake *et al*., 2015). Most of the fibres of the inguinal ligament attach to the pubic tubercle, however, some attach to the superior ramus of the pubis as the lacunar ligament or arch superiorly and combine with the contralateral external oblique aponeurosis as the reflected inguinal ligament (Moore *et al*., 2014).

The inguinal ligament folds under itself thereby forming a channel which plays a vital role in the formation of the inguinal canal (Drake *et al*., 2015). The inguinal canal is formed in relation to the relocation of the gonads (Moore *et al*., 2014). Taghavi *et al*. (2016) emphasised that the development of the inguinal canal has not been well described in literature. The embryological development of the inguinal canal is said to occur in both sexes as if the body was preparing for the migrating gonad, even though the migration only occurs in males (Taghavi *et al*., 2016). Taghavi *et al*. (2016) described that at twenty-two weeks, a mesenchymal ridge forms and attaches to the inferior pole of the gonadal bud and blends distally with the inguinal canal.

In adults, the inguinal canal lies superior and parallel to the medial half of the inguinal ligament (Moore *et al*., 2014). The inguinal canal conveys the spermatic cord or round ligament of the uterus, ilioinguinal nerve, blood vessels, and lymphatics (Moore *et al*., 2014; Drake *et al*., 2015). The inguinal canal has an opening on each end known as the deep and superficial inguinal rings. The inguinal canal is bounded by an anterior wall, posterior wall, roof and floor. The anterior wall is formed by the external oblique aponeurosis and posterior wall by the transversalis fascia (Moore *et al*., 2014). The roof is formed laterally by the transversalis fascia, centrally by the internal oblique and transversalis abdominis arches as well as the medial crus medially (Moore *et al*., 2014; Drake *et al*., 2015). Furthermore, the floor is formed laterally by the iliopubic tract, centrally by the inguinal ligament and medially by the lacunar ligament (Moore *et al*., 2014).

2.1.3 Neighbouring structures

Various important anatomical structures lie within the anterior pelvic wall. However, not all the structures are relevant to the current study. Therefore, the study focused on the iliohypogastric nerve (IHN), ilioinguinal nerve (IIN), lateral femoral cutaneous nerve (LFCN), superficial epigastric vessels (SEV), superficial circumflex iliac vessels (SCIV), femoral neurovasculature and spermatic cord or round ligament of the uterus (Figure 2.1).

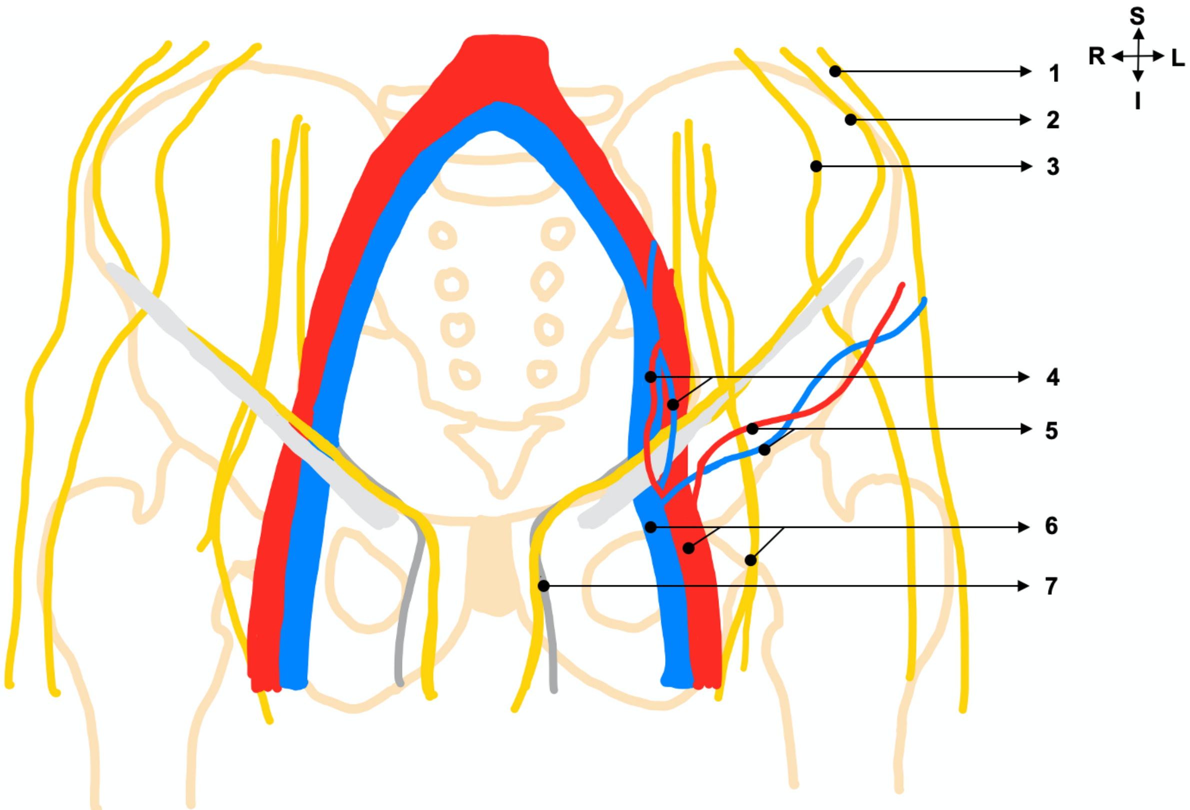

Figure 2.1: Anatomical illustration of the relevant structures
The image indicates most of the neighbouring structures as well as their rough anatomical locations for illustration purposes.
(1) IHN; (2) IIN; (3) LFCN; (4) SEV; (5) SCIV; (6) FV; (7) Spermatic cord.
Key: IHN – iliohypogastric nerve, IIN – ilioinguinal nerve, LFCN – lateral femoral cutaneous nerve, SEV – superficial epigastric vessels, SCIV – superficial circumflex iliac vessels, FV – femoral neurovasculature (femoral vein, femoral artery, femoral nerve).

2.1.3.1 Iliohypogastric nerve (IHN)

The Iliohypogastric nerve (IHN) originates from the lumbar plexus as the superior terminal branch of the anterior ramus of spinal nerve L1 (Anloague & Huijbregts, 2009; Moore *et al*., 2014; Tubbs *et al*., 2018) (Figure 2.1). The IHN is approximately 210 mm long with a diameter of approximately 4 mm (Tubbs *et al*., 2018). The L1 spinal nerve bifurcates into the IHN and ilioinguinal nerve (IIN) posterior to the psoas major muscle (Tubbs *et al*., 2018). The IHN enters the abdominal cavity, where it then descends laterally between the quadratus lumborum muscle and inferior pole of the kidney (Tubbs *et al*., 2018). It then pierces the transversus abdominis muscle where it continues anteriorly between the internal oblique muscles and transversus abdominis muscles (Drake *et al*., 2015; Tubbs *et al*., 2018). The IHN pierces the internal oblique muscle, approximately 15 mm – 80 mm medial to the anterior superior iliac spine (ASIS) on the left and 23 mm - 36 mm on the right (Avsar *et al*., 2002). The IHN courses parallel to the iliac crest and divides into anterior and lateral cutaneous branches (Moore *et al*., 2014).

The IHN has both a motor and sensory component which innervates various structures in the abdomen as well as the pelvic region (Tubbs *et al*., 2018). The motor component innervates the transversus abdominis muscles and internal oblique muscles whereas the sensory component supplies the skin over the gluteal region, hypogastric region, and upper lateral aspect of the thigh (Tubbs *et al*., 2018). Tubbs *et al*. (2018) published findings that indicated that injury to the IHN can result in motor dysfunction as well as sensory disturbances of the lower abdominal wall.

Several publications have indicated variations of the IHN (Anloague & Huijbregts, 2009; Klaassen *et al*., 2011). Al-dabbagh's (2002) findings were similar in that variations were found in 58.2% of the sample. These variations included accessory nerves, absence or a common trunk with the IIN (Al-dabbagh, 2002). Anloague & Huijbregts (2009) found that in 20.58% of lumbar plexuses, the IHN was completely absent with minimal sensory deficits and that the other lumbar nerves closely overlap. Klaassen *et al*. (2011) reported that the origin of the IHN varies and thus was classified into several groups. In 7% of their sample, the IHN originated from T12, 14% from T12 and L1, 10% from L1 and 6% from T11 and T12 (Klaassen *et al*., 2011). The subcostal nerve has also been reported to directly contribute to the IHN (Anloague & Huijbregts, 2009; Klaassen *et al*., 2011). Variations of the IHN is common, however identification of the variation is rare clinically; but prompt identification would considerably reduce the associated post-operative complications (Al-dabbagh, 2002).

2.1.3.2 Ilioinguinal nerve (IIN)

The ilioinguinal nerve (IIN) courses inferior to the IHN and originates from the lumbar plexus as the inferior terminal branch of the anterior ramus of spinal nerve L1 (Moore *et al*., 2014; Drake *et al*., 2015) (Figure 2.1). The diameter of the IIN ranges between 1.3 mm – 3.3 mm (Klaassen *et al*., 2011).

The IIN courses laterally past the lateral border of the psoas major muscle, and travels inferolaterally, anterior to the quadratus lumborum and transversus abdominis muscles, piercing the transversus abdominis muscle (Tubbs *et al*., 2018). Reinpold *et al*., (2015) reported that in 87% of cases, the IIN pierces the transversus abdominis muscle 30 mm cranially and in 13% of cases 6 mm caudally to the midpoint between the iliac spines on the iliac crest. Reinpold *et al*., (2015) commented that the IIN has a very inconsistent course superior and inferior to the iliac crests. The IIN travels between the transversus abdominis muscle and internal oblique muscle, where it will supply the inferior muscle fibres of the transversus abdominis muscle before it pierces the internal oblique muscle and innervates it (Avsar *et al*., 2002; Tubbs *et al*., 2018). Avsar *et al*. (2002) reported that the IIN pierces the internal oblique muscle approximately 48.5 mm inferomedially on the right and 33.7 mm inferomedially on the left from the ASIS. The IIN is concealed by the external oblique fascia until it reached the spermatic cord in males or the round ligament of the uterus in females (Klaassen *et al*., 2011). The IIN enters the inguinal canal by piercing the canal wall, later dividing into a femoral branch and either a scrotal or labial branch while coursing through the canal (Moore *et al*., 2014; Drake *et al*., 2015; Tubbs *et al*., 2018).

The IIN often receives contributions from either T12, L2 or L3 (Klaassen *et al*., 2011). Moreover, it was reported that the IIN origin had a prevalence of 65% for L1, 14% for T12 and L1, 11% for L1 and L2 and lastly 10% from L2 and L3 (Klaassen *et al*., 2011). Klaassen *et al*. (2011) reported that in 20% of cases, both the IHN and IIN originate from a common trunk before bifurcating shortly after leaving the intervertebral foramen. Furthermore, the IIN was found to communicate using accessory branches to other nerves, namely subcostal (17.5%), IHN (55%) and LFCN (27.5%) (Klaassen *et al*., 2011). Ndiaye *et al*. (2007) reported that in 7% of their cases, the IIN was absent.

2.1.3.3 Lateral femoral cutaneous nerve (LFCN)

The lateral femoral cutaneous nerve (LFCN) originates from the anterior rami of roots L2 - L3 of the lumbar plexus (Moore *et al*., 2014; Drake *et al*., 2015; Tubbs *et al*., 2018) (Figure 2.1). The LFCN exits from the lateral border of the psoas major muscle where it then passes obliquely inferior across the iliacus muscle (Anloague & Huijbregts, 2009; Drake *et al*., 2015; Tubbs *et al*., 2018). The LFCN courses 20 mm - 30 mm inferomedial towards the ASIS where it passes deep to the inguinal ligament (Doklamyai *et al*., 2008; Drake *et al*., 2015). The LFCN enters the thigh region by piercing through the fascia lata inferior to the inguinal ligament (Tubbs *et al*., 2018). The LFCN supplies the skin of the lateral and anterior thigh to the level of the knee (Drake *et al*., 2015).

Tubbs *et al*. (2018) described the LFCN as having a particularly variable course. Reinpold *et al*. (2015) published cases in which the LFCN had up to three sub-branches or bi-/trifurcations. The LFCN was determined to enter the abdomen 5 mm - 6 mm laterally (5%), 3 mm - 56 mm medially (95%), 10 mm cranially (10%) and 14 mm caudally (90%) to the ASIS using 58 cases (Reinpold *et al*., 2015). However, other publications have reported that the LFCN coursing superolateral to the ASIS in 2.9% – 4% of the samples (Aszmann *et al*., 1997; Mischkowshi *et al*., 2006). Ray *et al*., (2010) reported the mean distance from the ASIS to the point where the LFCN passes the inguinal ligament as 18.7 ± 4.8 mm and the mean distance from the ASIS to the point where it crosses the lateral border of the sartorius muscle as 61.5 ± 17.9 mm.

In their publication, de Ridder *et al*., (1999) reported that at least 25% of the population had a form of anatomical variation of the LFCN. Anatomical variation has also been found in the nerves that contribute to the formation of the LFCN. In normal situations, the LFCN originates from L2 - L3, however, instances have been reported where it arises from L1 - L2 or L3 - L4 (Apaydin, 2015). This variation is supported by Anloague & Huijbregts (2009) who reported that in four plexuses (11.8%), the LFCN originated from L1 - L2 and in one plexus (2.9%) it arose from only L2.

2.1.3.4 Superficial epigastric vessels (SEV)

The superficial epigastric artery and vein are grouped into the superficial epigastric vessels (SEV) as they course together. The superficial epigastric artery is a branch from the anterior aspect of the proximal femoral artery (Moore *et al*., 2014; Drake *et al*., 2015) (Figure 2.1). The artery arises just inferior to the inguinal ligament (de Rosnay *et al*., 2011). The superficial epigastric artery travels through the saphenous opening in the fascia lata and ascends in the superficial fascia of the external oblique muscle (de Rosnay *et al*., 2011). The artery runs towards the umbilicus in subcutaneous tissue and supplies the subcutaneous tissue and skin over the pubic and inferior umbilical region (Moore *et al*., 2014).

The superficial epigastric vein travels with the superficial epigastric artery (Moore *et al*., 2014; Drake *et al*., 2015). The vein drains into the great saphenous vein (Moore *et al*., 2014).

2.1.3.5 Superficial circumflex iliac vessels (SCIV)

The superficial circumflex iliac artery is a branch from the anterior aspect of the proximal femoral artery (Moore *et al*., 2014; Drake *et al*., 2015) (Figure 2.1). Ogami *et al*. (2017) reported that in 81.1% of their sample, the superficial circumflex iliac artery originated from the femoral artery. Of these cases, 96.7% of arteries originated between the origin of the femoral artery and its first bifurcation. The artery is usually identified approximately 19.81 ± 11.85 mm distal to the inguinal ligament (Ogami *et al*., 2017). The superficial circumflex iliac artery runs parallel to the inguinal ligament, in subcutaneous tissue (Moore *et al*., 2014; Ogami *et al*., 2017). The artery runs laterally to the ipsilateral ASIS and supplies the superficial abdominal wall and adjacent anterior thigh (Moore *et al*., 2014; Ogami *et al*., 2017).

The superficial circumflex iliac vein travels with the superficial circumflex iliac artery (Moore *et al*., 2014; Drake *et al*., 2015). Therefore, the artery and vein are grouped into the superficial circumflex iliac vessels (SCIV). The vein is a tributary of the great saphenous vein (Moore *et al*., 2014).

2.1.3.6 Femoral neurovasculature (FV, FA, FN)

The femoral artery (FA), the main source of blood supply to the lower limbs, is divided into a common and superficial part. The common FA is the segment of the artery proximal to the origin of the profunda femoris artery (Ogeng'o *et al*., 2015) (Figure 2.1). The superficial FA is the segment distal to the origin of the profunda femoris artery (Ogeng'o *et al*., 2015). The FA is a continuation of the external iliac artery as it passes posterior to the inguinal ligament and terminates as the popliteal artery at adductor hiatus (Moore *et al*., 2014; Drake *et al*., 2015). The FA is located halfway between the ASIS and pubic symphysis (Ellis, 2010). The FA lies anterior to the iliopsoas and pectineus muscles in the femoral triangle (Moore *et al*., 2014). The FA descends through the femoral triangle and travels medially in the adductor canal enroute to the popliteal fossa posteriorly (Moore *et al*., 2014). The FA is accompanied by the femoral vein along its course (Moore *et al*., 2014). The FA gives off several branches along its course, with the largest one being the profunda femoris artery (Moore *et al*., 2014). Two patterns of branching variations were identified by Ogeng'o *et al*. (2015). Firstly, a bifurcation of the common FA into the profunda femoris artery and superficial FA which had an incidence of 72.1%. Secondly, a trifurcation into the profunda femoris artery, superficial FA and lateral femoral circumflex artery with an incidence of 27.8%.

Proximal to the adductor hiatus, the femoral vein (FV) is a continuation of the popliteal vein (Moore *et al*., 2014). The FV enters the femoral sheath lateral to the femoral canal. The FV continues as the external iliac vein after it passes posterior to the inguinal ligament (Moore *et al*., 2014). The FV is located one fingers breadth medial to the FA along the line between the ASIS and pubic symphysis (Ellis, 2010).

The femoral nerve (FN) is one of the largest nerves originating from the anterior rami of nerves L2 – L4 from the lumbar plexus (Moore *et al*., 2014; Drake *et al*., 2015) (Figure 2.1). The FN originates posterior to the psoas major muscle and emerges at the lower lateral border of the psoas major muscle (Anloague & Huijbregts, 2009; Moore *et al*., 2014; Drake *et al*., 2015; Tubbs *et al*., 2018) or around 40 mm superior to the inguinal ligament (Gustafson *et al*., 2009). The FN lies between the anterior surface of the iliacus muscle and the lateral border of the psoas major muscle as it descends inferiorly (Anloague & Huijbregts, 2009; Drake *et al*., 2015). The FN, which courses outside the femoral sheath, firstly runs deep to the iliacus fascia and then lateral to the femoral artery (Anloague & Huijbregts, 2009). This nerve courses posterior to the inguinal ligament and is found emerging along the lateral third of the anterior thigh (Gustafson *et al*., 2009; Moore *et al*., 2014; Drake *et al*., 2015; Tubbs *et al*., 2018). The FN is found at ± half the distance between the ASIS and pubic symphysis (Tubbs *et al*., 2018), but Ellis (2010) defined it as one finger breadth lateral to the FA along the line between the ASIS and pubic symphysis. The FN, which has both motor and sensory components, enters the femoral triangle and immediately divides into several branches that supply the anterior thigh muscles and part of the knee joint (Moore *et al*., 2014). The cutaneous branches include the saphenous nerve, medial femoral cutaneous nerve, and intermediate femoral cutaneous nerve (Drake *et al*., 2015). The muscular branches supply the iliacus, pectineus, rectus femoris, vastus medialis, vastus intermedius, vastus lateralis, and sartorius muscles (Drake *et al*., 2015).

2.1.3.7 Spermatic cord and round ligament of the uterus

The spermatic cord carries structures to and from the testis such as ductus deferens, the testicular artery, artery of ductus deferens, cremasteric artery, pampiniform venous plexus, genital branch of genitofemoral nerve, lymphatic vessels, and sympathetic nerve fibres (Moore *et al*., 2014; Collinge & Beltran, 2015; Drake *et al*., 2015) (Figure 2.1). The spermatic cord is known to have several fascial coverings. These include the internal, cremasteric and external spermatic fascia. The internal spermatic fascia is derived from the transversalis fascia at the deep inguinal ring. The cremasteric fascia is derived from the superficial and deep surfaces of the internal oblique fascia. Finally, the external spermatic fascia is derived from the external oblique aponeurosis (Moore *et al*., 2014). The spermatic cord begins proximally to the deep inguinal ring, passes through the inguinal canal and exits the superficial inguinal ring where it runs inferiorly to end at the posterior border of the testis (Moore *et al*., 2014; Drake *et al*., 2015). The spermatic cord is located directly lateral to the pubic tubercle after it exits deep to the inguinal ligament (Collinge & Beltran, 2015) with an average distance reported as 5.196 ± 0.251 mm by Yu *et al*., (2015).

The round ligament of the uterus courses from the uterus to the deep inguinal ring and enters the inguinal canal (Drake *et al*., 2015). This ligament courses through the inguinal canal and finally exits through the superficial inguinal ring and attaches to the connective tissue associated with the labia majora (Drake *et al*., 2015). The round ligament of the uterus is a remnant of the ovarian gubernaculum, which assisted with the relocation of the gonad from where it developed within the abdomen (Moore *et al*., 2014). The round ligament of the uterus receives similar contributions from the abdominal wall, as with the spermatic cord, as it courses through the inguinal canal (Moore *et al*., 2014). The round ligament of the uterus has been reported to course 4.408 ± 0.304 mm from the pubic tubercle (Yu *et al*., 2015).

2.2 PELVIC TRAUMA

Pelvic trauma is considered the "most complex management in trauma care" according to the World Society of Emergency Surgery guidelines (Coccolini *et al*., 2017). High energy trauma, for example, a fall from a height, car or sport related accidents, are all considered dominant mechanisms of pelvic ring injuries (Coccolini *et al*., 2017). Arieux *et al*. (2012) reported in one-hundred and fifty-nine (n = 159) cases, that the following were the cause prevalence: car accidents accounted for 49%, falls 33%, mountain sports 24%, suicide attempts 6%, and aggressions for 3%. The prevalence of vehicle accidents causing pelvic trauma is supported by Costantini *et al*. (2015) who reported a prevalence of 42.7% and Ashkal *et al*. (2021) with a prevalence of 50.33% in South Africa.

High energy trauma is commonly related to unstable pelvic fractures with both high morbidity and mortality, which accounts for roughly 1.5% – 3.9% of all fractures according to Yin *et al*. (2019) or 3% of all skeletal injuries as stated by Niola *et al*., (2012) and Coccolini *et al*., (2017). The mortality rates of pelvic trauma have decreased over the past decade from 25% to 10% due to the medical advancements (Dyer & Vrahas, 2012). In severe pelvic fractures, 80% of cases have a minimum of two other traumatic injuries (Arvieux *et al*., 2012). Complex pelvic injuries are one of the most life-threatening trauma related injuries (Coccolini *et al*., 2017).

Whether the patient is considered stable, unstable or extremely unstable, also known as the hemodynamic status, depicts the appropriate management strategy as the pelvis has rich vascularisation (Arvieux *et al*., 2012). Patients who present as haemodynamically unstable, ± 15% – 30% of pelvic trauma cases, is usually as a result of blood loss (Ashkal *et al*., 2021). In 80% of cases, bleeding occurs from veins and the remaining from arteries or cancellous bone (Arvieux *et al*., 2012; Costantini *et al*., 2015; Coccolini *et al*., 2017). Although pelvic trauma with pelvic ring fractures may result in arterial bleeding, it only accounts for 10% – 20% of all haemorrhages; it is most commonly related to hemodynamic instability (Niola *et al*., 2012; Martin *et al*., 2017). Pre-peritoneal packing or interventional radiology may be required to reduce blood loss (Ashkal *et al*., 2021). Therefore, it can be reasoned that the patient survival thus is dependent on quick diagnosis and intervention (Niola *et al*., 2012).

Treatment of pelvic fractures should be based upon the patient's hemodynamic status as well as anatomic pelvic ring function and any other related injuries (Arvieux *et al*., 2012; Coccolini *et al*., 2017). The aim of all treatments would be to restore stability of the pelvic ring and homeostasis (Coccolini *et al*., 2017; Ashkal *et al*., 2021). Thus, treatments of pelvic injuries are considered multidisciplinary and based on both the anatomy and physiology associated with the injury (Coccolini *et al*., 2017). A multidisciplinary approach is usually required in the first time period directly after the trauma for the management of the patients bleeding, resuscitation and bone injuries (Coccolini *et al*., 2017). The timeline for definitive fixation depends on the patient's overall condition (Coccolini *et al*., 2017).

2.3 CLINICAL IMPORTANCE

Various methods of anterior fixation have been established and include retrograde pubic rami screws, external fixation, or open reduction internal fixation (ORIF) (Hiesterman *et al*., 2012). Retrograde pubic rami screws are a minimally invasive, percutaneous technique that requires precise placement of medullary screws (Starr *et al*., 2008). The screw can be placed percutaneously after the closed manipulation and reduction of a pelvic fracture. This technique has been described to have minimal blood loss and low infection rates (Mosheiff & Leibergall, 2002). A high rate of reduction loss or fracture displacement has been reported for this approach (Mosheiff & Leibergall, 2002; Starr *et al*., 2008). Furthermore, retrograde pubic rami screws are limited in their use as they are not suitable for all fracture types or for use in obese patients (Mosheiff & Leibergall, 2002; Starr *et al*., 2008). In addition, retrograde pubic rami screws are not suitable for patients with anatomical variations. An improved technique described by Mosheiff & Leibergall (2002) accommodates insertion in difficult anatomical variations, such as curved or narrow rami, with the use of a thick medullary screw and a manoeuvring method. The technique entails the usage of a halfway inserted temporary screw and a connected cannulated screw driver to serve as a manoeuvring device. The device gives control of the proximal fragment which helps to reduce the fracture.

2.3.1 External fixation methods

External fixation methods have been well described in the literature (Hiesterman *et al*., 2012). External fixation of the anterior pelvic ring has been described in a manner to complement posterior fixation, which renders increased stability to the pelvic ring as a whole (Hiesterman *et al*., 2012). External fixation surgeries have been described as a moderately easy and a quick procedure to stabilize the pelvis (Cole *et al*., 2012). Pelvic external fixation promotes the early mobilisation of the patient post-surgery through the enhanced stability of the pelvic ring (Cole *et al*. 2012). External fixation has proven to reduce the rate of morbidity and mortality of patients who have sustained unstable pelvic ring injuries (Cole *et al*., 2012; Cole *et al*., 2017). Although external fixation permits for easy removal, it has shown a high complication rate of up to 62% and is cumbersome for the patient (Cole *et al*., 2012; Vaidya *et al*., 2012b; Cole *et al*., 2017; Steer *et al*., 2019). Anterior pelvic external fixation (APEF) techniques have known complications that include wound infection, neurologic compromise, impingement of the fixator on the skin, and fixator loosening (Cole *et al*., 2012; Cole *et al*., 2017). Furthermore, surgeons might choose not to use APEF due to nursing care requirements or abdominal access challenges (Cole *et al*., 2012; Cole *et al*., 2017).

2.3.2 Internal fixation methods

The ORIF technique has two notable benefits that include, no need to remove the implant and anatomical reduction (Steer *et al*., 2019; Strydom & Snyckers, 2021). Despite the benefits of ORIF, the use of more extensive surgical approaches such as the Pfannenstiel and modified Stoppa approaches are not without risk. These open procedures are associated with longer surgical times and increased blood loss, which not only places greater physiological stress on the patient's cardiovascular system, but is also associated with prolonged recovery time (Grewal & Starr, 2020). It is also important to note that there is a paucity in literature when looking specifically at the complication rates of such extensile procedures in the elderly and frail population groups.

2.3.2.1 Minimally invasive techniques

Minimally invasive internal fixation techniques have become more popular for fracture fixation (Steer *et al*., 2019). Furthermore, these techniques are preferable if they allow for both reduction and stability (Hiesterman *et al*., 2012). Minimally invasive internal fixation has a reduced rate of complications and provides equivalent fixation when compared to APEF (Cole *et al*., 2017). Internal fixation has the benefits of external fixation that includes minimal blood loss, minimal dissection of soft tissue during surgery, reduced surgery times, and reduced risk of infection and recovery time in comparison to ORIF (Hiesterman *et al*., 2012; Vaidya *et al*., 2012b; Steer *et al*., 2019). Furthermore, there is a reduced risk of surgical site infection, nursing care demands, and interference with daily activities as a result of the subcutaneous location of internal fixation (Steer *et al*., 2019). Examples of these minimally invasive internal fixation techniques include the INFIX and pelvic bridge. Cole *et al*. (2017) suggested that the pelvic bridge can be used as a substitute for APEF.

Indications for both external fixation and internal fixation are the same, thus it is up to the surgeon's discretion which method is to be utilised (Cole *et al*., 2012). Cole *et al*. (2012) published a study in which a comparison was made between APEF and anterior pelvic internal fixation (APIF). It was found that amongst 24 patients in each group, the APIF patients, with moderate to severe unstable pelvis fractures, had a significantly lower rate of wound complications, surgical site pain persistence, and associated morbidity events (Cole *et al*., 2012). Nevertheless, Cole *et al*. (2012) also reported that there was no significant difference for the maintenance of the pelvic reduction between the aforementioned two groups. Patients who underwent APIF did not have the downsides of APEF in their quality of life, which includes difficulty with wearing clothing, sitting at a table, public stigmatism, and intercourse hindrance (Cole *et al*., 2012). Cole *et al*. (2012) and Hiesterman *et al*. (2012) stated that the main contraindication for APIF is a pure symphyseal disruption, in which case ORIF is recommended.

2.3.2.1.1 INFIX

The INFIX was one of the first minimally invasive internal fixation techniques described (Vaidya *et al*., 2012a; Yin *et al*., 2019). The INFIX requires the placement of a pedicle screw along with a connecting rod from the anterior inferior iliac spines bilaterally (Reichel *et al*., 2018).

Non-union is an uncommon occurrence for pelvic fracture healing using the INFIX and Vaidya *et al*. (2018) reported that it only occurred in 2 / 456 patients in a systematic review. However, potential drawbacks of this technique include the need for deep dissection and there is a potential risk of impingement or iatrogenic compression injuries to the surrounding neurovascular structures (Vaidya *et al*., 2012b; Reichel *et al*., 2018). Furthermore, the INFIX position is variable as it depends upon the placement of the pedicle screw in the ASIS as well as the actual curvature of the rod (Reichel *et al*., 2018). Dahill *et al*. (2017) reported that in forty-seven patients treated with the INFIX construct, 55% presented with LFCN injury of which in 34% the damage was permanent. Moreover, Vaidya *et al*. (2018) completed a systematic review, with a patient sample size of 496, in which the complication findings included LFCN irritation in 26.3%, heterotopic ossification in 36%, infections in 3%, and femoral nerve palsy in 1%. Implant removal is performed between ten weeks and nine months post-operatively without complication in an operating theatre, unlike with the external fixator that can be done in a clinic setting (Vaidya *et al*., 2018).

In addition, Reichel *et al*. (2018) using a cadaveric study, found that the INFIX application position and curvature was variable, which results in a larger risk of impingement. The screw placement depth is subjective, however if the screw is placed incorrectly the patient could experience discomfort or impingement (Reichel *et al*., 2018). In addition, it was found that the LFCN was at-risk in ten out of eleven cadavers, as it had close proximity to the INFIX construct (Reichel *et al*., 2018). In contrast, Hesse *et al*. (2015) reported eight cases from six patients who developed femoral nerve palsy, either uni- or bilaterally, with lasting effects after surgical removal. As the connecting rod is not as static as the surrounding anatomic structures, which include the pubic symphysis, inguinal ligament and iliac crests, there is a risk of injury to the femoral neurovasculature and nerve (Reichel *et al*., 2018).

2.3.2.1.2 Pelvic bridge

Hiesterman *et al*. (2012) and Cole *et al*. (2012; 2017) described another minimally invasive subcutaneous technique called the pelvic bridge, for anterior pelvic ring fixation. This method does require adequate posterior ring stability (Hiesterman *et al*., 2012). The pelvic bridge is a percutaneous method with minimal incisions (Hiesterman *et al*., 2012). Incisions are made extending roughly 50 mm over the iliac crests as well as a 60 mm – 80 mm incision over the pubic symphysis (Hiesterman *et al*., 2012; Cole *et al*., 2017). During dissection, down to the musculature, care must be taken to stay anterior to the inguinal ligament (Cole *et al*., 2017). The pelvic bridge involves the placement of a plate-rod construct, either a spinal rod or locking reconstruction plate, which spans between the ipsilateral iliac crest and either the ipsilateral or contralateral pubic symphysis (Hiesterman *et al*., 2012). The pelvic bridge is an off-label use of an occipito-cervical plate-rod construct (Cole *et al*., 2017). The pelvic bridge is placed subcutaneously above the external oblique fascia (Hiesterman *et al*., 2012). Stability is achieved through the fixation of the construct into the iliac crests and pubis (Hiesterman *et al*., 2012). The pelvic bridge allows for percutaneous placement from the hemi-pelvis either utilising the uninjured side or using two separate constructs that overlap with rod-to-rod connections at the pubic symphysis, which is a benefit of the pelvic bridge (Hiesterman *et al*., 2012). The plate-rod construct is placed superficial to the inguinal ligament, thereby protecting the neurovasculature deep to the ligament (Cole *et al*., 2017).

Cole *et al*. (2017) reported that with the use of visualisation, the spermatic cord or round ligament of the uterus can be avoided. However, if visualisation is lacking during implant placement, some anatomic structures at risk include, the LFCN, genitiofemoral nerve, IIN, IHN, FA, FV, and FN (Hiesterman *et al*., 2012). The IHN and IIN have been shown to be protected by musculature with the pelvic bridge plates, remaining a mean distance of 15 mm and 21 mm away from the plate, respectively (Moazzam *et al*., 2012; Cole *et al*., 2017). The LFCN was found to be safe posterior to the inguinal ligament with a mean distance of 15 mm away from the pelvic bridge fixator (Moazzam *et al*., 2012; Cole *et al*., 2017). The femoral neurovascular bundle was found to be a mean distance of 22 mm away from the fixator and therefore safe from risk of compression (Moazzam *et al*., 2012; Cole *et al*., 2017). Both Moazzam *et al*. (2012) and Reichel *et al*. (2018) conducted anatomical studies on cadaver specimens in which they concluded that the IHN, IIN, LFCN, FN, FV, spermatic cord and round ligament of the uterus were safe in relation to the pelvic bridge.

An advantage of the pelvic bridge is that it can be applied to any type of physique (Cole *et al*., 2017). However, Cole *et al*. (2017) emphasised that the pelvic bridge procedure should not be performed by inexperienced surgeons, nor surgeons that are not immensely familiar with pelvic anatomy. Cole *et al*. (2012; 2017) and Hiesterman *et al*. (2012) reported that the current practice is the removal of the implants as there is a lack of long-term outcomes for the construct.

Indications for using the pelvic bridge approach include unstable pelvic rings, obesity, avoidance of APEF, improve stability for early mobilisation or improve stability after posterior fixation (Cole *et al*., 2017). Contraindications for the usage of the pelvic bridge include degloving wounds over the iliac wing, simple pubic diastasis, iliac wing dissociations, or open pelvic injuries with peritoneal contamination (Cole *et al*., 2017).

Hiesterman *et al*. (2012) reported that after a six-month follow-up on eleven patients, no complications or pain was reported for the APIF group.

2.3.2.1.3 Bridging Infix

The pelvic Bridging Infix is a new modified technique that is a combination of both the pelvic bridge and the INFIX. Surgical incisions similar to that of the pelvic bridge procedure are made along the iliac crests and pubic symphysis with dissection down to the musculature. A subcutaneous tunnel is made similar to the pelvic bridge technique through which a contoured plate-rod construct is passed. Three cortical screws allow for definitive fixation. The pelvic Bridging Infix construct is shown in an anterior-posterior radiograph of the pelvis in Figure 2.2.

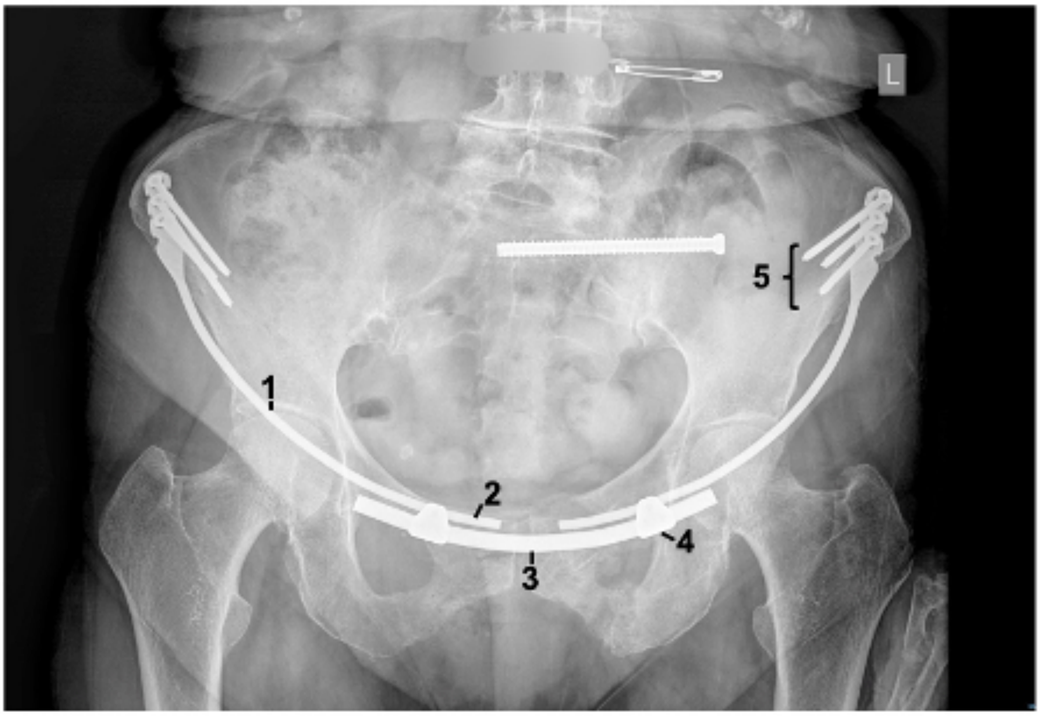

Figure 2.2: Pelvic Bridging Infix (Strydom & Snyckers, 2021)
An anterior-posterior pelvis radiograph showing a patient with the pelvic Bridging Infix implant post-surgery.
1: Plate rod construct; 2: Rod end; 3: 5 mm connector rod; 4: Rod-to-rod connector; 5: Cortical screws 50 mm, 45 mm, 40 mm.

This novel approach aims to have the benefits of both established methods whilst reducing the risks associated with either (Strydom & Snyckers, 2021). The pelvic Bridging Infix combines the extra-pelvic fixation methods with the low-profile benefits of the pelvic bridge and ORIF (Strydom & Snyckers, 2021). The benefits of ORIF include no need for removal of the implant as well as anatomic reduction. However, it has been referred to as the most rigid fixation construct and has a high surgical morbidity rate (Vaidya *et al.*, 2018). The pelvic Bridging Infix aims to reduce the risks of the INFIX, which is in close proximity to the LFCN and can lead to injury by following the same course as the pelvic bridge. Furthermore, patient discomfort and neuropraxia are also aimed to be reduced in comparison (Strydom & Snyckers, 2021). The lack of medial fixation nullifies the risk of bladder injury when placing screws and allows the construct to be used in cases with medial pubic rami comminution; which would not allow for adequate screw purchase.

In a case study, the authors reported that the patient was able to mobilise quickly postoperatively. The patient was able to walk unaided and was pain free at the six-week follow-up (Strydom & Snyckers, 2021). At the one-year follow-up, the patient reported no discomfort and examinations showed a good bony union thus the decision was made to not remove the implant (Strydom & Snyckers, 2021).

As this is a new, adapted method, no previous studies have been completed to identify which anatomic structures might be at risk during the placement of the Bridging Infix. Thus, the purpose of our study was to determine if any structures are at risk which could preclude this new modified method as the preferred new method for anterior pelvic fixation surgeries to reduce intra- and post-operative complications. The use of fresh cadavers allowed the study to determine if measurements differ between a standing and seated position when flexing the hip. This is still an area of uncertainty with these pelvic fixation techniques and as to the researcher's knowledge no other studies have done this dynamic assessment.

CHAPTER 3: MATERIALS AND METHODS

3.1 SAMPLE

The sample used in this study comprised of fifty (n = 50) adult (age > 18 years) formalin fixed cadavers and two (n = 2) fresh frozen cadavers. The age of the cadaver sample ranged from 30 to 102 years (mean = 71.00; SD ± 15.36). Nineteen (n = 19) female and thirty-three (n = 33) male cadavers were included in the study, of which forty-eight (n = 48) were white and four (n = 4) were black. The cadavers used in the study were obtained from the Department of Anatomy, University of Pretoria. The fresh frozen cadaver specimens were obtained from the National Tissue Bank (Ethical clearance: 182/2021- Annexure 1). Prior to any procedures being performed on the fresh frozen specimens, the specimens were thawed at room temperature for two days and dissected accordingly. The proximity of surrounding anatomical structures to the Bridging Infix was investigated through superficial and deep dissections of the anterior abdomino-pelvic wall. The Bridging Infix implant methods used followed the technique guidelines as to be published by Strydom & Snyckers, (2022) with some modifications to suit the current study. The bending angles of the implant were also investigated.

3.2 INCLUSION CRITERIA

Only undissected cadavers were included in the study. The sample included specimens of various body mass index (BMI) (range = 10.43 kg/m^2 – 31.77 kg/m^2). The BMI was calculated as per the definition, wherein the weight (in kilograms) of each cadaver was divided by their height (in metres) squared. The sample consisted of cadavers of different population groups, and this was not seen as an exclusion criteria. The weight measurements of a few cadavers were unavailable, but the cadavers were included in the study as certain parameters could still be attained. The inclusion was also due to the limited cadaver availability; the missing variables were therefore not included in the final analysis.

3.3 EXCLUSION CRITERIA

Cadavers with evidence of previous pelvic or abdominal surgeries were excluded from the study. Furthermore, specimens with visible damage or pathology in the pelvic or abdominal region were also excluded. Cadavers with an age below 18 years were not included in the study.

3.4 METHODS

The methods described were standardized for the cadaveric and fresh frozen samples. The instruments used included the 4 mm plate-rod construct with a straight rod and two rod-to-rod clamps that are currently described for use in occipito-cervical fusion from the company DePuy Synthes (Figure 3.1).

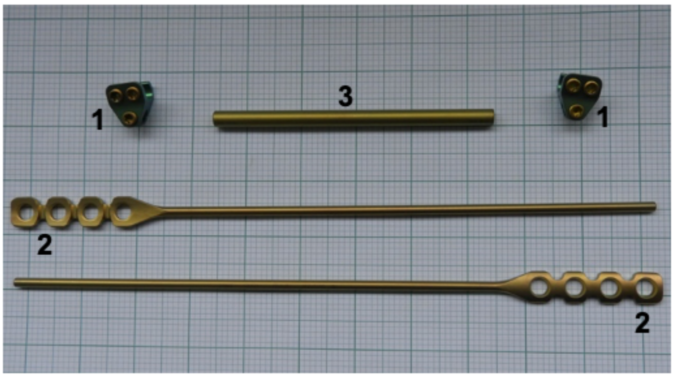

Figure 3.1: Bridging Infix instruments
(1) rod-to-rod clamps; (2) 4 mm plate-rods; (3) straight rod.

Prior to implanting the Bridging Infix, each plate-rod was externally contoured, by an orthopaedic surgeon, according to the curvature of each cadaver's pelvis using a dry articulated pelvis as template. The Bridging Infix was gently bent to passively lie on the iliac crest as can be seen in Figure 3.2 (number 1) which clearly shows the first contour. The second contour is known as a lazy-S bend at the plate-rod junction (Figure 3.2; number 2). The final contour bent the rod medially to align with the inguinal ligament, with the distal portion aligning ± 10 mm parallel superior to the pubic symphysis (Figure 3.2; number 3). Visualisation with the naked eye was used to determine if the construct was adequately contoured as no imaging was available. The rod ends were cut to allow a ± 15 mm gap between the two rod ends.

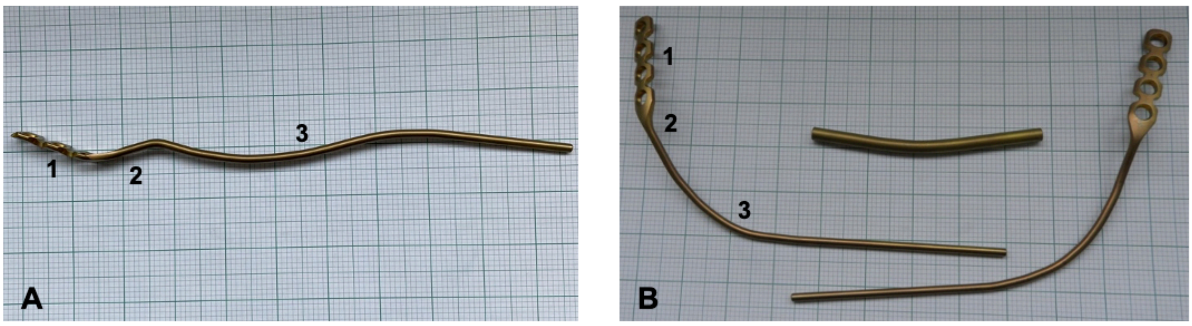

Figure 3.2: Bridging Infix contours
A: Contoured plate-rod to indicate three contours; B: Contoured Bridging Infix, as seen during placement.
(1) iliac crest contour; (2) lazy-S contour; (3) inguinal ligament contour.

3.3.1 Superficial and intermediate dissection procedure

Both the formalin-fixed and fresh-frozen cadaver samples followed identical dissection procedures:

With the cadaver in a supine position, easily palpable bony landmarks were identified; these included the iliac crest, anterior superior iliac spine (ASIS), and pubic tubercle (PT). Furthermore, the suspected course of the LFCN was marked (Figure 3.3).

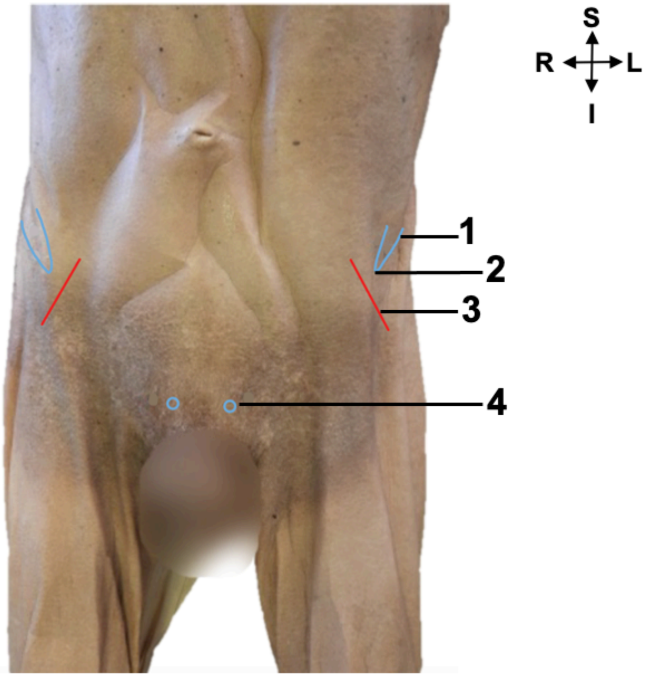

Figure 3.3: Cadaver in a supine position with the palpable landmarks marked
(1) iliac crest; (2) ASIS; (3) LFCN suspected course; (4) PT.
Key: I- Inferior, L- Left, R- Right, S- Superior, ASIS- Anterior Superior Iliac Spine, LFCN- Lateral Femoral Cutaneous Nerve, PT- Pubic Tubercle.

An incision originating inferior to the umbilicus, extending to the inferior aspect of the pubic symphysis was made, line AC (Figure 3.4). A second transverse incision extending bilaterally from the inferior aspect of the umbilicus to the mid-axillary line was made, line AB. A final transverse skin incision extending bilaterally from the inferior aspect of the pubic symphysis to the mid-axillary line was made, line CD.

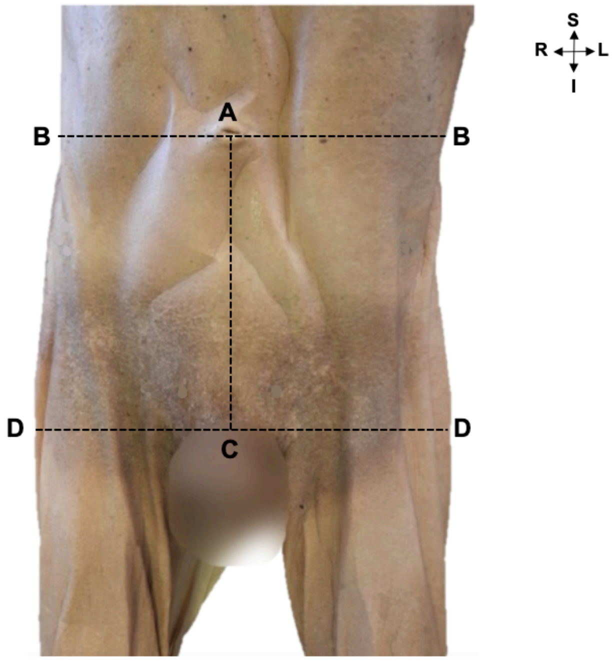

Figure 3.4: Cadaver in a supine position with the dissection incisions annotated
A-C: Inferior umbilicus to inferior aspect of pubic symphysis; A-B: Umbilicus bilaterally to mid-axillary line; C-D: Pubic symphysis bilaterally to mid-axillary line.
Key: I- Inferior, L- Left, R- Right, S- Superior.

The skin was carefully reflected laterally to the midaxillary line, preserving all superficial arteries, veins, and nerves (Figure 3.5). Both Camper's and Scarpa's fascia were also preserved. The two easily palpable bony landmarks, the ASIS and PT, were pinned for easy identification.

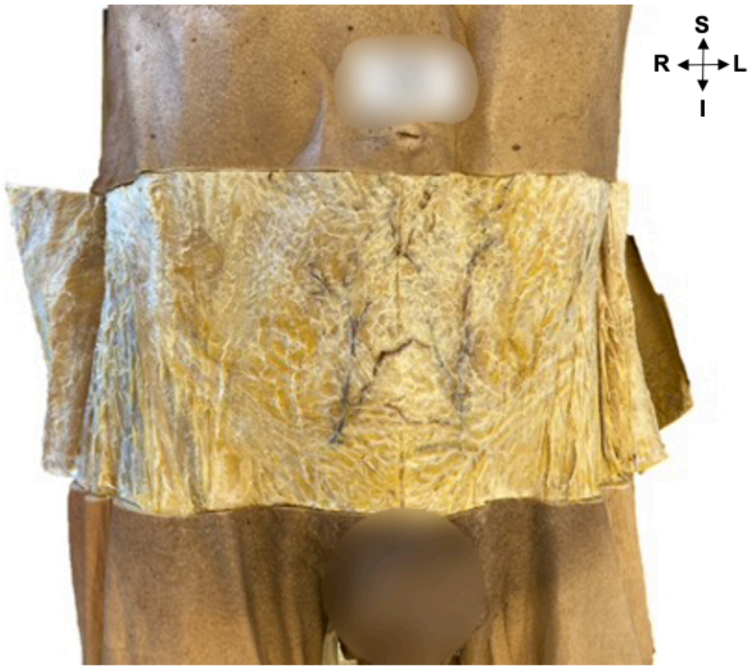

Figure 3.5: Cadaver in a supine position with the skin reflected laterally
Key: I- Inferior, L- Left, R- Right, S- Superior.

The superficial epigastric vessels (SEV) were identified by slowly dissecting through the camper's fascia located lateral to the linea alba (Figure 3.6; number 3). The course of the SEV was pinned to avoid movement during further dissection. The tissues surrounding the ASIS were dissected to locate the superficial circumflex iliac vessels (SCIV) (Figure 3.6; number 4). The course of the SCIV was fully dissected and pinned in place. Approximately 10 mm medial to the ASIS, a vertical incision was made into the fascia lata to expose the lateral femoral cutaneous nerve (LFCN) as it emerged from the inguinal ligament. Parts of the tenser fascia lata were removed to fully expose the LFCN and its course was pinned (Figure 3.6; number 5).

Figure 3.6: Anterior view of the abdomen showing the superficial dissection on the left (1) ASIS; (2) PT; (3) SEV; (4) SCIV; (5) LFCN.
Key: I- Inferior, L- Left, R- Right, S- Superior, ASIS- Anterior Superior Iliac Spine, PT- Pubic Tubercle, SEV- Superficial Epigastric Vessels, SCIV- Superficial Circumflex Iliac Vessels, LFCN- Lateral Femoral Cutaneous Nerve.

After the dissection procedure of the superficial structures, dissection of the intermediate structures was conducted. The intermediate dissection procedure involved removing both the rectus sheath and the external oblique aponeurosis. Furthurmore, the inferior fibres of the external oblique muscle were relected superolaterally. The iliohypogastric nerve (IHN), as emerging anteriorly, was identified as it coursed medial to the ASIS (Figure 3.7; number 6). The IHN was carefully followed to expose its course medially without detaching it from the fascia layer to prevent movement. The visible emergence and disappearance points were pinned. The ilioinguinal nerve (IIN) was also identified on the internal oblique muscle and its course was fully exposed, from its point of emergence on the internal oblique muscle to its re-emergence from the inguinal canal in close proximity to the pubis (Figure 3.7; number 7). The course of the IIN was also pinned.

Finally, the emergence of the spermatic cord from the superficial inguinal ring was identified in male cadavers and pinned. The analogous structure in females, the round ligament of the uterus, was difficult to locate in the older female cadavers. Therefore, it was excluded from the study as it is not such a prominent structure in comparison to the spermatic cord and as such, it was determined as a no great risk structure.

All structures were identified and pinned on both the left and right side of each cadaver. Measurements were taken and recorded in the excel spreadsheet data collection sheet (Annexure 2).

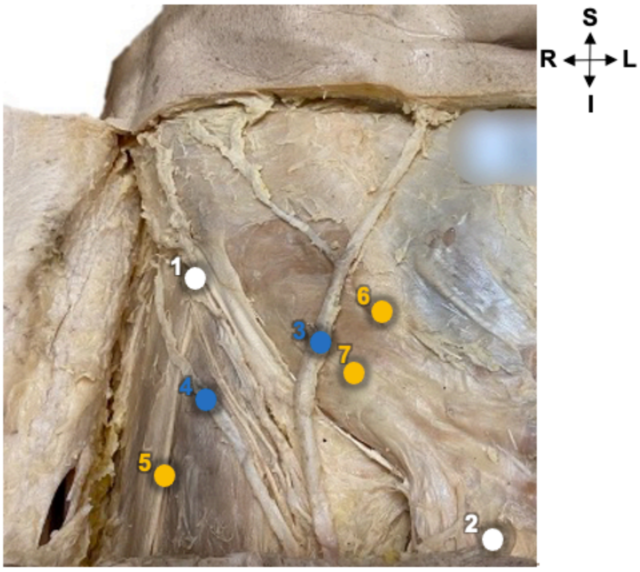

Figure 3.7: Superficial and intermediate dissection of the lower quadrant of the abdomen
(1) ASIS; (2) PT; (3) SEV; (4) SCIV; (5) LFCN; (6) IHN; (7) IIN.
Key: I- Inferior, L- Left, R- Right, S- Superior, ASIS- Anterior Superior Iliac Spine, PT- Pubic Tubercle, SEV- Superficial Epigastric Vessels, SCIV- Superficial Circumflex Iliac Vessels, LFCN- Lateral Femoral Cutaneous Nerve, IHN- Iliohypogastric nerve, IIN- Ilioinguinal nerve.

3.3.2 Implant procedure

In the two different sample groups, the formalin fixed and fresh frozen cadavers, the Bridging Infix implantation procedures differed slightly. Both implantation procedures were carried out by an orthopaedic surgeon followed by dissection of the inferior abdominal wall by the primary investigator.

For the formalin fixed cadaveric sample, the superficial and intermediate dissection procedures were completed prior to implantation. This was done due to the rigidity of the cadaver tissue which resulted in it being unfeasible to easily create the subcutaneous tunnels required. In addition, no complications as a result of the implantation procedure were expected. The implantation procedure was a modified version of the surgical technique (Section 3.3.2.2).

However, in the fresh frozen cadaveric sample, it was decided to closely follow the surgical technique as the tissue was more flexible and best represented actual patients undergoing the surgical procedure.

3.3.2.1 Formalin fixed cadaveric sample

Subsequent to the superficial and intermediate dissection procedures, the implants were secured on the formalin fixed cadaveric samples. With the cadaver in a supine position, and all the structures pinned, the external oblique fascia was lifted off of the iliac crest.

The periosteum was also cleaned off of the iliac crest to create a bare area for fixation.
The plate of implant was placed on the bare area to identify if any last bending adjustments are required for the plate-rod to fit ± 10 mm superior to the pubic symphysis. A hole was drilled into the most anteromedial space on the plate, in line with the iliac crest, and the 40 mm cortical screw was placed. Next the most posterolateral hole was drilled and the 50 mm cortical screw was inserted. Lastly, the middle hole was drilled and the 45 mm cortical screw was placed. The definitive fixation was carried out bilaterally.

The rod ends were cut to allow a ± 15 mm gap between the two rod ends. In the study, only two sets of Bridging Infix implants were available thus they had to be reused. As a result, the plate-rods were only cut once on an intermediate size cadaver to allow the implants to fit both large and small pelvic girdle sizes throughout the study. To connect each plate-rod, a 5 mm connector rod was used with two rod-to-rod connectors (Figure 3.8).

Figure 3.8: Formalin fixed cadaver with the Bridging Infix implanted between the iliac crests and pubic symphysis
Key: I- Inferior, L- Left, R- Right, S- Superior.

3.3.2.2 Fresh frozen cadaveric sample simulation
Prior to anatomical dissection, an orthopaedic surgeon performed the Bridging Infix surgical procedure on two fresh frozen specimens as per the modified methods developed by Strydom & Snyckers (2022).

With the fresh frozen cadaver in a supine position, a marker was used to indicate the three surgical incision sites (Figure 3.9). Two incisions for the lateral windows were made extending from the ASIS 40 mm along the crest on both the left and right side (Figure 3.9; number 1). Dissection continued posteriorly until the external oblique fascia. The musculature was carefully lifted away from the iliac crest to create a bare area for fixation. A third horizontal incision of 60 – 80 mm for the medial window was made approximately 10 mm superior to the pubic symphysis (Figure 3.9; number 2). Dissection continued into the deeper layers of the third incision site, until the rectus abdominis fascia was identified.

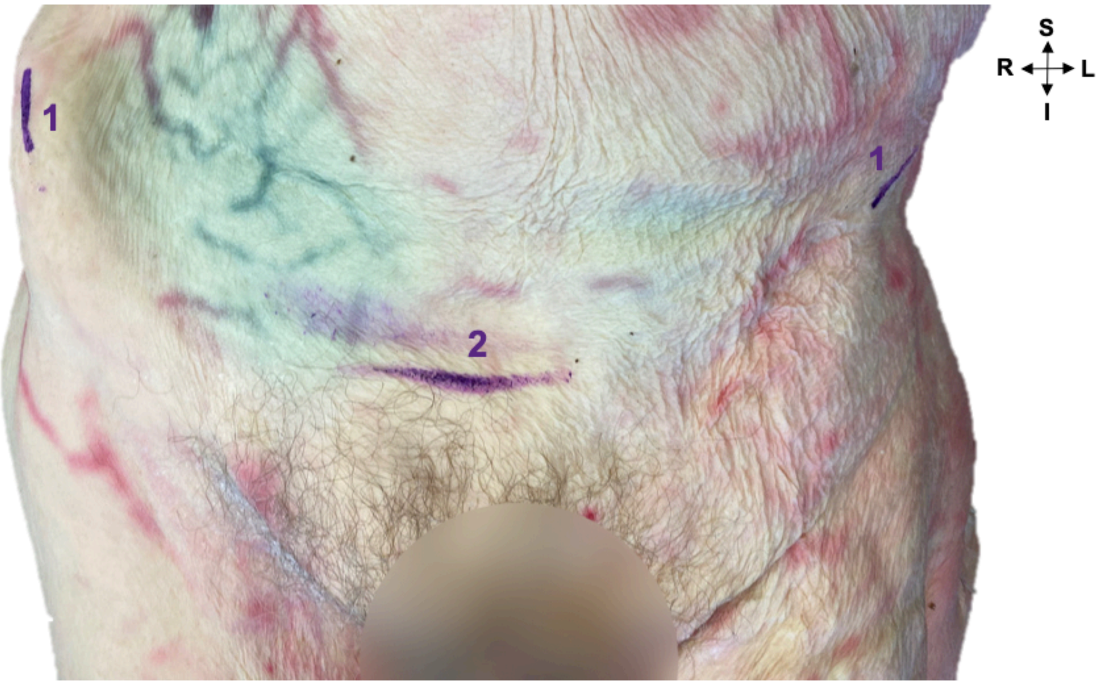

Figure 3.9: Fresh frozen cadaver with surgical incision lines marked on the anterior abdominal wall
(1) Lateral windows; (2) Medial window.
Key: I- Inferior, L- Left, R- Right, S- Superior.

Using a Cobb elevator and blunt dissection, a single subcutaneous tunnel was made traversing between the medial and lateral windows. Kocher forceps were placed between the medial and lateral windows to later pull the Bridging Infix through the tunnel (Figure 3.10).

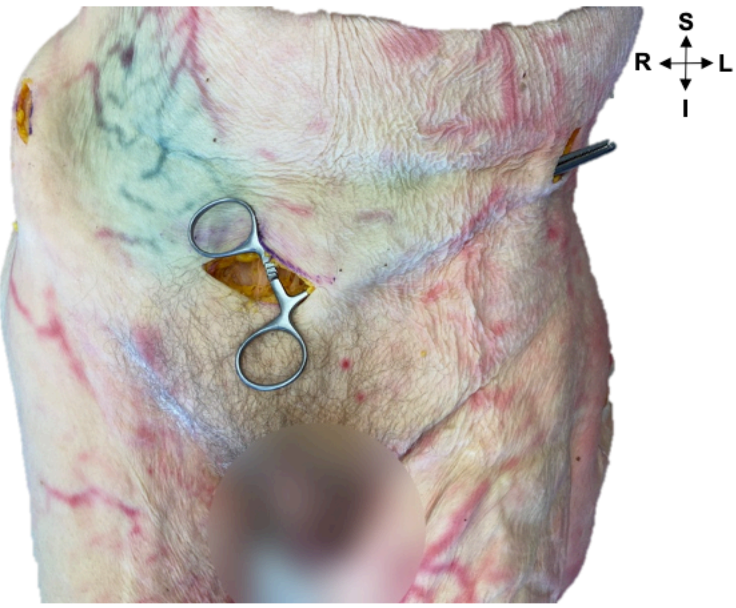

Figure 3.10: Kocher forceps indicating the subcutaneous tunnel from the pubic symphysis to the iliac crest on the fresh frozen specimen
Key: I- Inferior, L- Left, R- Right, S- Superior.

The Kocher forceps were used to clamp the tip of the rod and gently pull the rod through the subcutaneous tunnel from the lateral to medial windows. Visualisation was used to determine if the construct was adequately contoured as no imaging was available. A set of standard cortical screw lengths, 50 mm, 45 mm and 40 mm (from proximal to distal) were used on both sides for definitive fixation. To connect each plate-rod, a 5 mm connector rod was used with rod-to-rod connectors (Figure 3.11).

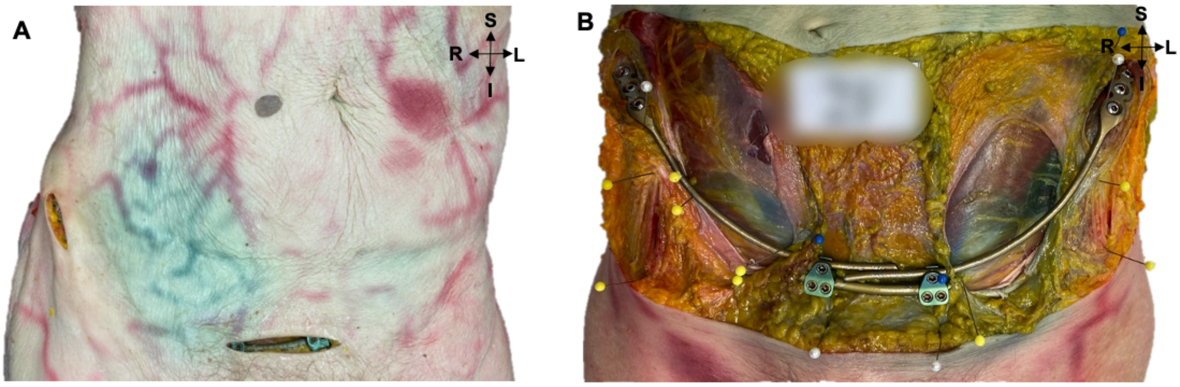

Figure 3.11: The Bridging Infix in-situ
A: Implant in-situ prior to dissection; B: Implant in-situ after dissection.
Key: I- Inferior, L- Left, R- Right, S- Superior.

Subsequent to the surgical technique, the normal superficial and intermediate dissection procedures, as described in section 3.3.1 were followed.

3.3.3 Superficial measurements

Following the superficial and intermediate dissections of both cadaveric samples, measurements were taken using a sliding mechanical calliper of 0.1 mm accuracy. Each measurement originated at either a specific point of the implant (midpoint of the 40 mm cortical screw head or midpoint of the implant rod-to-rod connector single screw) or at a specific bony landmark (ASIS or PT). Each measurement ended at a specific point of an anatomical structure coursing along (or in relation to) the implant.

Firstly, measurements were taken of the distance from the midpoint of the 40 mm cortical screw head to the closest point of the following structures (Figure 3.12):

- IHN emergence from the internal oblique muscle (number 1)
- IIN emergence from the internal oblique muscle (number 3)
- LFCN emergence at the inguinal ligament (number 4)
- SCIV course (number 5)
- Spermatic cord emergence from the inguinal canal (number 2)

Secondly, the most prominent point of the ASIS to the closest point of the (Figure 3.12):

- IHN emergence from the internal oblique muscle (number 1)
- IIN emergence from the internal oblique muscle (number 3)

- LFCN emergence at the inguinal ligament (number 4)
- SCIV course (number 5)
- Spermatic cord emergence from the inguinal canal (number 2)
- PT most prominent point (number 6)

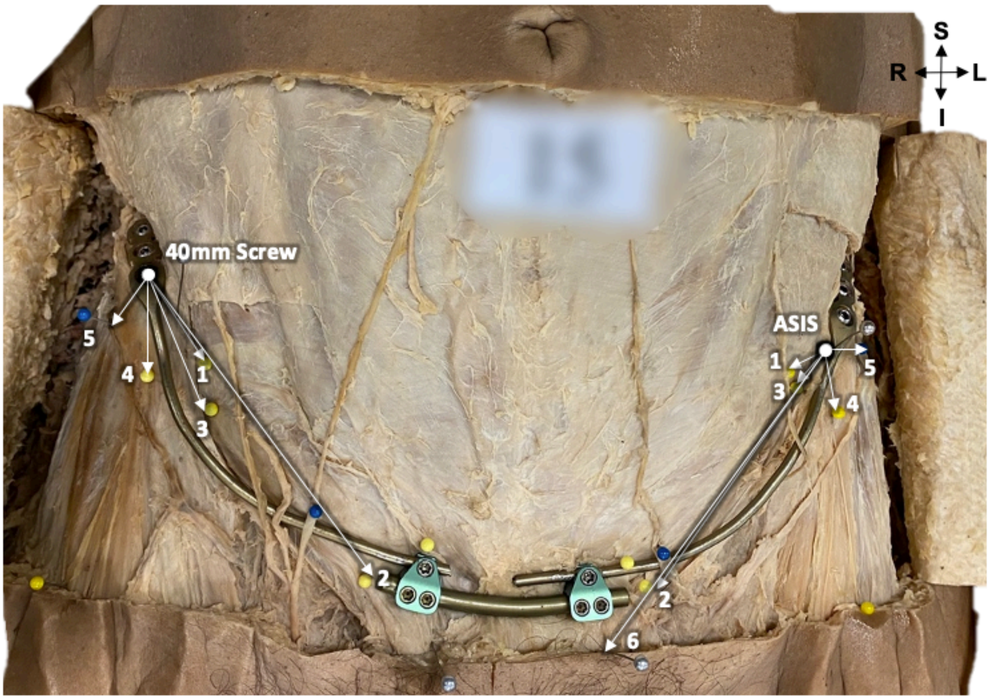

Figure 3.12: Measurements originating laterally from either the left ASIS or right 40 mm screw head illustrated on the anterior surface of a formalin fixed cadaver
(1) IHN; (2) Spermatic cord; (3) IIN; (4) LFCN; (5) SCIV; (6) PT.
Key: I- Inferior, L- Left, R- Right, S- Superior, ASIS- Anterior Superior Iliac Spine, IHN- Iliohypogastric nerve, IIN- Ilioinguinal nerve, LFCN- Lateral Femoral Cutaneous Nerve, SCIV- Superficial Circumflex Iliac Vessels, PT- Pubic Tubercle.

Thirdly, the midpoint of the implant rod-to-rod connector single screw to the closest point of the (Figure 3.13):

- IHN close to implant rod-to-rod connector single screw (number 4)
- IIN close to implant rod-to-rod connector single screw (number 5)
- LFCN emergence at the inguinal ligament (number 2)
- SCIV at the ASIS (number 1)
- SEV as they pass superior to the Bridging Infix rod (number 3)
- Spermatic cord emergence from the inguinal canal (number 6)

Fourthly, the most prominent point of the pubic tubercle to the closest point of the (Figure 3.13):

- IHN close to implant rod-to-rod connector single screw (number 4)
- IIN close to implant rod-to-rod connector single screw (number 5)
- LFCN emergence at the inguinal ligament (number 2)
- SCIV at the ASIS (number 1)

- SEV as they pass superior to the Bridging Infix rod (number 3)
- Spermatic cord emergence from the inguinal canal (number 6)
- Implant rod-to-rod connector single screw (number 7)

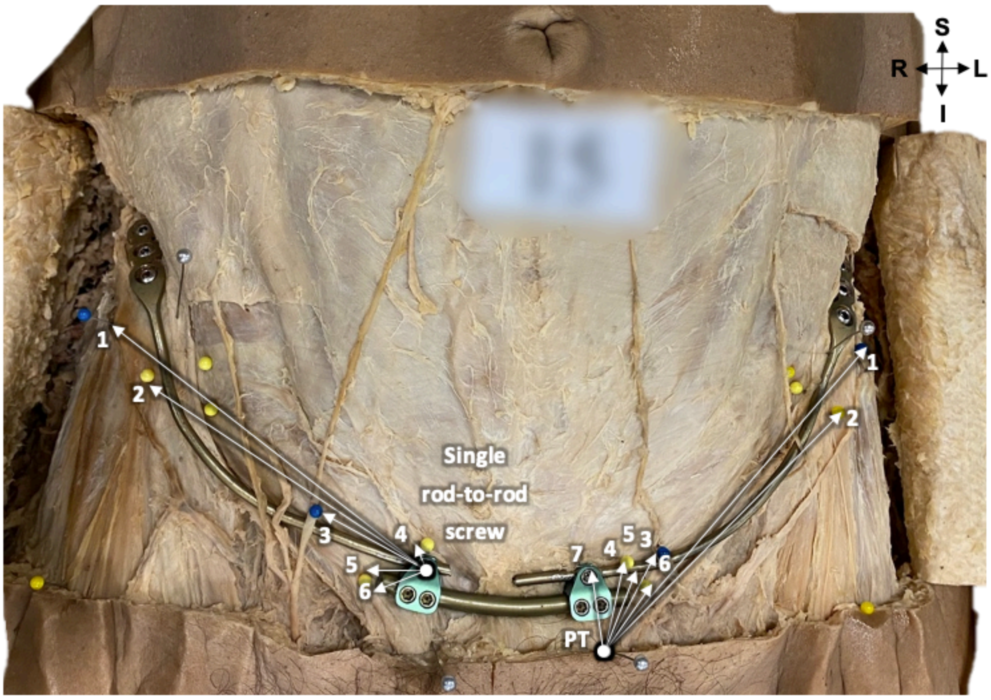

Figure 3.13: Measurements originating medially from either the single right rod-to-rod screw head or left PT illustrated on the anterior surface of a formalin fixed cadaver
(1) SCIV; (2) LFCN; (3) SEV; (4) IHN; (5) IIN; (6) Spermatic cord; (7) Rod-to-rod connector single screw.
Key: I- Inferior, L- Left, R- Right, S- Superior, PT- Pubic Tubercle, SCIV- Superficial Circumflex Iliac Vessels, LFCN- Lateral Femoral Cutaneous Nerve, SEV- Superficial Epigastric Vessels, IHN- Iliohypogastric nerve, IIN- Ilioinguinal nerve.

Lastly, an osteological measurement from ASIS to ASIS was taken to determine the length of the pelvic girdle. The bony measurements were taken to assist the surgeons with the implant procedure as well as to aid in determining a safe zone for the placement of the lateral aspect of the plate-rod.

All measurements were taken bilaterally and recorded for data analysis (Annexure 2). However, in some cadavers, a few structures were damaged, cut or not found in the dissection procedure and therefore could not be measured.

3.3.4 Deep dissection procedure

With the cadaver in a supine position, the fatty tissue, fascia and femoral sheath covering the femoral neurovasculature were carefully removed to expose the femoral vein (FV) and femoral artery (FA) from their emergence below the inguinal ligament. Each structure was pinned as it emerged inferior to the inguinal ligament, coursing inside or in relation to the femoral sheath.

3.3.5 Deep measurements

After the completion of the deep dissections, the following measurements were taken. Firstly, the distance from the midpoint of the 40 mm cortical screw head to the closest point of the FV (number 1), FA (number 2), and FN (number 3) as they emerged inferior to the inguinal ligament (Figure 3.14).

Secondly, the most prominent point of the ASIS to the closest point of the FV (number 1), FA (number 2), and FN (number 3) as they emerged inferior to the inguinal ligament (Figure 3.14).

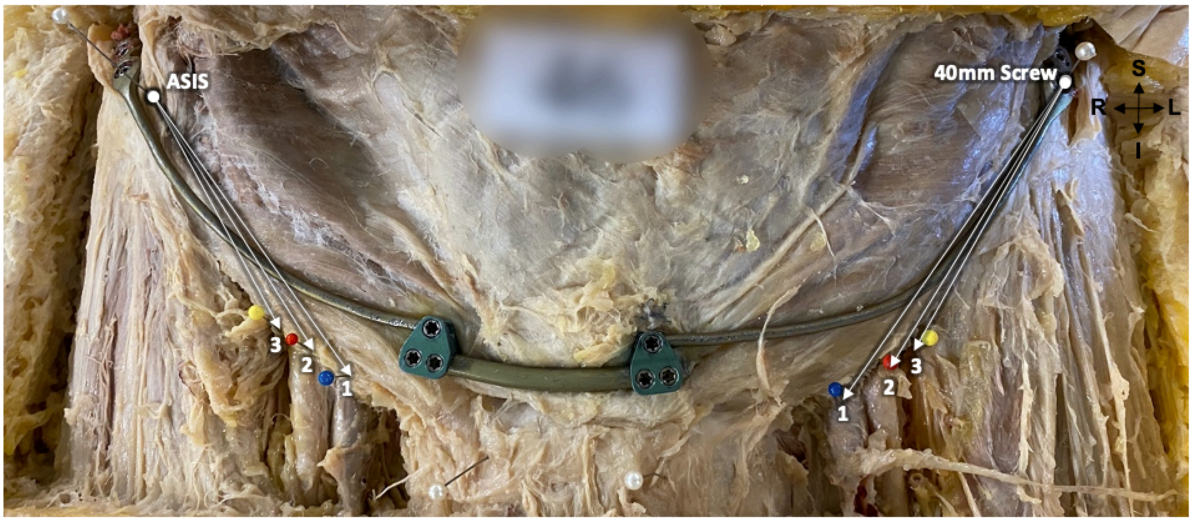

Figure 3.14: Deep measurements originating laterally from either the right ASIS or left 40 mm screw head illustrated on the anterior surface of a formalin fixed cadaver
(1) FV; (2) FA; (3) FN.
Key: I- Inferior, L- Left, R- Right, S- Superior, ASIS- Anterior Superior Iliac Spine, FV- Femoral Vein, FA- Femoral Artery, FN- Femoral Nerve.

Thirdly, the midpoint of the implant rod-to-rod connector single screw to the closest point of the FV (number 1), FA (number 2), and FN (number 3) as they emerge inferior to the inguinal ligament (Figure 3.15).

Lastly, the most prominent point of the pubic tubercle to the closest point of the FV (number 1), FA (number 2), and FN (number 3) as they emerge inferior to the inguinal ligament (Figure 3.15).

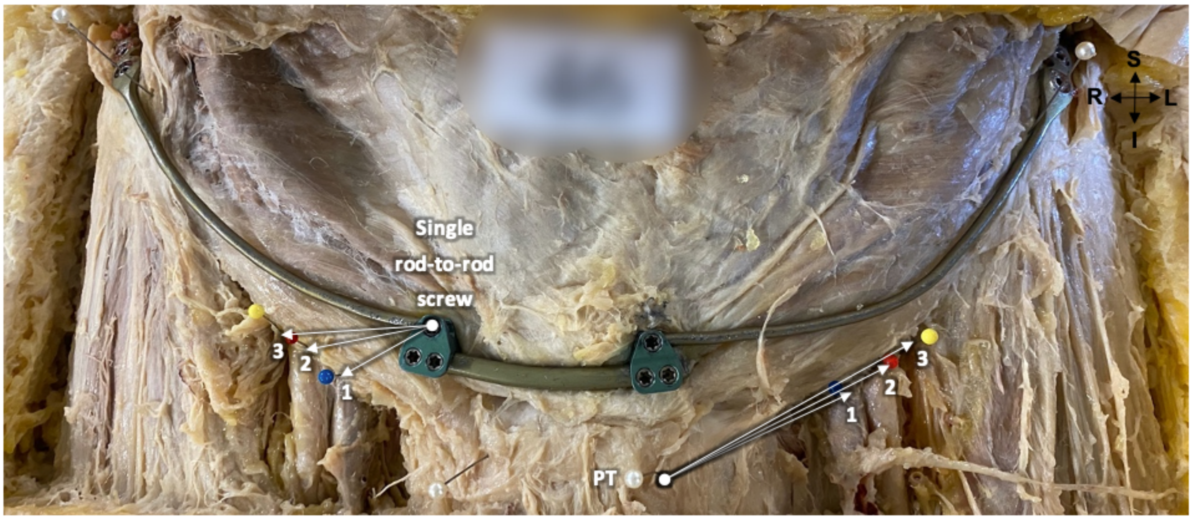

Figure 3.15: Deep measurements originating medially from either the right single rod-to-rod connector screw head or left PT illustrated on the anterior surface of a formalin fixed cadaver
(1) FV; (2) FA; (3) FN.
Key: I- Inferior, L- Left, R- Right, S- Superior, PT- Pubic Tubercle, FV- Femoral Vein, FA- Femoral Artery, FN- Femoral Nerve.

All measurements were taken bilaterally and recorded for data analysis.

3.3.6 Effect of flexion

To determine if flexion of the hip influences the measurements taken, the hips of the fresh frozen cadavers (n = 4) were flexed > 45° (Mean: 70.44; Range: 69.30 - 71.33). Only the fresh frozen cadavers were included in the investigation as the formalin fixed cadavers were too rigid to move the joints.

With the cadavers in a supine position, one hip at a time was flexed. Observations were recorded if the observer noticed a structure move. Furthermore, measurements were taken from the three most important superficial structures, IHN, IIN and LFCN. The following two sets of measurements were taken:

- The distance from the midpoint of the 40mm cortical screw head to the closest point of the IHN, IIN and LFCN.
- The distance from the midpoint of the implant rod-to-rod connector single screw to the closest point of the IHN, IIN and LFCN.

The measurements taken were later analysed and compared to the same measurements taken with the legs straight to determine if hip flexion has an effect on the location of the superficial structures.

3.3.7 Explant procedure

Each Bridging Infix was carefully removed and placed on scaled (2 mm x 2 mm squared) graphical paper. It was rotated and captured to see all the contours of the implant. As only two sets of implants were available, each set of the implants were then re-contoured according to the next cadaver and reused.

The images taken of the Bridging Infix on the scaled paper were imported to *ImageJ* software to analyse the contoured angles. The analysis was conducted to determine if a one size fits all implant can be manufactured.

3.4 INTEROBSERVER AND INTRAOBSERVER ERROR

To ensure the accuracy and repeatability of the results obtained from the study, intra- and inter-rater reliability were determined with the use of intraclass correlation coefficients (ICC). The ICC values were determined for 10% of each sample (n = 5 for formalin fixed sample; n = 2 for fresh frozen sample) by the primary investigator and by using an independent observer. The results pertaining to the error testing is presented in Chapter 4, Table 4.11.

3.5 ETHICAL CLEARANCE

Ethical approval was obtained from the Faculty of Health Sciences Research Ethics Committee, University of Pretoria (Ethical clearance: 182/2021) prior to the commencement of the study (Annexure 1). The cadavers used in this study were obtained and dissected in accordance with the rules and regulations stated within the South African National Health Act (Act 61 of 2003). The formalin fixed cadavers were obtained from the Department of Anatomy, University of Pretoria, and the fresh frozen cadavers from the National Tissue Bank. All the data collected was from full body cadavers. All cadavers are obtained through donation as a personal choice of the deceased before death, by the family members or due to the deceased being unclaimed by family members from senior citizen homes, hospitals, or investigative cases. The cadavers were handled with respect and properly safeguarded at all times. No information which could possibly reveal the identities of the cadavers was obtained. Access to personal information regarding the cadaver's age, ancestry, height, and weight were noted, and restricted to the primary investigator. No other personal information was obtained.

3.6 DATA PROCESSING

The *SPSS IBM Statistics* version 27 (1989, 2020) software was used to perform the analysis. Thedata analysis included descriptive statistics (means, standard deviations, 99% confidence intervals, minimum and maximum) for the continuous variables (distance measurements from the implant to adjacent anatomical structures, age and BMI) and frequency tables (counts and percentages) for categorical variables (gender and ancestry).

The measurements were tested for normality prior to further testing. Tests for difference between the measurements were conducted. The parametric *paired t-test* was conducted to compare the left- and right-side measurements for normally distributed measurements and the non-parametric *Wilcoxon Signed Ranks Test* was performed on the skewed measurements.

To test for difference between sex groups, a *t-test for equality of means* was conducted for normally distributed data or a *Mann Whitney-U test* for skewed data. To test for possible differences in BMI groups, a *Kruskal Wallis test* was performed.

Furthermore, for comparisons between the fresh cadavers with flexed and straight hips, *Mann Whitney-U tests* were conducted.

CHAPTER 4: RESULTS

4.1 FORMALIN FIXED CADAVER SAMPLE

4.1.1 Descriptive statistics

Fifty (n = 50) formalin fixed cadavers were utilized in the study of which eighteen (n = 18) were female and thirty-two (n = 32) were male. The mean age of the sample was 71 years with a mean BMI of 20.14 kg/m^2. The sample size (n) may differ slightly between all measurements due to either the structure being cut, damaged, or not found during dissection. These samples were still included due to the limited availability of cadavers. All measurements originated from either a specific point of the implant, the 40 mm implant cortical screw head (40mm) and the implant single screw of the rod-to-rod connector (IRTR) or a bony landmark, the anterior superior iliac spine (ASIS) or pubic tubercle (PT). The measurements were taken from one of the previously mentioned origins to one of the following structures: iliohypogastric nerve (IHN), ilioinguinal nerve (IIN), lateral femoral cutaneous nerve (LFCN), superficial epigastric vessels (SEV), superficial circumflex iliac vessels (SCIV), spermatic cord, femoral vein (FV), femoral artery (FA) or femoral nerve (FN). Descriptive statistics are presented in Table 4.1 in section 4.1.3 for all measurements depending on the normality results.

4.1.2 Normality test

When the left and right measurements were paired, and tested for normality, the distance between the 40 mm screw and FA (p-value = 0.011; statistic = 0.937; df = 50) and FN (p-value = 0.025; statistic = 0.947; df = 50) were skewed. Moreover, the measurements from the IRTR – SCIV (p-value = 0.006; statistic = 0.909; df = 36) and PT – spermatic cord (p-value = 0.013; statistic = 0.912; df = 32) were skewed. The distance between the PT – ASIS (p-value = 0.013; statistic = 0.940; df = 50) was also skewed. For further testing, non-parametric tests were used for the skewed measurements and non-normally distributed data is highlighted in blue throughout.

4.1.3 Difference between sides (left vs right)

To assess whether a difference exists between equivalent measurements taken on the left and right side of the cadaver, a *paired t-test* or *Wilcoxon signed rank test* for skewed data was performed. The results are indicated in Table 4.1 below with the statistically significant results highlighted in grey.

A significant difference was found for all measurements originating from the IRTR, with the exception of the measurement to the PT, indicating that the left and right-side measurements are different. Furthermore, a difference between left and right sides was detected for the measurement from the implant 40 mm screw to the IHN. No other statistically significant differences were detected. In the cases where no difference was detected between the sides, the data was pooled together for further testing.

The data was tested for normality again after testing for statistical differences between the sides using a *Shapiro Wilk test*. On the left side, the distances between the IRTR to the IHN (p-value = 0.005; statistic = 0.927; df = 49) and SCIV (p-value = 0.033; statistic = 0.942; df = 42) were found to not follow a normal distribution. On the right side, only the distance between the 40mm – IHN (p-value = 0.028; statistic = 0.946; df = 48) was skewed.

For the pooled data, several significant differences were detected. Originating from the 40 mm cortical screw to the IIN (p-value = 0.016; statistic = 0.968; df = 98), LFCN (p-value = 0.001; statistic = 0.949; df = 100), FA (p-value = 0.036; statistic = 0.973; df = 100) and FN (p-value = 0.042; statistic = 0.974; df = 100) were found to be skewed. Furthermore, the distance between the ASIS to IHN (p-value = 0.013; statistic = 0.966; df = 97), IIN (p-value = 0.011; statistic = 0.966; df = 98), LFCN (p-value = 0.003; statistic = 0.959; df = 100) and FN (p-value = 0.034; statistic = 0.972; df = 100) were not normally distributed. Lastly, the measurement from the PT – SEV (p-value = 0.039; statistic = 0.965; df = 73) was skewed. For further testing, the measurements which were found to not follow a normal distribution underwent non-parametric testing and are indicated with blue highlighting throughout.

Table 4.1: Analysis results for significant differences between the left and right sides

Measurement Origin	To	n	Side	Mean	Minimum	Maximum	SD	Median	IQR	99% CI for mean Lower	Upper	t or Z	df	Sig. [2-tailed]
	IHN	49	L	44.29	19.62	81.08	14.42	45.48	24.68	38.76	49.81	-2.358	46	**0.023**
		48	R	38.14	10.86	81.25	15.71	36.27	15.47	32.05	44.23			
	IIN	50	L	61.96	23.99	97.62	21.05	62.78	29.40	53.98	69.94	-1.502	47	0.140
		48	R	57.20	16.60	90.02	19.68	62.63	32.91	49.58	64.83			
		98	Total	59.63	16.60	97.62	20.43	62.63	32.74	54.21	65.05			
	LFCN	50	L	38.89	18.79	68.68	12.96	35.13	19.93	33.98	43.80	-0.872	49	0.388
		50	R	37.04	18.00	64.98	11.45	35.86	19.56	32.71	41.38			
		100	Total	37.97	18.00	68.68	12.20	35.13	19.80	34.76	41.17			
	SCIV	39	L	20.94	8.52	37.36	7.40	19.61	9.81	17.73	24.15	-0.282	31	0.780
		37	R	19.64	6.74	34.16	6.74	19.36	8.31	16.63	22.65			
		76	Total	20.31	6.74	37.36	7.06	19.49	9.11	18.16	22.45			
40mm	SC	31	L	120.45	86.89	141.92	12.23	120.92	18.90	114.41	126.49	0.524	29	0.604
		30	R	122.47	98.11	142.79	11.04	124.07	16.92	116.92	128.02			
		61	Total	120.50	86.89	141.92	11.96	120.73	17.31	116.46	124.54			
	FV	50	L	104.03	89.54	124.76	8.95	103.85	13.62	100.64	107.42	0.051	49	0.959
		50	R	104.09	72.28	129.79	9.79	104.21	9.81	100.38	107.80			
		100	Total	104.06	72.28	129.79	9.33	104.21	11.58	101.61	106.51			
	FA	50	L	90.77	73.03	116.29	9.77	90.43	11.23	87.06	94.47	-0.690^{Z}	-	0.490
		50	R	90.85	63.40	114.20	8.25	91.35	7.50	87.72	93.98			
		100	Total	90.81	63.40	116.29	9.00	91.06	9.59	88.44	93.17			
	FN	50	L	78.78	59.41	100.40	8.27	78.16	11.13	75.64	81.91	-1.511^{Z}	-	0.131
		50	R	80.12	47.22	96.46	8.10	80.79	8.90	77.05	83.19			
		100	Total	79.45	47.22	100.40	8.17	78.67	9.58	77.30	81.59			
	IHN	49	L	33.32	7.42	59.14	14.36	35.13	23.69	27.81	38.82	-1.143	46	0.259
		48	R	29.74	10.34	72.89	14.46	27.09	13.95	24.14	35.35			
		97	Total	31.55	7.42	72.89	14.45	29.31	21.35	27.69	35.40			
	IIN	50	L	50.32	10.21	85.26	21.53	54.27	33.89	42.16	58.48	-1.103	47	0.276
		48	R	47.54	10.42	84.61	19.83	49.39	34.28	39.86	55.23			
		98	Total	48.96	10.21	85.26	20.65	51.64	32.36	43.48	54.44			
	LFCN	50	L	29.59	7.92	60.89	12.98	27.85	19.18	24.67	34.51	-0.828	49	0.411
		50	R	27.95	8.21	56.00	10.74	26.97	16.07	23.89	32.02			
		100	Total	28.77	7.92	60.89	11.88	27.42	16.85	25.65	31.89			
	SCIV	40	L	21.26	2.45	43.08	8.32	22.45	9.73	17.70	24.82	-0.038	31	0.970
		37	R	20.53	4.16	35.96	7.48	20.49	10.77	17.19	23.87			
		77	Total	20.91	2.45	43.08	7.88	20.90	10.02	18.54	23.28			
ASIS	SC	31	L	109.67	74.46	131.84	13.71	110.26	24.21	102.90	116.45	0.587	29	0.562
		30	R	111.96	82.99	131.91	11.60	112.09	18.10	106.13	117.80			
		61	Total	110.80	74.46	131.91	12.66	111.65	18.69	106.49	115.11			
	FV	50	L	93.02	76.28	119.61	10.25	91.16	14.03	89.13	96.90	-0.502	49	0.618
		50	R	92.36	58.46	116.02	10.16	92.82	12.52	88.51	96.22			
		100	Total	92.69	58.46	119.61	10.16	91.94	12.67	90.02	95.36			
	FA	50	L	78.93	62.82	99.00	9.05	78.90	13.25	75.50	82.36	0.501	49	0.619
		50	R	79.58	49.63	102.54	9.10	80.73	9.58	76.14	83.03			
		100	Total	79.26	49.63	102.54	9.03	79.77	11.34	76.88	81.63			
	FN	50	L	67.93	51.18	89.18	8.77	68.26	11.47	64.61	71.26	0.674	49	0.503
		50	R	68.78	35.74	84.20	8.47	69.78	9.18	65.57	71.99			
		100	Total	68.36	35.74	89.18	8.59	69.01	9.87	66.10	70.61			
	ASIS	50	-	254.39	176.84	379.66	32.58	249.59	35.91	245.14	263.65	-	-	-
	IHN	49	L	19.48	5.40	44.82	8.90	17.95	9.15	16.07	22.89	-3.885	47	**0.000**
		49	R	14.38	3.14	29.87	6.66	14.64	9.64	11.83	16.94			
	IIN	50	L	29.94	12.36	55.96	10.49	29.73	16.67	25.97	33.92	-5.377	49	**0.000**
		50	R	20.08	7.12	37.38	7.56	19.55	12.56	17.22	22.95			
	LFCN	50	L	105.57	67.28	135.06	15.71	105.45	23.92	99.61	111.52	-4.169	49	**0.000**
		50	R	96.04	74.07	119.08	11.79	95.34	16.73	91.57	100.50			
	SCIV	42	L	132.76	103.07	178.10	19.61	129.03	32.30	124.59	140.94	-3.472^{Z}	-	**0.001**
		40	R	123.54	92.64	166.51	18.87	122.42	23.30	115.46	131.62			
	SC	35	L	27.36	15.29	47.19	8.61	25.52	10.60	23.38	31.33	-6.112	34	**0.000**
		35	R	19.88	10.23	35.97	5.38	18.57	6.71	17.40	22.36			
IRTR	SEV	38	L	37.30	7.55	65.20	14.64	37.99	24.37	30.86	43.75	-2.237	32	**0.032**
		33	R	31.36	9.32	48.86	10.41	32.74	15.56	26.39	36.32			
	FV	50	L	47.07	27.57	66.47	10.22	46.88	15.77	43.20	50.94	-7.141	49	**0.000**
		50	R	36.75	22.06	51.17	6.50	34.96	9.14	33.28	38.21			
	FA	50	L	57.35	36.09	77.41	10.73	56.91	14.18	53.29	61.42	-7.095	49	**0.000**
		50	R	45.52	27.30	60.90	7.03	45.23	9.21	42.86	48.19			
	FN	50	L	68.57	45.98	93.90	11.32	68.76	16.65	64.28	72.86	-7.071	49	**0.000**
		50	R	56.54	40.02	72.86	7.65	57.44	10.76	53.64	59.44			
	PT	50	L	29.95	14.67	50.63	8.34	30.43	11.42	26.79	33.11	1.623	49	0.111
		50	R	31.24	5.78	53.28	10.15	31.17	16.18	27.39	35.08			
		100	Total	30.59	5.78	53.28	9.26	30.65	12.41	28.16	33.03			
	IHN	49	L	39.86	15.46	65.50	11.21	41.05	15.33	35.56	44.15	-0.087	47	0.931
		49	R	39.34	12.58	61.52	11.87	41.09	17.66	34.79	43.89			
		98	Total	39.60	12.58	65.50	11.48	41.07	16.10	36.55	42.65			
	IIN	50	L	33.30	13.83	60.64	11.34	33.54	15.68	29.01	37.60	-0.516	49	0.608
		50	R	35.57	0.00	51.75	11.47	32.86	16.20	28.22	36.92			
		100	Total	32.94	0.00	60.64	11.35	33.54	15.91	29.96	35.92			
	LFCN	50	L	114.54	71.15	143.98	14.90	115.08	19.13	108.89	120.19	1.236	49	0.222
		50	R	117.40	85.60	145.97	14.57	118.15	25.94	111.88	122.92			
		100	Total	115.97	71.15	145.97	14.73	116.25	20.80	112.10	119.84			
	SCIV	42	L	141.82	119.80	180.54	13.05	141.08	15.17	136.38	147.26	-0.248	35	0.806
		40	R	141.77	103.27	172.73	13.79	143.40	14.99	135.87	147.67			
		82	Total	141.80	103.27	180.54	13.33	142.87	15.09	137.91	145.68			
	SC	34	L	27.67	16.51	46.43	8.06	25.27	11.69	23.89	31.44	-1.244^{Z}	-	0.214
		33	R	25.93	0.00	56.49	13.65	24.86	18.14	19.42	32.43			
PT		67	Total	26.81	0.00	56.49	11.11	25.20	14.08	23.21	30.41			
	SEV	38	L	50.84	20.42	76.64	14.96	49.72	23.00	44.25	57.43	1.100	34	0.279
		35	R	53.24	8.01	74.36	15.41	54.74	15.20	46.13	60.35			
		73	Total	51.99	8.01	76.64	15.12	52.79	19.24	47.31	56.67			
	FV	50	L	47.67	32.82	62.26	7.53	47.49	11.47	44.81	50.52	-0.227	49	0.822
		50	R	47.41	26.40	71.96	9.36	45.76	10.89	43.86	50.96			
		100	Total	47.54	26.40	71.96	8.45	46.89	11.57	45.32	49.76			
	FA	50	L	61.00	44.36	78.92	8.98	61.98	11.87	57.60	64.40	-0.241	49	0.811
		50	R	60.72	37.46	85.30	10.07	60.29	11.00	56.90	64.54			
		100	Total	60.86	37.46	85.30	9.49	60.42	11.07	58.37	63.35			
	FN	50	L	74.01	53.02	92.65	9.51	75.23	14.15	70.40	77.62	-0.449	49	0.655
		50	R	73.49	48.69	101.96	10.56	73.16	14.26	69.48	77.49			
		100	Total	73.75	48.69	101.96	10.00	73.73	13.83	71.12	76.38			
	ASIS	50	L	135.07	104.06	161.80	12.87	136.02	18.08	130.19	139.95	-1.197^{Z}	-	0.231
		50	R	135.63	106.92	162.58	12.63	135.66	16.06	130.85	140.42			
		100	Total	135.35	104.06	162.58	12.69	135.90	17.50	132.02	138.68			

where n = sample size, SD = standard deviation, IQR = interquartile range, CI = confidence interval, t or Z = test statistic or Z value for skewed data, df = degrees of freedom; significant differences (p ≤ 0.05) between groups are highlighted in grey, not normally distributed measurements are highlighted in blue.

4.1.4 Difference between sex (female vs male)

To assess whether a difference exists between sex groups for the left and right measurements as well as the pooled measurements, a *t-test for equality of means* was performed for the normally distributed data. If data was skewed, a *Mann Whitney-U test* was conducted with the results highlighted in blue.

The distance between the IRTR to both the IIN and LFCN on the left were found to be statisitically different as indicated in Table 4.2, while no measurements on the right exhibited any statistically significant difference as seen in Table 4.3.

Furthermore, when the measurements were pooled, significant differences were found for all the measurements to the IIN as well as from the 40 mm screw to FV, ASIS to the femoral neurovasculature and the PT to the LFCN. Results are displayed in Table 4.4 for the pooled measurements.

Table 4.2: Left side analysis for the test of difference between the sexes

Measurement		n	Sex	Mean	SD	Median	IQR	99% CI of difference		t or Z	df	Sig. [2-tailed]
Origin	To							Lower	Upper			
40mm	IHN	18 31	F M	42.68 45.22	14.02 14.79	38.61 47.40	24.14 25.04	-14.087	9.009	-0.590	47	0.558
IRTR	IHN	18 31	F M	19.17 19.66	10.27 8.18	16.47 18.00	12.21 8.68	-	-	-1.046^{Z}	-	0.296
	IIN	18 32	F M	23.57 33.53	8.26 9.98	20.32 32.03	14.54 14.25	-17.396	-2.529	-3.595	48	**0.001**
	LFCN	18 32	F M	98.29 109.66	15.53 14.48	97.53 108.45	23.00 23.47	-23.122	0.363	-2.599	48	**0.012**
	SCIV	14 28	F M	134.42 131.93	20.71 19.37	129.98 127.11	32.93 29.27	-	-	-0.403^{Z}	-	0.687
	SEV	11 27	F M	34.11 38.61	14.04 14.94	30.61 41.58	18.23 22.97	-18.786	9.797	-0.855	36	0.398
	FV	18 32	F M	44.63 48.45	9.39 10.55	45.26 47.88	12.31 18.32	-11.846	4.205	-1.277	48	0.208
	FA	18 32	F M	54.57 58.92	9.61 11.15	55.04 60.02	10.64 18.10	-12.749	4.054	-1.388	48	0.172
	FN	18 32	F M	65.53 70.28	10.50 11.56	67.76 71.07	16.74 17.34	-13.604	4.089	-1.443	48	0.156

where n = sample size, SD = standard deviation, IQR = interquartile range, CI = confidence interval, t or Z = test statistic or Z value for skewed data, df = degrees of freedom, F = female, M = male; significant differences (p ≤ 0.05) between groups are highlighted in grey, not normally distributed measurements are highlighted in blue. Note: Mann-Whitney value for IRTR – IHN = 215.000, IRTR – SCIV = 132.000.

Table 4.3: Right side analysis for the test of difference between the sexes

Measurement Origin	To	n	Sex	Mean	SD	Median	IQR	99% CI of difference Lower	Upper	t or Z	df	Sig. [2-tailed]
40mm	IHN	16	F	35.74	11.67	35.64	13.33	-	-	-0.109^{Z}	-	0.913
		32	M	39.34	17.43	37.01	22.39					
IRTR	IHN	17	F	15.49	7.72	14.87	10.56	-3,691	7.081	0.845	47	0.402
		32	M	13.79	6.08	14.09	7.77					
	IIN	18	F	18.91	7.73	18.22	12.25	-7.823	4.159	-0.820	48	0.416
		32	M	20.74	7.50	21.58	12.67					
	LFCN	18	F	91.89	10.08	93.80	15.52	-15.554	2.598	-1.914	48	0.062
		32	M	98.37	12.18	99.85	19.39					
	SCIV	13	F	128.05	21.88	124.18	44.39	-10.574	23.934	1.050	38	0.300
		27	M	121.37	17.27	121.30	21.65					
	SEV	9	F	32.34	8.24	34.50	10.67	-9.972	12.677	0.328	31	0.745
		24	M	30.99	11.25	32.22	17.35					
	FV	18	F	37.36	6.97	34.71	10.50	-2.572	7.624	1.329	48	0.190
		32	M	34.84	6.15	34.96	8.19					
	FA	18	F	46.53	7.55	44.28	13.26	-4.000	7.164	0.760	48	0.451
		32	M	44.95	6.78	45.93	7.81					
	FN	18	F	57.86	7.85	57.25	12.24	-4.002	8.111	0.910	48	0.367
		32	M	55.80	7.56	57.62	9.64					

where n = sample size, SD = standard deviation, IQR = interquartile range, CI = confidence interval, t or Z = test statistic or Z value for skewed data, df = degrees of freedom, F = female, M = male; significant differences (p ≤ 0.05) between groups are highlighted in grey, not normally distributed measurements are highlighted in blue. Note: Mann-Whitney value for 40mm – IHN = 251.000.

Table 4.4: Pooled analysis for the test of difference between the sexes

Measurement Origin	To	n	Sex	Mean	SD	Median	IQR	99% CI of difference Lower	Upper	t or Z	df	Sig. [2-tailed]
40mm	IIN	35 63	F M	49.10 65.48	21.57 17.32	45.48 68.48	38.44 27.38	-	-	-3.652^{Z}	-	**0.000**
40mm	LFCN	36 64	F M	39.94 36.86	13.75 11.20	36.74 34.99	20.48 19.49	-	-	-0.898^{Z}	-	0.369
40mm	SCIV	27 49	F M	21.39 19.71	5.37 7.83	20.46 18.01	9.10 10.37	-2.799	6.156	0.991	74	0.325
40mm	FV	36 64	F M	100.68 105.96	9.14 8.96	98.96 104.88	11.54 10.56	-10.220	-0.344	-2.810	98	**0.006**
40mm	FA	36 64	F M	88.25 92.25	9.31 8.56	88.03 91.91	8.59 8.15	-	-	-2.377^{Z}	-	0.0178
40mm	FN	36 64	F M	77.53 80.53	9.53 7.15	77.34 79.86	11.20 8.55	-	-	-1.605^{Z}	-	0.108
ASIS	IHN	34 63	F M	29.99 32.39	12.70 15.34	27.35 30.06	21.34 21.45	-	-	-0.620^{Z}	-	0.535
ASIS	IIN	35 63	F M	38.44 54.80	22.11 17.39	33.90 57.21	40.91 28.01	-	-	-3.614^{Z}	-	**0.000**
ASIS	LFCN	36 64	F M	30.25 27.94	13.94 10.57	28.20 26.97	18.53 16.32	-	-	-0.661^{Z}	-	0.509
ASIS	SCIV	28 49	F M	21.64 20.49	8.61 7.49	22.53 20.49	9.79 9.55	-3.809	6.102	0.612	75	0.543
ASIS	FV	36 64	F M	88.51 95.04	9.59 9.77	88.34 93.87	11.56 11.75	-11.840	-1.213	-3.227	98	**0.002**
ASIS	FA	36 64	F M	75.53 81.35	8.43 8.74	75.70 81.59	9.50 9.73	-10.550	-1.105	-3.241	98	**0.002**
ASIS	FN	36 64	F M	65.63 69.89	9.42 7.75	66.69 69.56	12.46 7.99	-	-	-2.133^{Z}	-	**0.033**
ASIS	ASIS	36 64	F M	243.20 260.69	15.38 37.52	245.42 258.19	26.95 51.14	-	-	-2.643^{Z}	-	0.008
IRTR	PT	36 64	F M	28.71 31.65	9.81 8.84	30.12 31.16	11.49 12.64	-7.975	2.094	-1.534	98	0.128
PT	IHN	35 63	F M	41.19 38.71	12.11 11.12	43.36 39.61	20.49 13.99	-3.882	8.840	1.024	96	0.308
PT	IIN	36 64	F M	29.12 35.09	8.67 12.15	28.60 34.84	13.30 15.63	-12.013	0.067	-2.598	98	**0.011**
PT	LFCN	36 64	F M	110.05 119.30	13.49 14.44	109.47 118.61	16.47 22.13	-16.971	-1.526	-3.146	98	**0.002**
PT	SCIV	27 55	F M	140.47 142.45	14.20 12.97	140.87 143.25	13.61 15.79	-10.268	6.326	-0.627	80	0.533
PT	SEV	21 52	F M	51.47 52.20	10.71 16.66	51.92 53.77	13.35 19.93	-	-	-0.658^{Z}	-	0.511
PT	FV	36 64	F M	48.24 47.15	8.53 8.45	46.35 47.03	15.39 10.57	-3.551	5.731	0.617	98	0.539
PT	FA	36 64	F M	60.82 60.88	9.63 9.49	59.96 60.52	16.51 9.38	-5.280	5.164	-0.029	98	0.977
PT	FN	36 64	F M	73.07 74.13	9.82 10.16	72.32 75.23	16.23 14.09	-6.562	4.429	-0.510	98	0.611
PT	ASIS	36 64	F M	132.48 136.97	12.06 12.84	133.30 137.60	19.58 15.41	-9.685	0.709	-1.714	98	0.090

where n = sample size, SD = standard deviation, IQR = interquartile range, CI = confidence interval, t or Z = test statistic or Z value for skewed data, df = degrees of freedom, F = female, M = male; significant differences (p ≤ 0.05) between groups are highlighted in grey, not normally distributed measurements are highlighted in blue. Note: Mann-Whitney value for 40mm – IIN = 610.000, 40mm – LFCN = 1027.000, 40mm – FA = 821.000, 40mm – FN = 928.500, ASIS – IHN = 989.000, ASIS – IIN = 615.000, ASIS – LFCN = 1060.000, ASIS – FN = 855.000, ASIS – ASIS = 784.000, PT – SEV = 492.000.

4.1.5 Difference between BMI (underweight, healthy, overweight/obese)

The cadaver sample was divided into three different BMI categories, namely underweight (BMI < 18.5 kg/m^2), healthy (18.5 kg/m^2 ≥ BMI < 25 kg/m^2) and overweight (BMI ≥ 25 kg/m^2). For six cadavers (n = 6), BMI was unavailable thus those cadavers were excluded from this analysis. A *Kruskal-Wallis test* was performed to investigate the influences of BMI on the measurements taken.

In general, the overweight category was found to have larger distances with 90% and 70% of all measurements on the left and right, respectively.

On the left side, significant differences were found from the IRTR to the IIN, LFCN, SC, SEV, FV, FA and FN. In contrast, on the right side no significant differences were found. The results are indicated below in Table 4.5. In the pooled measurements, a significant difference was found for the distance between the PT and the IIN, LFCN, FA and FN as indicated in Table 4.6. Furthermore, the measurement between ASIS – ASIS was found to be significant.

Table 4.5: Left and right side analysis for test of difference between three BMI categories

Measurement Origin	Measurement To	Side	Underweight n	Underweight MR	Underweight Mean	Underweight SD	Underweight Median	Underweight IQR	Healthy n	Healthy MR	Healthy Mean	Healthy SD	Healthy Median	Healthy IQR	Overweight n	Overweight MR	Overweight Mean	Overweight SD	Overweight Median	Overweight IQR	Kruskal Wallis H	df	Sig.
40mm	IHN	L	19	22.11	43.89	14.55	47.40	30.14	16	23.69	46.75	16.53	50.06	28.53	8	18.38	40.81	11.01	45.46	18.24	0.957	2	0.620
		R	19	20.00	35.45	13.59	33.21	17.55	15	21.67	40.37	20.47	35.71	30.52	8	24.75	39.87	9.30	38.07	5.63	0.848	2	0.654
IRTR	IHN	L	19	18.95	17.36	8.26	14.64	5.79	16	22.25	17.10	5.18	16.87	6.12	8	28.75	25.04	12.03	25.05	22.24	3.441	2	0.179
		R	19	22.00	13.81	6.28	14.64	6.78	16	19.88	13.57	7.50	11.14	10.96	8	26.25	17.10	7.47	17.42	14.38	1.375	2	0.503
	IIN	L	19	18.03	26.56	9.20	25.65	12.51	17	23.12	29.86	10.10	30.10	13.59	8	31.81	37.49	9.87	38.18	14.96	6.549	2	**0.038**
		R	19	19.89	18.17	7.20	16.32	11.44	17	24.18	20.63	7.68	18.28	11.82	8	25.13	21.40	8.47	21.97	14.63	1.405	2	0.495
	LFCN	L	19	16.47	98.20	14.77	94.68	19.07	17	23.94	106.47	10.99	105.20	20.21	8	33.75	116.77	10.42	118.52	13.91	10.532	2	**0.005**
		R	19	19.32	93.16	13.30	94.14	22.64	17	23.12	97.02	10.13	97.10	11.10	8	28.75	103.48	11.57	106.08	21.96	3.101	2	0.212
	SCIV	L	15	13.83	125.45	17.97	118.36	28.57	14	21.54	139.83	21.51	139.45	36.09	7	22.43	140.62	20.09	140.44	42.49	5.079	2	0.079
		R	12	14.25	118.04	17.21	114.63	19.87	15	19.40	129.50	24.03	125.33	50.26	8	21.00	127.70	8.96	129.23	6.49	2.573	2	0.276
	SC	L	14	12.21	22.94	5.75	23.94	11.43	11	17.27	29.39	11.73	24.06	20.35	7	23.86	31.34	3.75	31.30	6.08	7.302	2	**0.026**
		R	14	13.57	18.09	4.20	17.71	6.67	11	20.91	22.92	6.35	23.20	8.58	7	15.43	19.02	5.55	19.05	6.62	3.886	2	0.143
	SEV	L	16	13.19	31.96	15.04	35.05	26.62	11	18.73	41.19	14.36	37.01	20.44	6	24.00	47.26	8.52	50.65	12.89	5.983	2	**0.050**
		R	15	12.60	29.29	10.38	31.81	17.09	9	15.22	33.22	8.04	32.20	11.10	5	21.80	39.26	5.40	40.32	9.40	4.387	2	0.112
	FV	L	19	17.68	42.26	9.52	43.69	13.55	17	23.71	48.08	10.81	46.99	18.38	8	31.38	52.81	8.80	49.85	14.38	6.639	2	**0.036**
		R	19	19.26	33.80	5.31	33.68	11.11	17	26.35	37.36	7.26	35.89	9.54	8	22.00	34.52	6.64	34.09	6.96	2.748	2	0.253
	FA	L	19	17.24	52.03	9.94	52.20	14.44	17	23.18	57.34	10.71	56.61	18.29	8	33.56	64.95	7.94	62.83	14.20	9.171	2	**0.010**
		R	19	18.26	42.73	5.62	43.62	8.30	17	26.12	47.00	6.97	46.71	11.07	8	24.88	44.70	7.82	46.55	7.77	3.689	2	0.158
	FN	L	19	17.37	63.27	10.35	63.04	14.59	17	23.35	68.75	10.72	67.68	17.76	8	32.88	77.57	9.93	74.78	16.45	8.326	2	**0.016**
		R	19	17.76	53.09	6.60	53.20	10.00	17	26.00	58.47	7.64	58.59	8.28	8	26.31	57.47	8.35	49.75	7.48	4.551	2	0.103

where n = sample size, MR = mean rank, SD = standard deviation, IQR = interquartile range, df = degrees of freedom; significant differences ($p \leq 0.05$) between groups are highlighted in grey, not normally distributed measurements are highlighted in blue.

Table 4.6: Pooled analysis for test of difference between BMI categories

Measurement Origin	To	Underweight n	MR	Mean	SD	Median	IQR	Healthy n	MR	Mean	SD	Median	IQR	Overweight n	MR	Mean	SD	Median	IQR	Kruskal Wallis H	df	Sig.
40mm	IIN	38	44.11	59.42	18.83	62.66	31.04	32	41.50	56.95	24.31	61.42	48.11	16	46.06	61.95	18.62	61.18	26.99	0.396	2	0.820
	LFCN	38	45.80	38.45	13.64	35.46	20.75	34	45.50	37.51	11.29	34.96	19.53	16	39.28	34.60	9.48	32.35	17.49	0.819	2	0.664
	SCIV	28	32.07	19.20	7.29	19.95	11.05	24	35.25	20.73	6.17	20.40	9.01	13	30.85	19.39	6.82	17.74	9.91	0.576	2	0.750
	SC	26	29.15	120.82	11.58	124.92	22.07	18	25.61	117.13	13.14	118.49	12.23	12	31.42	123.55	12.61	120.54	25.75	0.990	2	0.609
	FV	38	45.64	104.47	7.77	105.28	12.61	34	41.93	103.01	9.76	101.68	11.84	16	47.25	106.08	10.46	104.11	12.72	0.607	2	0.738
	FA	38	48.64	92.15	7.54	92.48	9.68	34	39.54	89.60	8.71	90.43	8.27	16	45.19	92.28	11.60	90.24	11.79	2.291	2	0.318
	FN	38	48.08	80.77	6.93	81.91	10.73	34	41.29	78.55	8.61	78.21	9.33	16	42.81	79.35	9.79	78.58	10.45	1.351	2	0.509
ASIS	IHN	38	41.84	30.55	14.70	27.82	24.06	31	43.65	32.32	16.97	25.67	24.10	16	44.50	30.02	8.57	30.77	7.67	0.164	2	0.921
	IIN	38	44.50	49.13	19.30	50.64	31.62	32	39.97	45.00	23.03	47.35	42.09	16	48.19	52.69	20.04	55.60	25.71	1.265	2	0.531
	LFCN	38	46.01	29.57	13.79	28.52	20.54	34	42.68	27.32	10.98	26.34	14.81	16	44.78	27.39	7.49	26.63	11.64	0.308	2	0.857
	SCIV	28	36.43	22.43	9.60	21.59	11.83	25	27.08	17.73	7.19	16.87	13.67	13	39.54	23.05	5.08	22.43	7.07	4.734	2	0.094
	SC	26	26.92	109.71	12.81	113.39	20.13	17	27.76	110.92	13.43	110.80	14.12	12	30.67	113.32	13.15	113.29	25.89	0.454	2	0.797
	FV	38	47.00	93.91	8.88	95.15	13.62	34	39.03	90.61	10.27	90.34	9.90	16	50.19	96.69	12.55	93.17	15.17	2.716	2	0.257
	FA	38	48.74	81.19	8.18	82.07	10.98	34	37.25	77.21	8.22	77.44	10.15	16	49.84	82.18	10.88	81.31	13.61	4.483	2	0.106
	FN	38	47.95	69.92	7.51	70.17	9.68	34	39.50	66.59	9.24	68.43	11.05	16	46.94	69.87	9.23	70.22	9.16	2.140	2	0.343
	ASIS	38	36.87	246.81	25.51	243.13	30.74	34	47.85	256.45	20.65	250.60	24.88	16	55.50	271.24	58.07	280.83	68.28	6.946	2	**0.031**
IRTR	PT	38	45.61	30.17	7.88	30.87	11.48	34	44.03	30.33	11.81	30.12	14.37	16	42.88	29.59	7.30	28.48	10.96	0.147	2	0.929
PT	IHN	38	44.82	39.64	8.79	41.43	13.30	32	39.50	37.63	13.81	34.67	19.87	16	48.38	40.43	13.16	40.97	13.57	1.537	2	0.464
	IIN	38	48.12	34.51	8.21	33.86	10.30	34	34.31	28.17	12.68	24.49	19.59	16	57.56	39.76	13.50	39.66	24.65	10.356	2	**0.006**
	LFCN	38	39.39	112.42	16.06	111.94	21.27	34	41.97	114.39	12.13	113.83	17.31	16	62.00	125.15	11.10	126.07	18.71	9.358	2	**0.009**
	SCIV	27	31.19	140.62	17.29	140.06	20.42	29	36.41	141.54	10.78	143.44	11.82	15	43.87	145.73	10.93	148.55	9.06	3.660	2	0.160
	SC	28	27.61	24.71	8.69	23.45	14.06	20	30.35	26.21	14.10	24.77	17.58	13	39.31	31.73	9.92	30.10	19.56	3.897	2	0.143
	SEV	32	27.88	47.46	15.13	50.28	22.86	21	34.24	53.80	14.45	52.29	20.22	11	42.64	59.81	12.61	65.17	20.66	5.418	2	0.067
	FV	38	38.38	44.50	8.38	43.91	13.02	34	46.07	47.69	7.72	46.14	12.07	16	55.69	49.84	5.75	49.90	7.31	5.377	2	0.068
	FA	38	37.97	57.06	9.05	58.78	14.70	34	43.85	60.47	9.17	58.30	10.41	16	61.38	64.58	5.74	64.72	5.72	9.483	2	**0.009**
	FN	38	37.89	69.99	9.98	72.37	16.54	34	43.97	73.48	9.60	72.92	11.74	16	61.31	78.74	5.57	80.14	8.87	9.984	2	**0.009**
	ASIS	38	41.71	30.17	7.88	30.87	11.48	34	43.66	134.16	12.10	134.86	17.88	16	52.91	140.07	11.39	140.38	10.10	2.222	2	0.329

where n = sample size, MR = mean rank, SD = standard deviation, IQR = interquartile range, df = degrees of freedom; significant differences (p ≤ 0.05) between groups are highlighted in grey, not normally distributed measurements are highlighted in blue.

The samples were not tested for the possible significant differences between ancestry (Black = 4; White = 46) and age (Age ≤ 50 = 5; Age > 50 = 45) with the measured distances as a result of the small sample sizes in the comparison groups which would not yield accurate results.

4.2 FRESH FROZEN CADAVER SAMPLE

4.2.1 Descriptive statistics

4.2.1.1 Straight hip

The fresh frozen cadaver sample consisted of two (n = 2) specimens, one female (n = 1) and one male (n = 1). Equivalent measurements were taken on both the formalin fixed and fresh frozen cadavers with the hips straight. Descriptive statistics for the fresh frozen sample with the hips straight are displayed below in Table 4.7.

Table 4.7: Descriptive statistics for straight fresh frozen cadaver measurements

Measurement Origin	To	n	Side	Mean	Minimum	Maximum	SD
40mm	IHN	2	L	26.56	20.56	32.93	8.75
		2	R	52.76	39.65	65.86	18.53
	IIN	2	L	70.91	69.29	72.53	2.29
		2	R	50.80	46.06	55.53	6.70
	LFCN	2	L	28.53	26.06	31.00	3.49
		2	R	29.29	27.66	30.92	2.31
	SCIV	1	L	32.56	-	-	-
		2	R	18.17	12.54	23.79	7.95
	SC	1	L	112.92	-	-	-
		1	R	115.45	-	-	-
	FV	2	L	106.38	104.31	108.44	2.92
		2	R	99.28	91.42	107.13	11.11
	FA	2	L	94.57	94.10	95.03	0.66
		2	R	89.28	84.22	94.34	7.16
	FN	2	L	85.86	80.59	91.12	7.45
		2	R	81.75	77.23	86.26	6.39
ASIS	IHN	2	L	38.30	15.84	60.76	31.76
		2	R	44.66	28.30	61.01	23.13
	IIN	2	L	66.76	60.93	72.59	8.24
		2	R	40.44	35.16	45.72	7.47
	LFCN	2	L	23.10	17.68	28.52	7.67
		2	R	18.96	18.10	19.82	1.22
	SCIV	1	L	38.00	-	-	-
		2	R	29.30	27.46	31.14	2.60
	SC	1	L	110.70	-	-	-
		1	R	106.95	-	-	-
	FV	2	L	100.42	96.14	104.70	6.05
		2	R	87.64	79.22	96.05	11.90
	FA	2	L	90.58	86.92	94.24	5.18
		2	R	78.57	72.92	84.21	7.98
	FN	2	L	79.22	70.51	87.92	12.31
		2	R	70.57	65.66	75.47	6.94
	ASIS	2	-	219.83	206.54	233.11	18.79
IRTR	IHN	2	L	21.20	16.01	26.39	3.54
		2	R	22.66	17.76	27.56	6.93
	IIN	2	L	18.16	15.66	20.66	3.54
		2	R	25.82	15.93	35.71	13.99
	LFCN	2	L	94.02	84.81	103.22	13.02
		2	R	92.69	84.07	101.30	12.18
	SCIV	1	L	136.48	-	-	-
		2	R	128.44	126.92	129.96	2.15
	SC	1	L	23.44	-	-	-
		1	R	17.33	-	-	-
	SEV	2	L	21.48	7.52	35.44	19.74
		2	R	14.36	12.79	15.93	2.22
	FV	2	L	41.43	39.30	43.56	3.01
		2	R	36.24	28.69	43.78	10.67
	FA	2	L	45.89	44.10	47.68	2.53
		2	R	43.96	41.05	46.86	4.11
	FN	2	L	53.63	47.38	59.88	8.84
		2	R	50.45	48.11	52.78	3.30
	PT	2	L	18.09	15.01	21.17	4.36
		2	R	23.00	20.34	25.66	3.76
PT	IHN	2	L	31.30	24.16	38.43	10.09
		2	R	44.45	40.53	48.36	5.54
	IIN	2	L	27.69	22.01	33.37	8.03
		2	R	38.99	31.93	46.04	9.98
	LFCN	2	L	106.38	95.74	117.02	15.05
		2	R	110.00	100.00	120.00	14.14
	SCIV	1	L	49.04	-	-	-
		2	R	146.41	142.92	149.90	4.94
	SC	1	L	28.06	-	-	-
		1	R	26.18	-	-	-
	SEV	2	L	41.68	34.54	48.81	10.09
		2	R	34.93	31.21	38.64	5.25
	FV	2	L	39.17	33.35	44.98	8.22
		2	R	34.99	34.36	35.61	0.88
	FA	2	L	47.31	40.99	53.62	8.93
		2	R	44.23	42.52	45.93	2.41
	FN	2	L	53.15	42.00	64.30	15.77
		2	R	53.25	48.99	57.50	6.02
	ASIS	2	L	121.89	118.34	125.43	5.01
		2	R	124.77	118.31	131.22	9.13

where n = sample size, SD = standard deviation, L = Left, R = Right. Note: where n = 1, the mean reflects the true value.

4.2.1.2 Flexed hip

To investigate whether hip position influences the anatomical structures' proximity to the implant, the specimens' hips were flexed > 45°. The descriptive statistics for these measurements are indicated below in Table 4.8.

Table 4.8: Descriptive statistics for flexed fresh frozen cadaver measurements

Measurement		n	Side	Mean	Minimum	Maximum	SD
Origin	To						
40mm	IHN	2	L	44.55	23.86	65.23	29.25
		2	R	53.37	41.20	65.54	17.21
	IIN	2	L	71.26	69.33	73.19	2.73
		2	R	50.98	47.36	54.59	5.11
	LFCN	2	L	28.94	26.30	31.58	3.73
		2	R	28.68	27.07	30.28	2.27
IRTR	IHN	2	L	73.95	46.94	100.95	38.19
		2	R	69.55	67.23	71.86	3.27
	IIN	2	L	51.38	41.68	61.07	13.71
		2	R	62.57	58.49	66.64	5.76
	LFCN	2	L	94.08	84.10	104.05	14.11
		2	R	92.77	85.63	99.91	10.10

where n = sample size, SD = standard deviation, L = Left, R = Right.

Due to the small sample size of the fresh frozen specimens, statistical analysis regarding the normality of the sample could not be accurately determined. The specimens' demographic data, including age, weight and height was unavailable. The ancestry of both cadavers was white, therefore no difference between ancestry could be determined. Furthermore, due to the limited sample size, potential differences associated between sex and sides of the specimen's statistical analysis could also not be determined.

4.2.2 Difference between hip positions (straight vs flexed)

A *Mann Whitney-U test* was run to establish whether hip position, either straight (180°) or flexed (> 45°) influences the distance measurements of the important nerves to the implant. As the formalin fixed specimens were too rigid, flexion of the hip could only be carried out with the fresh frozen cadaver specimens (n = 2). No statistically significant differences were found; however, the sample size was limited (n = 2). The results are reported in Table 4.9 and Table 4.10 below for the left and right sides, respectively.

Table 4.9: Left side analysis for test of difference between straight vs flexed hip positions

Measurement Origin	To	n	Leg position	Mean Rank	Mann Whitney-U	Z	Sig. [2*1-tailed]
40mm	IHN	2 2	Straight Flexed	3.00 2.00	1.000	-0.775	0.667
	IIN	2 2	Straight Flexed	3.00 2.00	1.000	-0.775	0.667
	LFCN	2 2	Straight Flexed	3.00 2.00	1.000	-0.775	0.667
IRTR	IHN	2 2	Straight Flexed	3.50 1.50	0.000	-1.549	0.333
	IIN	2 2	Straight Flexed	3.50 1.50	0.000	-1.549	0.333
	LFCN	2 2	Straight Flexed	2.50 2.50	2.000	0.000	1.000

where n = sample size, Z = Z value; significant differences (p ≤ 0.05) between groups are highlighted in grey.

Table 4.10: Right side analysis for test of difference between straight vs flexed hip positions

Measurement Origin	To	n	Leg position	Mean Rank	Mann Whitney-U	Z	Sig. [2*1-tailed]
40mm	IHN	2 2	Straight Flexed	2.50 2.50	2.000	0.000	1.000
	IIN	2 2	Straight Flexed	2.50 2.50	2.000	0.000	1.000
	LFCN	2 2	Straight Flexed	2.00 3.00	1.000	-0.775	0.667
IRTR	IHN	2 2	Straight Flexed	3.50 1.50	0.000	-1.549	0.333
	IIN	2 2	Straight Flexed	3.50 1.50	0.000	-1.549	0.333
	LFCN	2 2	Straight Flexed	2.50 2.50	2.000	0.000	1.000

where n = sample size, Z = Z value; significant differences (p ≤ 0.05) between groups are highlighted in grey.

A statistical comparison between the formalin fixed and fresh frozen sample could not accurately be conducted. This was as a result of a very small sample for the fresh frozen sample (n = 2) and a much larger sample for the formalin fixed sample (n = 50).

4.3 INTRA- AND INTER- OBSERVER RELIABILITY

To determine the reliability of the measurements conducted, intra- and inter-observer reliability were determined with the use of interclass correlation coefficients (ICC). The ICCs were determined for 10% of the sample (n = 5 for formalin fixed) using an independent observer to ensure accuracy.

It was found that majority of the ICCs, 90.54% were greater than 0.9, therefore a high reliability can be concluded. Lower ICC values were found for the distances between the SCIV to both the 40 mm cortical screw and ASIS bilaterally, and FN to both the IRTR and PT on the right. Further inconsistencies were found between the LFCN – 40mm, FV – ASIS and IRTR – PT. The ICC results are indicated in Table 4.11. ICC values are not reported for the fresh frozen sample due to the limited sample size (n = 2) which is a limitation of the study.

Table 4.11: Interclass correlation coefficients for the formalin fixed sample

Measurement Origin	To	n	Side	ICC	95% CI Lower	95% CI Upper
40mm	IHN	4	L	0.999	0.987	1.000
		4	R	0.997	0.956	1.000
	IIN	4	L	0.999	0.986	1.000
		5	R	0.992	0.928	0.999
	LFCN	5	L	0.998	0.980	1.000
		5	R	0.204	-6.645	0.917
	SCIV	5	L	0.262	-6.087	0.923
		3	R	-0.693	-65.032	0.957
	SC	3	L	0.916	-2.270	0.998
		3	R	0.997	0.890	1.000
	FV	5	L	0.999	0.987	1.000
		5	R	0.989	0.895	0.999
	FA	5	L	0.942	0.447	0.994
		5	R	0.977	0.777	0.998
	FN	5	L	0.990	0.906	0.999
		5	R	0.996	0.962	1.000
ASIS	IHN	4	L	0.997	0.957	1.000
		4	R	0.987	0.797	0.999
	IIN	4	L	0.998	0.974	1.000
		5	R	0.994	0.942	0.999
	LFCN	5	L	0.998	0.979	1.000
		5	R	0.987	0.871	0.999
	SCIV	5	L	-0.003	-8.635	0.896
		3	R	0.312	-25.822	0.982
	SC	3	L	0.997	0.882	1.000
		3	R	0.996	0.842	1.000
	FV	5	L	0.989	0.896	0.999
		5	R	0.664	-2.225	0.965
	FA	5	L	0.992	0.925	0.999
		5	R	0.980	0.806	0.998
	FN	5	L	0.985	0.853	0.998
		5	R	0.986	0.867	0.999
	ASIS	5	-	0.990	0.902	0.999
IRTR	IHN	4	L	0.946	0.164	0.996
		4	R	0.996	0.932	1.000
	IIN	4	L	0.998	0.975	1.000
		5	R	0.996	0.957	1.000
	LFCN	5	L	0.999	0.990	1.000
		5	R	0.993	0.937	0.999
	SCIV	5	L	0.999	0.992	1.000
		4	R	0.978	0.655	0.999
	SC	3	L	0.996	0.837	1.000
		3	R	0.904	-2.749	0.998
	SEV	3	L	0.999	0.976	1.000
		3	R	0.991	0.640	1.000
	FV	5	L	0.998	0.979	1.000
		5	R	0.948	0.504	0.995
	FA	5	L	0.991	0.915	0.999
		5	R	0.896	0.003	0.989
	FN	5	L	0.987	0.878	0.999
		5	R	-0.138	-9.931	0.882
	PT	5	L	-0.057	-9.150	0.890
		5	R	0.964	0.654	0.996
PT	IHN	4	L	0.826	-1.680	0.989
		4	R	0.985	0.775	0.999
	IIN	4	L	0.992	0.883	1.000
		5	R	0.927	0.298	0.992
	LFCN	5	L	0.998	0.977	1.000
		5	R	0.914	0.174	0.991
	SCIV	5	L	0.999	0.991	1.000
		4	R	0.975	0.614	0.998
	SC	3	L	0.996	0.836	1.000
		3	R	0.995	0.792	1.000
	FV	5	L	0.994	0.945	0.999
		5	R	0.994	0.942	0.999
	FA	5	L	0.972	0.734	0.997
		5	R	0.982	0.829	0.998
	FN	5	L	0.995	0.953	0.999
		5	R	-1.771	-25.612	0.712
	ASIS	5	L	0.986	0.864	0.999
		5	R	0.952	0.540	0.995

where n = sample size, ICC = interclass correlation coefficient, CI = confidence interval.

CHAPTER 5: MANUSCRIPT 1

TITLE: Establishing the safety of the lateral femoral cutaneous nerve when using the Bridging Infix for anterior pelvic fixation

5.1 ABSTRACT

BACKGROUND:

Established subcutaneous internal fixation techniques have shown reduced wound complications, better quality of life, and reduced pain. However, these techniques still have specific indications, contraindications, and complications. The most significant known complication for these techniques is injury of the lateral femoral cutaneous nerve (LFCN). A novel minimally invasive modified technique, the Bridging Infix, has been proposed to further assist in the reduction of the negative effects of anterior fixation of unstable pelvic fractures. The safety of the LFCN during the novel procedure is currently unknown. Therefore, the aim of the study was to determine the relationship between the Bridging Infix and the LFCN.

METHODS:

Fifty formalin-fixed cadaveric specimens (n = 50) and two fresh frozen cadaver specimens (n = 2) were utilized in the study. Any cadavers with evidence of previous pelvic or abdominal surgery, visible pelvic pathology, or pelvic damage were excluded from the study. The pelvic Bridging Infix was inserted by experienced orthopaedic surgeons as per the recommended technique guide. Superficial dissection of the surgical site was subsequently conducted and bilateral measurements of the distance between the LFCN and the implant as well as palpable bony landmarks were taken to determine safe zones for implant placement.

RESULTS:

In all cases the LFCN was identified coursing deep to the inguinal ligament. Therefore, during the implantation procedure of the Bridging Infix, the LFCN was not compromised and did not pose a significant risk of impingement. The minimum distance from the LFCN to the most proximal cortical screw was 18.00 mm. The mean distance from the most proximal screw to the LFCN was 37.97 mm (SD ± 12.20).

CONCLUSION:

The LFCN was not injured or impinged by the Bridging Infix in any of the cadaver specimens used in this study. Thus, the surgical procedure can be considered safe if layer by layer dissection is employed and the screws are directly inserted on the iliac crest, with no pressure being applied within three finger breadths medial to the anterior superior iliac spine (ASIS).

KEYWORDS: Bridging Infix, lateral femoral cutaneous nerve, anterior pelvic fixation, minimally invasive, anterior superior iliac spine, pubic tubercle

5.2 INTRODUCTION

Pelvic ring injuries account for approximately 8% of injuries in trauma cases (Mason *et al*., 2005; Moazzam *et al*., 2012; Hung *et al*., 2018), and between 0.3% - 6% of all fractures (Court-Brown & Caesar, 2006; Cole *et al*., 2012; Küper *et al.,* 2019). Although the prevalence of pelvic ring injuries is lower in comparison to other fractures, these injuries are known to have both high morbidity and mortality rates (Mason *et al*., 2005; Moazzam *et al*., 2012). Surgical interventions for anterior pelvic fixation have been well established. Established subcutaneous internal fixation techniques have shown reduced wound complications, better quality of life, and reduced pain. However, these techniques still have specific indications, contraindications and complications. The most significant known complication for these techniques is injury of the lateral femoral cutaneous nerve (LFCN).

The LFCN originates from the anterior rami of roots L2 - L3 of the lumbar plexus and (Moore *et al*., 2014; Drake *et al*., 2015; Tubbs *et al*., 2018) supplies the skin of the lateral and anterior thigh to the level of the knee (Drake *et al*., 2015). The LFCN comes out from the lateral border of the psoas major muscle where it then passes obliquely inferior across the iliacus muscle (Drake *et al*., 2015; Tubbs *et al*., 2018). The LFCN courses 20 - 30 mm inferomedial towards the ASIS where it passes deep to the inguinal ligament (Doklamyai *et al*., 2008; Drake *et al*., 2015). The LFCN enters the thigh region by piercing through the fascia lata inferior to the inguinal ligament (Tubbs *et al*., 2018).

De Ridder *et al*., (1999) reported that at least 25% of their sample population had a form of anatomical variation of the LFCN and this was further corroborated by Tubbs *et al*. (2018) who described the course of the LFCN to be particularly variable. Anatomical variations have been found in the nerves that contribute to the formation of the LFCN. In normal situations, the LFCN originates from L2 - L3, however, instances have been reported where it arises from L1 - L2 or L3 - L4 (Apaydin, 2015). This variation is supported by Anloague & Huijbregts, (2009) who reported that in four plexuses (11.8%), the LFCN originated from L1 - L2 and in one plexus (2.9%) it arose from only L2. Reinpold *et al*. (2015) published cases in which the LFCN had up to three sub-branches or bi-/trifurcations. They reported that the LFCN entered the abdomen 5 mm - 6 mm laterally (5%), 3 mm - 56 mm medially (95%), 10 mm cranially (10%), and 14 mm caudally (90%) to the ASIS using 58 cases (Reinpold *et al*., 2015). However, other publications have reported that the LFCN coursing superolateral to the ASIS in 2.9% - 4% of the samples (Aszmann *et al*., 1997; Mischkowshi *et al*., 2006).

The LFCN is at a potentially high risk for damage due to its variable course (Grossman *et al*., 2001; Ray *et al*., 2010). Damage can occur as a complication to several procedures, which include anterior pelvic surgeries (Ray *et al*., 2010). The LFCN is susceptible to injury and compression along its entire course; but injuries are most prevalent as the nerve exits the pelvis (Grossman *et al*., 2001). A common pathology associated with LFCN injury, a symptom complex known as meralgia paresthetica, can occur which manifests as loss of sensation, burning, pain or itching over the area that the LFCN supplies (Grossman *et al*., 2001; Grothaus *et al*., 2005; Ray *et al*., 2010; Tomaszewski *et al*., 2016).

A modified technique using an internal bridge plate and rod technique has been proposed by Dr Strydom and Dr Snyckers (2021). This technique combines the benefits of the pelvic bridge and open reduction internal fixation (ORIF) with the extra-pelvic fixation methods, with the aim of reducing known complications (Strydom & Snyckers, 2021). As the Bridging Infix follows the same course as the pelvic bridge, it is suspected that the incidence of LFCN injury would be similar to that of the pelvic bridge, thereby reducing a significant risk of the INFIX technique. However, the safety of the LFCN during the novel procedure is currently unknown. Therefore, the aim of the study is to determine the relationship between the Bridging Infix and the LFCN as well as a safe zone for implantation.

5.3 METHODS

The study sample consisted of fifty (n = 50) formalin fixed cadavers and two (n = 2) fresh frozen specimens dissected. The samples were obtained in accordance with the National Health Act no. 61 of 2003 (Ethical clearance: 182/2021). Cadavers with evidence of previous abdomino-pelvic surgeries, pathology or damage in the abdomino-pelvic region were excluded. The proximity of surrounding anatomical structures to the Bridging Infix was investigated through superficial dissections of the anterior abdomino-pelvic wall.

Prior to implanting the Bridging Infix, each plate-rod was externally contoured, by an orthopaedic surgeon, according to the curvature of each cadaver's pelvis using a dry articulated pelvis as a template. Naked eye visualisation was used to determine if the construct was adequately contoured as no imaging was available.

Both samples followed similar dissection procedures. With the cadaver in a supine position, the skin and subcutaneous tissue was reflected laterally and removed, respectively. A vertical incision was made ± 10 mm inferior to the ASIS, into the tensor fascia latae to expose the LFCN as it emerged from the inguinal ligament. Parts of the tensor fasciae latae were removed to fully expose the LFCN course. In cases where the nerve emerged as more than one branch, the most lateral branch was measured.

In the two different samples, the Bridging Infix implantation procedures differed. Due to the rigidity of the formalin fixed cadavers, it was deemed unfeasible to easily create a subcutaneous tunnel as required. Therefore, the implantation procedure was a modified version of the surgical technique guidelines as published by Strydom & Snyckers (2021). However, in the fresh frozen sample, it was decided to closely follow the surgical technique as the cadavers were flexible and best represented patients undergoing the surgical procedure.

In the fresh frozen specimens, the surgical implantation procedure was followed before dissection. Three surgical incisions were made. Two incisions for the lateral windows, extending from the ASIS, 40 mm along the iliac crest and a horizontal incision for the medial window ± 10 mm superior to the pubic symphysis. A subcutaneous tunnel was created between the medial and lateral windows. Kocher forceps were used to pull the plate-rod through the tunnel.

In both samples, the external oblique fascia was lifted off the iliac crest and the periosteum was cleaned off the iliac crest to create a bare area for fixation. The plate was placed on the bare area and secured using a standard set of cortical screws for definitive fixation (40 mm, 45 mm, 50 mm). To connect each plate-rod, a 5 mm connector rod was used with two rod-to-rod connectors (Figure 5.1).

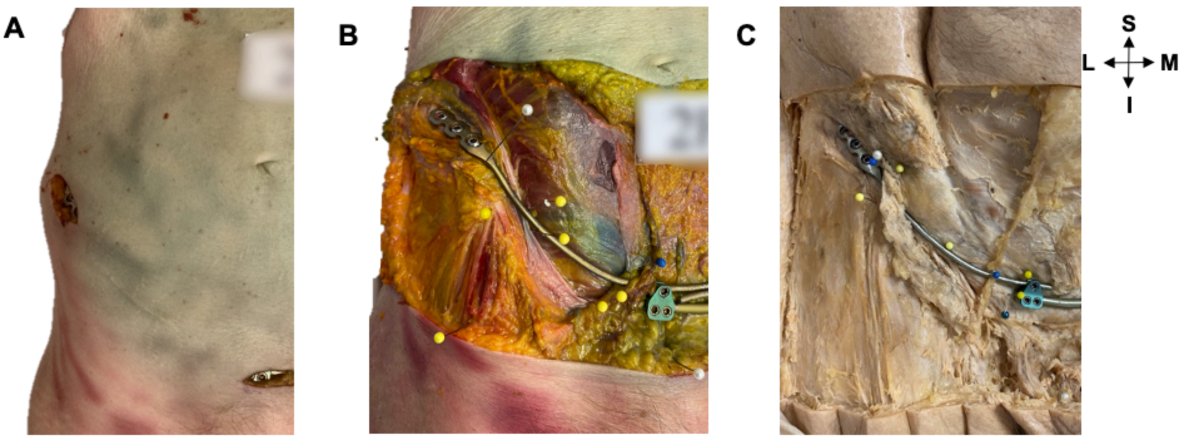

Figure 5.1: Bridging Infix implanted between the iliac crests and pubic symphysis on the right
A: Bridging Infix implanted in a fresh frozen cadaver prior to dissection; B: Bridging Infix implanted in a fresh frozen cadaver shown after dissection; C: Bridging Infix implanted in a formalin fixed cadaver.
Key: I- Inferior, L- Lateral, M-Medial, S- Superior.

Following the dissection and implantation procedures, the following distances were measured using a sliding mechanical calliper of 0.1 mm accuracy (Figure 5.2). Firstly, the distance from the midpoint of the most medial screw head (40 mm cortical screw) to the LFCN emergence at the inguinal ligament. Next, the distance between the ASIS and the LFCN emergence at the inguinal ligament was determined. Thirdly, a measurement was taken from the midpoint of the implant rod-to-rod connector single screw to the LFCN as it emerges from the inguinal ligament. Finally, the distance originating from the most prominent point of pubic tubercle to the LFCN emergence was measured. In addition, the distance between the ASIS and pubic tubercle was measured. All measurements were taken bilaterally and recorded for data analysis.

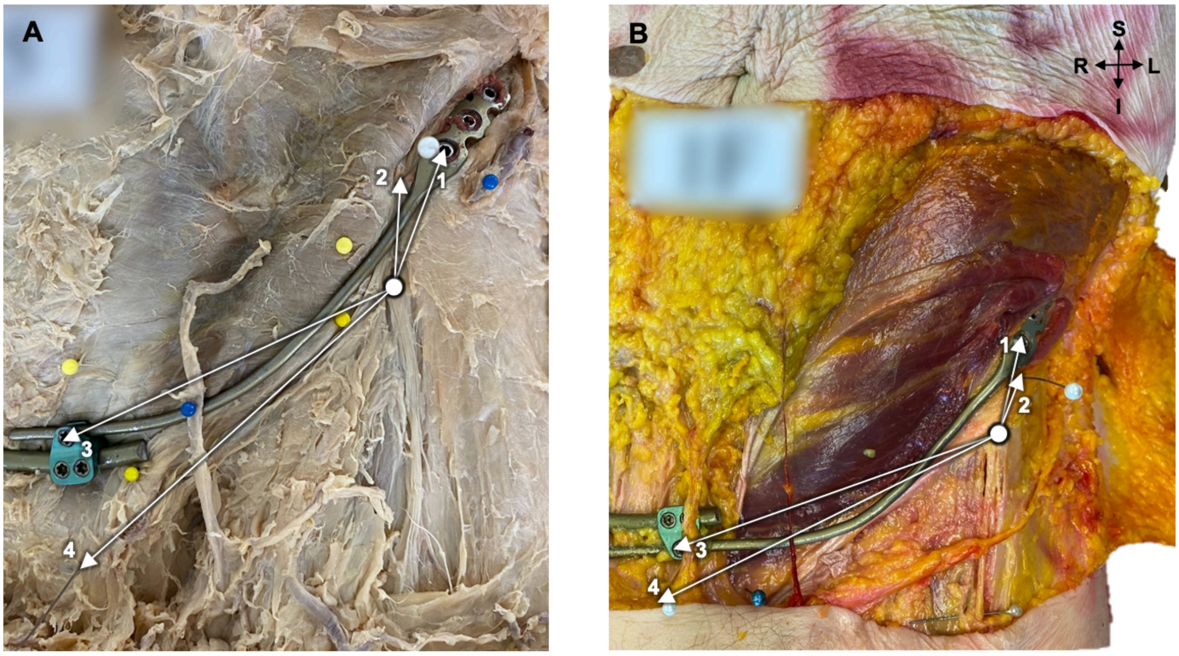

Figure 5.2: Cadaver images indicating the LFCN measurements of the right proximal thigh
A: Formalin fixed cadaver; B: Fresh frozen cadaver. (1) LFCN – 40mm cortical screw; (2) LFCN – ASIS; (3) LFCN – single rod-to-rod connector screw; (4) LFCN – PT.
Key: LFCN: lateral femoral cutaneous nerve, ASIS: anterior superior iliac spine, PT: pubic tubercle, royal blue pins indicate vascular structures, metallic blue pin indicates the spermatic cord, yellow pins indicate nerves, white pins indicate palpable bony structures.

In the fresh frozen cadaver sample (n = 4), additional measurements were recorded to determine if flexion of the hips (> 45°) influences the measurements taken. In order to accurately evaluate the impact flexion had on the measured distances, only one hip was flexed at a time. The following two distances were re-measured thereafter the distance from the 40 mm cortical screw head as well as the distance from the midpoint of the implant rod-to-rod connector single screw to the emergence of the LFCN from the inguinal ligament. The measurements were later analysed and compared to the same measurements taken with the hips straight.

Statistical analysis was conducted using *SPSS IBM Statistics* version 27. The data analysis included descriptive statistics and statistical tests. The samples were tested for normality, followed by a paired t-test or Wilcoxon signed rank test to test for differences between the left and right-side measurements . To test for differences between sex, a t-test was conducted for normally distributed data or a Mann Whitney-U test for skewed data. For testing difference in the BMI groups, a Kruskal Wallis test was performed. Furthermore, Mann Whitney-U tests were conducted for comparisons between the flexed and straight hips of the fresh frozen sample. A p-value ≤ 0.05 was considered statistically significant.

5.4 RESULTS

The LFCN was identified in all specimens (n = 52) on both the left and right sides. All measurements were determined to be normally distributed using a paired t-test. In order to determine if a difference exists between equivalent measurements taken on the left and right side of the cadavers, a paired t-test was performed in the formalin fixed sample only as a result of the small sample size of the fresh frozen sample. In the formalin fixed sample, a significant difference ($p < 0.05$) was only found between the measurements taken on the left and right side for the distance between the midpoint of the single rod-to-rod connecting screw and the LFCN emergence at the inguinal ligament. All the other measurements were determined to be analogous and therefore the measurements were pooled for further testing. The results are indicated below in Table 5.1.

The minimum distance, in the formalin fixed sample, from the midpoint of the 40 mm cortical screw head to the LFCN was 18.00 mm. In comparison, in the fresh frozen sample, the minimum distance was 26.06 mm and 27.07 mm on the left and right, respectively. The minimum distance from the LFCN to the single rod-to-rod connecting screw was 67.28 mm on the left and 74.07 mm on the right for the formalin fixed cadavers. However, in the fresh frozen cadaver sample, the minimum values were 84.10 mm and 84.07 mm on the left and right, respectively. The average distance between the ASIS – LFCN was found to be 28.77 mm for the formalin fixed sample and 23.10 mm on the left and 18.96 mm right for the fresh frozen specimens. Although the sample of fresh specimens was limited, based on the measurements taken there seems to be a large difference between them, but no inference can be made due to the small sample and should just be noted.

Table 5.1: Test for difference between LFCN on the left and right

Sample	Measurement Origin	n	Side	Mean	SD	99% CI Lower	99% CI Upper	p-value
Formalin fixed	40 mm Cortical screw	100	-	37.97	12.20	34.76	41.17	0.388
	ASIS	100	-	28.77	11.88	25.65	31.89	0.411
	Rod-to-rod connector screw	50	L	105.57	15.71	99.61	111.52	**0.000**
		50	R	96.04	11.79	91.57	100.50	
	PT	100	-	115.97	14.73	112.10	119.84	0.222
Fresh frozen	40 mm Cortical screw	2	L	28.74	2.96	20.09	37.38	-
		2	R	28.98	1.90	23.43	34.54	
	ASIS	2	L	23.10	7.67	-321.92	368.12	-
		2	R	18.96	1.22	-35.78	73.70	
	Rod-to-rod connector screw	2	L	94.05	11.08	61.68	126.41	-
		2	R	92.73	9.14	66.05	119.41	
	PT	2	L	106.38	15.05	-570.93	783.69	-
		2	R	110.00	14.14	-526.57	746.57	

where n = sample size, SD = standard deviation, CI = confidence interval, ASIS = anterior superior iliac spine, PT = pubic tubercle. (Grey highlight indicates statistically significant values p < 0.05).

An independent sample t-test was performed to determine if sex had an influence on the measurements taken in the formalin fixed cadaver sample. A significant difference was only determined for the measurements originating from the implant rod-to-rod connector single screw to LFCN emergence on the left ($p = 0.012$) and the pubic tubercle to the LFCN emergence pooled ($p = 0.002$). In both cases, males were found to have larger values in comparison to females. Although a smaller sample was available for the female group, it can be said that due to the sexual dimorphic differences between males and females, it is likely that some measurements may differ between the two groups.

The sample was divided into the three known BMI categories, namely underweight (BMI < 18.5; n = 19), healthy weight (18.5 ≥ BMI < 25; n = 17) and overweight or obese combined (BMI ≥ 25; n = 8). BMI values were unavailable for six (n = 6) of the cadaver specimens therefore they were excluded from this statistical analysis. A Kruskal-Wallis test determined there was a significant difference for the distance from the rod-to-rod connecting single screw to the LFCN emergence on the left side only with a p-value of 0.005 and BMI; with overweight cadavers having longer measurements. Furthermore, the pooled distance between the pubic tubercle and LFCN ($p = 0.009$) was found to have a significant influence by BMI where overweight/obese patients were found to have larger distances again.

In the fresh frozen sample, selected measurements were taken with the cadavers' hips in both a straight and flexed position. A Mann Whitney-U test was conducted to determine if flexion > 45° would influence the measurements taken. No significant difference ($p < 0.05$) was determined. Although the sample is small, it is possible to assume that flexion does not seem to influence the measurements taken. However, observations noted during the measurement process indicate that the LFCN was seen having slightly moved from the straight position to the flexed position.

Interclass correlation coefficients (ICC) were determined to ensure the reliability of results. ICC's were determined for each measurement. It was found that all ICC's were greater than 0.9, with a minimum of 0.914 and a maximum of 0.999. One distance, from the 40mm – LFCN on the right, was an exception with a ICC value of 0.204. Therefore, a decent intra- and inter-observer reliability was concluded.

5.5 DISCUSSION

The current study demonstrated that the use of Bridging Infix for anterior pelvic fixation did not pose a significant risk to the LFCN. The procedure, if the technique guide is followed (Strydom & Snyckers, 2022), can be considered at low risk to the LFCN.

The LFCN is currently the most prevalent structure mentioned in literature relating to anterior pelvic fixation (Cole *et al*., 2012; Hiesterman *et al*., 2012; Moazzam *et al*., 2012; Osterhoff *et al*., 2017; Reichel *et al*., 2018; Yin *et al*., 2019; Strydom & Snyckers, 2021). Knowledge of the LFCN location and variations is important, as this is the location where surgeons dissect during surgical procedures. Numerous studies have been published that relate the LFCN to the ASIS (Dibenedetto *et el*., 1996; Sürücü *et al*., 1997; Hospodar *et al*., 1999; Grothaus *et al*., 2005; Mischkowski *et al*., 2006; Bjurlin *et al*., 2007; Doklamyai *et al*., 2008; Ropars *et al*., 2009; Bodner *et al*., 2009; Ray *et al*., 2010; Majkrzak *et al*., 2010; Üzel *et al*., 2011). However, additional and more pertinent distances were needed in order to establish the safety of the Bridging Infix in this reference sample. With regards to the placement of the Bridging Infix, structures in close relation to the ASIS and iliac crest would be at risk. Furthermore, due to the medial window position, structures in close relation to the pubic tubercle may also be in danger during dissection.

A common pathology described in literature pertaining to the LFCN is meralgia paresthetica. Meralgia paresthetica can be described as pain, burning or dysesthesia in the anterolateral or lateral aspects of the skin of the thigh that the LFCN supplies (Grossman *et al*., 2001; Ropars *et al*., 2009; Majkrzak *et al*., 2010; Tomaszewski *et al*., 2016). A cause of this condition has been described as impingement or surgical iatrogenic injury to the LFCN (Majkrzak *et al*., 2010; Tomaszewski *et al*., 2016). Possible treatments include both conservative and surgical possibilities; however, the results are irregular (Ropars *et al*., 2009). Thus, to avoid injury, knowledge of the anatomy and variations of the LFCN is key. The current study further emphasises the conclusion that the LFCN is variable and thus surgeons should be aware of the different locations presented in literature.

During the Bridging Infix procedure, cortical screws are inserted into the iliac crest. As a result, measurements were conducted from the LFCN to the most medial cortical screw (40 mm) and the ASIS. The mean distance from the LFCN to the 40 mm cortical screw was 37.96 ± 12.20 mm with the distances ranging between 18.00 – 68.68 mm. When comparing this to the INFIX, Reichel *et al*., (2018) found that the pedicle screws may cause potential nerve injury as there was no safety margin in 90.9% of cadavers. As this study is the first anatomical study for the novel method, the LFCN distance to the medial cortical screw could not be compared to the literature.

In the specimens dissected, the LFCN never crossed over the ASIS or iliac crest. Instead, the nerve was observed emerging deep to the inguinal ligament, which is consistent with the findings of Doklamyai *et al*., (2008) and Üzel *et al*., (2011). Furthermore, the LFCN was only found medial to the ASIS, consistent with Hospodar *et al*., (1999), Ropars *et al*., (2009) and Üzel *et al*., (2011). Tomaszewski and co-authors (2016) conducted a review and concluded that in 1473 lower limbs, 86.8% of LFCN emerged deep to the inguinal ligament and medial to the ASIS as per the general course (Tomaszewski *et al*., 2016). In only 1.9% of the cases, did the nerve course over the ASIS or 2.4% through the ASIS (Tomaszewski *et al*., 2016). Only in these rare circumstances, would the LFCN be injured if the surgeons followed the surgical technique for the Bridging Infix.

The ASIS is easily palpable for surgeons to use as a landmark. During surgical procedures, the ASIS is used to assume the location of LFCN (Üzel *et al*., 2011). A general guideline that surgeons use to estimate the LFCN course is two finger breadths medial to the ASIS (Majkrzak *et al*., 2010). However, in the present study, 30% of the measurements lay within a range of 30 mm – 40 mm medial to the ASIS. Finger breadths vary; as the variation was similarly pointed out by Tomaszewski *et al*. (2016) who suggested a 30 mm average. Thus, an average rule of 40 mm or three finger breadths medial to the ASIS may be a better approximation taking the current studies measurement proportions into consideration.

The current study's findings regarding the distance between the ASIS and LFCNs emergence at the inguinal ligament are most consistent with those presented by Bjurlin *et al*., (2007), Bodner *et al*., (2009) and Üzel *et al*., (2011) as seen in Table 5.2. In the present study, the mean distance between the ASIS – LFCN was 28.77 ± 11.88 mm. However, other studies have reported smaller mean distances. The differences in measurements may be attributed to the fact that not all studies directly defined the exact position on the ASIS where their measurements were taken from. The mean comparisons between various studies are presented below in Table 5.2. Some of the studies mentioned in Table 5.2 reported the measurements in centimetres, but for the sake of the current study and comparative purposes, all measurements were converted to millimetres.

Table 5.2: Measurements for ASIS – LFCN emergence compared between studies

Study	Left			Right			Total		
	n	Mean	SD	n	Mean	SD	n	Mean	SD
Dibenedetto *et el*., (1996)							114	17	12
Sürücü *et al*., (1997)	22			22			44	15.2	8.4
Hospodar *et al*., (1999)							68	20.4	10.7
Grothaus *et al*., (2005)	14			15			29	36	20
Mischkowski *et al*., (2006)							34	14.6	
Bjurlin *et al*., (2007)							22	26	19
Doklamyai *et al*., (2008)							43	20	
Ropars *et al*., (2009)							34	21.1	
Bodner *et al*., (2009)	8	28	12	7	29	14			
Ray *et al*., (2010)	29	21.1	6.3	18	14.9	7.8	47	18.7	4.8
Majkrzak *et al*., (2010)								14	15
Üzel *et al*., (2011)	20	30.9	23.2	22	27.1	17.3	42	29.5	20.1
Current study, (2021)	**50**	**29.59**	**12.98**	**50**	**27.95**	**10.74**	**100**	**28.77**	**11.88**

where n= sample size, SD= standard deviation. (Grey highlighting indicates measurements ± 10 mm from current study).

Articles published by both Grothaus *et al*., (2005) and Ropars *et al*., (2009) concluded that a danger zone for LFCN injury exists extending along the lateral border of the sartorius muscle and along the inguinal ligament for the common trunk of the LFCN, reaching as far as 73 mm and 72 mm, respectively. Our data is comparable with a maximum value of 60.89 mm.

In a meta-analysis conducted by Tomaszewski *et al*. (2016), the authors reported the mean distance from the ASIS – LFCN as 19.0 mm using 1099 lower limbs from North American, South American, and European population groups. Further analysis revealed that the North American and European groups had mean distances of 23.1 mm and 23.2 mm, respectively. In comparison, South Americans had a shorter distance of 9.9 mm between the ASIS – LFCN. In the current sample, the average ASIS – LFCN distance was found to be the largest reported, 28.77 mm. Tomaszewski *et al*. (2016) suggested that geographical differences may result in measurement differences of the LFCN – ASIS. To the authors knowledge, no published studies have been conducted on the South African population regarding the LFCN location.

In the current study, the average distance from ASIS – PT was 135.35 ± 12.69 mm which is similar to findings reported by Majkrzak *et al*. (2010) as 124 ± 13 mm. Üzel *et al*. (2011) made similar findings with 131.1 ± 10.8 mm (129.8 ± 10.4 mm on the left; 132.3 ± 11.3 mm on the right) recorded.

Bjurlin *et al*. (2007) related the distance from the ASIS to the LFCN emergence at the inguinal ligament as a percentage of the distance between the ASIS and pubic tubercle as 19% ± 14%. Similarly, in the current study, the LFCN – ASIS distance was 21.24% ± 8.57% of the ASIS – PT distance. Üzel *et al*. (2011) also calculated the ratio for LFCN – ASIS/ASIS – PT to assist surgeons with patients of different body types. Üzel *et al*. (2011) found the ratio to be 0.22 ± 0.16 (0.24 ± 0.20 for the left and 0.20 ± 0.12 for the right) which corresponds to a ratio of 0.21 ± 0.09 in the current study. Thus, the LFCN can be found medial to the ASIS approximately one fifth of the distance between the ASIS – PT along the inguinal ligament.

Doklamyai *et al*. (2008) measured the distance between the LFCN – PT. On average, they reported the distance as approximately 110 mm in males and 100 mm in females (Range: 83 mm – 127 mm). This is equivalent to the 115.97 mm documented in the current study.

When comparing hip flexion ± 70° and the cadaver in a supine position, flexion did not seem to influence the measurements taken between the Bridging Infix and surrounding structures ($p > 0.05$). In contrast, Osterhoff *et al*., (2017) investigated 90° hip flexion using the INFIX which indicated that the LFCN was compressed in 75% - 80% of the samples. The INFIX is however fastened to the anterior inferior iliac spine (AIIS) (Yin *et al*., 2019) and does not fully align with the inguinal ligament. It can be hypothesized that the Bridging Infix does not compress the LFCN due to its alignment with the inguinal ligament.

In the fresh frozen sample, selected measurements were taken with the cadavers' hips in both a straight and flexed position. A Mann Whitney-U test was conducted to determine if flexion > 45° would influence the measurements taken. No significant difference ($p < 0.05$) was determined. Although the sample is small, it is possible to assume that flexion does not seem to influence the measurements taken. However, observations noted during the measurement process indicate that the LFCN was seen having slightly moved from the straight position to the flexed position.

Majkrzak *et al*., (2010) reported that fresh and formalin fixed specimen data sets were statistically equivalent in their study. This analysis could not be conducted in the present study as a result of the varying sample sizes.

5.6 CONCLUSION

Clinically, the variations of the LFCN are of importance. Various surgical approaches relating to anterior internal fixation would put the LFCN at risk. Surgeons should be aware that the LFCN, on average emerges 28.77 mm medial to the most prominent point of the ASIS along the inguinal ligament. This is equivalent to approximately one fifth the distance between the

ASIS – PT. In the current study, the LFCN was only seen emerging deep to the inguinal ligament. If the layer-by-layer dissection procedure, as described in the technique guide is adhered to, the surgeon should visualize the LFCN if it happens to cross over the ASIS. Thus, relating specifically to the Bridging Infix procedure, the LFCN can be considered to be a safe distance from the cortical screws when they are directly inserted into the iliac crest.

5.7 LIMITATIONS

Limitations in the study include the small sample size of the fresh frozen sample (n = 2). A larger sample size can be employed to run statistical analysis on the results. Variations in the measurements originating from the implant rod-to-rod connector were seen as this is not a stable point. Further research of the LFCN should be conducted in the South African population.

Complications can be avoided by strict surgical technique and advanced knowledge of the known variation prevalence. Furthermore, as Mischkowski *et al*., (2006) pointed out, if the surgeon employs layer by layer dissection down to the level of the periosteum of the iliac crest, only then can a possible LFCN variation where the nerve passes over the ASIS or iliac crest be avoided and preserved. In the case of the Bridging Infix procedure, this technique has already been employed and therefore is believed to reduce the risk of damage due to anatomical variations.

5.8 REFERENCES

Anloague, P.A. & Huijbregts, P. 2009. Anatomical variations of the lumbar plexus: a descriptive anatomy study with proposed clinical implications. *J Manual Manip Ther*, 17(4): e107-e114.

Apaydin, N. Variations of the lumbar and sacral plexuses and their branches. In: Tubbs, R.S., Rizk, E., Shoja, M.M., Loukas, M., Barbaro, N., Spinner, R.J., eds. Nerves and Nerve Injuries. Vol 1. San Diego: Elsevier; 2015: 614-617.

Aszmann, O.C., Dellon, E.S. & Dellon, A.L. 1997. Anatomical course of the lateral femoral cutaneous nerve and its susceptibility to compression and injury. *Plast Reconstr Surg*, 100: 600-604.

Bjurlin, M.A., Davis, K.E., Allin, E.F. & Ibraheim, D.T. 2007. Anatomic variations in the lateral femoral cutaneous nerve with respect to pediatric hip surgery. *Am J Orthop*, 36(3): 143-146.

Bodner, G., Bernathova, M., Galiano, K., Putz, D., Martinoli, C. & Felfernig, M. 2009. Ultrasound of the Lateral Femoral Cutaneous Nerve. *Reg Anesth Pain Med*, 34: 265-268.

Cole, P.A., Gauger, E.M., Anavian, J., Ly, T.V., Morgan, R.A. & Heddings, A.A. 2012. Anterior pelvic external fixator versus subcutaneous internal fixator in the treatment of anterior ring pelvic fractures. *J Orthop Trauma*, 26(5): 269-277.

Court-Brown, C.M. & Caesar, B. 2006. Epidemiology of Adult Fractures: A Review. *Injury*, 37(8): 691–697. Doi: 10.1016/j.injury.2006.04.130.

de Ridder, V.A., de Lange, S. & Popta, J.V. 1999. Anatomical variations of the lateral femoral cutaneous nerve and the consequences for surgery. *J Orthop Trauma*, 13(3): 207-211.

Dibenedetto, L.M., Lei, Q., Gilroy, A.M., Hermey, D.C., Marks, S.C. & Page, D.W. 1996. Variations in the inferior pelvic pathway of the lateral femoral cutaneous nerve: Implications for laparoscopic hernia repair. *Clin Anat*, 9: 232-236.

Doklamyai, P., Agthong, S., Chentanez, V., Huanmanop, T., Amarase, C., Surunchupakorn, P. & Yotnuengnit, P. 2008. Anatomy of the lateral femoral cutaneous nerve related to inguinal ligament, adjacent bony landmarks and femoral artery. *Clin Anat*, 21: 769-774.

Drake, R.L., Vogl, A.W. & Mitchell, A.W.M. 2015. Gray's Anatomy for Students. 3rd ed. Philadelphia: Churchill Livingstone Elsevier, 398-401.

Grossman, M.G., Ducey, S.A., Nadler, S.S. & Levy, A.S. 2001. Meralgia Paresthetica: Diagnosis and Treatment. *J Am Acad Orthop Surg*, 9: 336-344.

Grothaus, M.C., Holt, M., Mekhail, A.O., Ebraheim, N.A. & Yeasting, R.A. 2005. Lateral Femoral Cutaneous Nerve: An Anatomic Study. *Clin Orthop Relat Res*, 437: 164-168.

Hiesterman, T., Hill, B. & Cole, P. 2012. Surgical technique: A percutaneous method of subcutaneous fixation for the anterior pelvic ring: The Pelvic Bridge. *Clin Orthop Relat Res*, 470(8): 2116-2123.

Hospodar, P.P., Ashman, E.S. & Traub, J.A. 1999. Anatomic study of the lateral femoral cutaneous nerve with respect to the ilioinguinal surgical dissection. *J Orthop Trauma*, 13(1): 17-19.

Hung, C., Wu, J., Li, Y., Cheng, Y., Wu, C., Shen, H. & Yeh, T. 2018. Minimally Invasive Treatment for Anterior Pelvic Ring Injuries with Modified Pedicle Screw-Rod Fixation: A Retrospective Study. *J Orthop Surg Res*, 13(1): 1–8. Doi: 10.1186/s13018-018-0945-4.

Küper, M.A., Trulson, A., Stuby, F.M. & Stöckle, U. 2019. Pelvic ring fractures in the elderly. EFORT Open Rev, 4: 313-320. Doi: 10.1302/2058-5241.4.180062.

Majkrzak, A., Johnston, J., Kacey, D. & Zeller, J. 2010. Variability of the lateral femoral cutaneous nerve: an anatomic basis for planning safe surgical approaches. *Clin Anat*, 23: 304-311.

Mason, W.T.M., Khan, S.N., James, C.L., Chesser, T.J.S. & Ward, A.J. 2005. Complications of temporary and definitive external fixation of pelvic ring injuries. *Injury*, 36: 599-604.

Mischkowski, R.A., Selbach, I., Neugebauer, J., Koebke, J. & Zöller, J.E. 2006. Lateral femoral cutaneous nerve and iliac crest bone grafts- anatomical and clinical considerations. *Int J Oral Maxillofac Surg*, 35: 366-372.

Moazzam, C., Heddings, A.A., Moodie, P. & Cole, P.A. 2012. Anterior Pelvic Subcutaneous Internal Fixator Application: An Anatomic Study. *J Orthop Trauma*, 26(5): 263-268.

Moore, K.L., Dalley, A.F. & Aguir, A.M.R. 2014. Moore Clinically Orientated Anatomy. 7th ed. Philadelphia: Lippincott Williams & Wilkins, 186.

Osterhoff, G., Aichner, E.V., Scherer, J., Simmen, H., Werner, C.M.I. & Feigl, G.C. 2017. Anterior subcutaneous internal fixation of the pelvis – what rod-to-bone distance is anatomically optimal. *Injury*, 48: 2162-2168.

Ray, B., D'Souza, A.S., Kumar, B., Marx, C., Ghosh, B., Gupta, N.K. & Marx, A. 2010. Variations in the course and Microanatomical Study of the Lateral Femoral Cutaneous Nerve and Its Clinical Importance. *Clinl Anat*, 23: 978-984.

Reichel, L.M., MacCormick, L.M., Dugarte, A.J., Rizkala, A.R., Graves, S.C. & Cole, P.A. 2018. Minimally invasive anterior pelvic internal fixation: An anatomic study comparing Pelvic Bridge to INFIX. *Injury*, 49: 309-314.

Reinpold, W., Schroeder, M., Berger, C., Rohr, M. & Wehrenberg, U. 2015. Retroperitoneal anatomy of the iliohypogastric, ilioinguinal, genitofemoral and lateral femoral cutaneous nerve: consequences for prevention and treatment of chronic inguinodynia. *Hernia*, 19(4): 539-548.

Ropars, M., Morandi, X., Huten, D., Thomazeau, H., Berton, E. & Darnault, P. 2009. Anatomical study of the lateral femoral cutaneous nerve with special reference to minimally invasive anterior approach for total hip replacement. *Surg Radiol Anat*, 31: 199-204.

Strydom, S. & Snyckers, C.H. 2021. Minimally invasive subcutaneous anterior fixation of pelvic fractures in the elderly: Case report and literature review. *S Afr Orthop J*, 20(4): 240-245.

Sürücü, H.S., Tanyeli, E., Sargon, M.F. & Karahan, S.T. 1997. An anatomic study of the lateral femoral cutaneous nerve. *Surg Radiol Anat*, 19: 307-310.

Tomaszewski, K.A., Popieluszko, P., Henry, B.M., Roy, J., Sanna, B., Kijek, M.R. & Walocha, J.A. 2016. The surgical anatomy of the lateral femoral cutaneous nerve in the inguinal region: a meta-analysis. *Hernia*, 20: 649-657.

Tubbs, R.S., Loukas, M., & Hanna, A.S. 2018. Surgical Anatomy of the Lumbar Plexus. Thieme Medical Publishers, Incorporated, New York. Available from: ProQuest Ebook Central. [17 February 2021].

Üzel, M., Akkin, S.M., Tanyeli, E. & Koebke, J. 2011. Relationships of the lateral femoral cutaneous nerve to bony landmarks. *Clin Orthop Relat Res*, 469: 2605-2611.

Yin, Y., Luo, J., Zhang, R., Li, S., Jiao, Z., Zhang, Y. & Hou, Z. 2019. Anterior subcutaneous internal fixator (INFIX) versus plate fixation for pelvic anterior ring fracture. *Sci Rep*, 9(1): 2578-2578.

CHAPTER 6: MANUSCRIPT 2

TITLE: Establishing the safe use of the Bridging Infix method for anterior pelvic fixation in relation to neighbouring anatomical structures

6.1 ABSTRACT

BACKGROUND:

Numerous techniques for anterior pelvic fixation have been established. A novel minimally invasive subcutaneous anterior pelvic fixation technique has been proposed, termed the Bridging Infix. As this is a new modified method, the exact at-risk anatomical structures in close proximity to the implant are not known as yet. Therefore, the current study aimed to investigate the proximity of the implant to neighbouring structures as well as palpable bony landmarks for easy identification.

METHODS:

An anatomical investigation was performed using fifty (n = 50) formalin fixed cadaver specimens and two (n = 2) fresh frozen specimens. Dissections were carried out to identify and measure the proximity of the Bridging Infix to neighbouring anatomical structures including the iliohypogastric nerve (IHN), ilioinguinal nerve (IIN), superficial epigastric vessels (SEV), superficial circumflex iliac vessels (SCIV), spermatic cord and femoral neurovasculature (FV, FA, FN). Each structure was measured to standard points on the Bridging Infix and bony landmarks.

RESULTS:

The implantation of the Bridging Infix following the technique guide, did not violate any of the surrounding anatomical structures. The IHN and IIN were protected by abdominal musculature with a mean of 31.55 mm and 48.96 mm from the anterior superior iliac spine (ASIS), respectively. The spermatic cord was easily visualized and observed to not be compressed by any part of the implant. The SEV were found to occasionally course within the medial window field and the SCIV close to the ASIS and lateral window, but if injured it can usually be easily cauterized or ligated prior to further dissection. The femoral neurovasculature were found deep to the implant but a safe distance from injury with no seen compression.

CONCLUSION:

The hypothesized potentially at risk anatomical structures during the placement of the Bridging Infix were found to all be at no significant danger. It should be noted that the musculature surrounding the iliac crest needs to be fully retracted prior to definitive fixation of the plate-rod.

KEYWORDS:

Bridging Infix, anterior pelvic fixation, iliohypogastric nerve, ilioinguinal nerve, superficial epigastric vessels, superficial circumflex iliac vessels, spermatic cord, femoral neurovasculature.

6.2 INTRODUCTION

Minimally invasive internal fixation techniques have become more popular for fracture fixation (Scheyerer *et al*., 2014; Rommens *et al*., 2017; Steer *et al*., 2019). These techniques have a reduced rate of complications and provides equivalent fixation when compared to external fixation (Scheyerer *et al*., 2014; Cole *et al*., 2017). There is a reduced risk of surgical site infection, nursing care demands, and interference with daily activities as a result of the subcutaneous location of internal fixation (Steer *et al*., 2019). Numerous internal fixation techniques have been established and include both the INFIX and pelvic bridge.

The INFIX requires the placement of a pedicle screw along with a connecting rod from the anterior inferior iliac spines (AIIS) bilaterally (Reichel *et al*., 2018). However, potential drawbacks of this technique include the need for deep dissection and there is a potential risk of impingement or iatrogenic compression injuries to the surrounding neurovascular structures (Vaidya *et al*., 2012; Reichel *et al*., 2018). Moreover, Vaidya *et al*. (2018) completed a systematic review, with a patient sample size of 496, in which the complication findings included lateral femoral cutaneous nerve irritation in 26.3%, heterotopic ossification in 36%, infections in 3%, and femoral nerve palsy in 1%. Hesse *et al*. (2015) reported eight cases from six patients who developed femoral nerve palsies, either uni- or bi-laterally, with lasting effects after surgical removal. As the connecting rod does not follow static surrounding anatomic structures, which include the pubic symphysis, inguinal ligament and iliac crests, there is a risk of injury to the femoral neurovasculature or for the rod to be misaligned (Reichel *et al*., 2018).

The pelvic bridge involves the placement of a rod-plate construct that spans between the ipsilateral iliac crest and either the ipsilateral or contralateral pubic symphysis (Hiesterman *et al*., 2012). Stability is achieved through the fixation of the construct into the iliac crests and pubis (Hiesterman *et al*., 2012). A merit of the pelvic bridge is that it has been said that it can be applied to any type of physique (Cole *et al*., 2017). However, Cole *et al*. (2017) emphasised the need for the pelvic bridge procedure to be performed by experienced surgeons, or surgeons immensely familiar with pelvic anatomy. Cole *et al*. (2012; 2017) and Hiesterman *et al*. (2012) have also reported that the current practice is the removal of the implants after postoperative healing, as there is a lack of long-term outcomes for the construct.

A modified technique using an internal bridge plate and rod technique has been proposed by Dr Strydom and Dr Snyckers (2021). This novel approach aims to have the benefits of both established methods whilst reducing the risks associated with either (Strydom & Snyckers, 2021). The Bridging Infix combines the extra-pelvic fixation methods with the low-profile benefits of the pelvic bridge and open reduction with internal fixation (ORIF) (Strydom & Snyckers, 2021). The benefits of ORIF include no need for removal of the implant as well as anatomic reduction. However, despite ORIF providing the most rigid fixation construct, it has a high surgical morbidity rate (Vaidya *et al*., 2018). The Bridging Infix aims to reduce the risks of the INFIX and moreover, patient discomfort and neuropraxia are also aimed to be reduced in comparison (Strydom & Snyckers, 2021). The lack of medial fixation nullifies the risk of bladder injury when placing screws and allows the construct to be used in cases with medial pubic rami comminution; which would not allow for adequate screw purchase when compared to the pelvic bridge.

In a case study, the authors reported that the patient was able to mobilise quickly postoperatively. The patient was able to walk unaided and was pain free at the six-week follow-up (Strydom & Snyckers, 2021). At the one-year follow-up, the patient reported no discomfort and examinations showed a good bony union, thus the decision was made to not remove the implant (Strydom & Snyckers, 2021).

The anterior pelvis has various important structures coursing in close proximity to the bony pelvis. During internal fixation, some of these structures are at risk of injury. As the Bridging Infix is a new, modified technique, the exact at-risk structures are not known as yet. Therefore, this study investigated the anatomical relationship of the iliohypogastric nerve (IHN), ilioinguinal nerve (IIN), superficial epigastric vessels (SEV), superficial circumflex iliac vessels (SCIV), spermatic cord, femoral vein (FV), femoral artery (FA) and femoral nerve (FN) to the Bridging Infix and associated bony landmarks. Thereby, assisting clinicians by determining a safe-zone and reducing associated complications with anterior pelvic fixation.

6.3 METHODS

The samples used in this study consisted of fifty (n = 50) formalin fixed and two (n = 2) fresh frozen cadaver specimens. Ethical clearance was obtained from the Department of Anatomy, Faculty of Health Sciences, University of Pretoria, in accordance with the National Health Act no. 61 of 2003 (Ethical clearance: 182/2021). An orthopaedic surgeon performed the Bridging Infix implantation procedures, and the primary investigator completed all the dissections. Specimens were excluded if there was evidence of surgical intervention involving the abdominal or pelvic regions. Dissection, implantation and measurements were conducted with the cadavers in a supine position to determine the proximity of the Bridging Infix to neighbouring anatomical structures. The implantation method of the Bridging Infix closely resembled the technique guidelines of Strydom & Snyckers, (2022) (to be published) with minor modifications to allow for both the cadaver samples.

Prior to implantation, the Bridging Infix was contoured to align with the cadaver's iliac crest and pubic symphysis. No imaging was available, thus naked eye visualization was used to determine if the contours were sufficient.

6.3.1 Superficial and intermediate dissection

For this study, the skin was reflected laterally from the inferior aspect of the umbilicus to the inferior aspect of the pubic symphysis. The subcutaneous tissue was carefully dissected to preserve the superficial structures, namely the superficial epigastric vessels (SEV) (Figure 6.1; number 3) and superficial circumflex iliac vessels (SCIV) (Figure 6.1; number 4). Furthermore, the emergence of the spermatic cord from the superficial inguinal ring was identified in male cadavers (Figure 6.1; number 7).

Following the exposure of the superficial structures, dissection of the intermediate structures followed. This dissection included the removal of the external oblique aponeurosis and rectus sheath, and the reflection of the inferior fibres of the external oblique muscle superolaterally. The iliohypogastric nerve (IHN) (Figure 6.1; number 5) and ilioinguinal nerve (IIN) (Figure 6.1; number 6) were identified on the internal oblique muscle and their course was fully exposed.

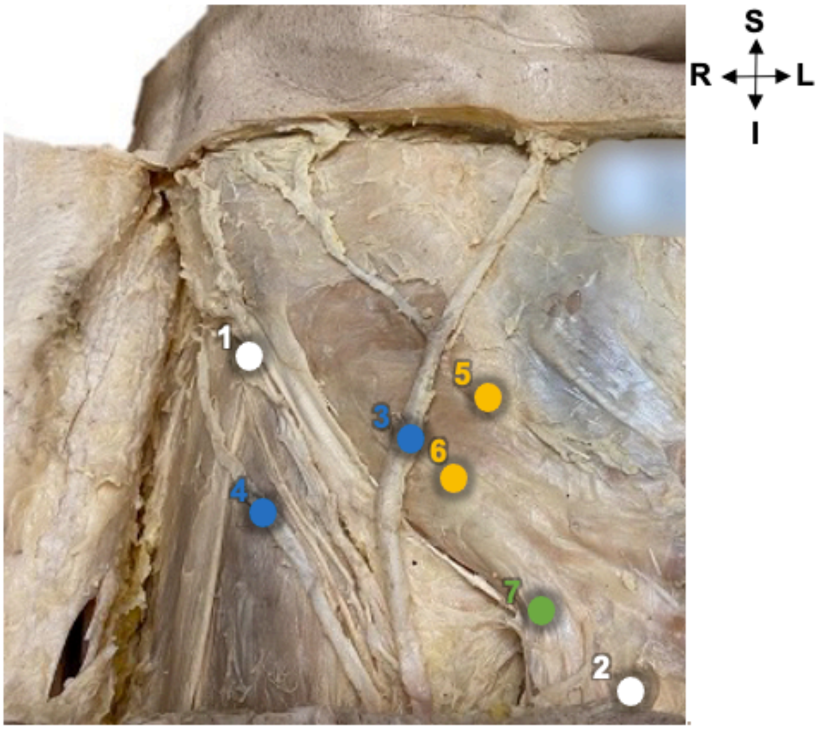

Figure 6.1: Superficial and intermediate dissection of the lower quadrant of the abdomen in a formalin fixed specimen
(1) ASIS; (2) PT; (3) SEV; (4) SCIV; (5) IHN; (6) IIN; (7) Spermatic cord.
Key: I- Inferior, L- Left, R- Right, S- Superior, ASIS- Anterior Superior Iliac Spine, PT- Pubic Tubercle, SEV- Superficial Epigastric Vessels, SCIV- Superficial Circumflex Iliac Vessels, IHN- Iliohypogastric nerve, IIN- Ilioinguinal nerve.

6.3.2 Implantation procedure

In the two different sample groups, the Bridging Infix procedures differed slightly. For the formalin fixed cadaveric sample, the superficial and intermediate dissection procedures were completed prior to implantation. This was done due to the rigidity of the cadaver tissue which resulted in it being impractical to easily create the subcutaneous tunnels required. In addition, no complications as a result of the implantation procedure were expected. However, in the fresh frozen cadaveric sample, it was decided to closely follow the surgical technique as the tissue was more pliable and best represented actual patients who would undergo the surgery.

In the fresh frozen specimens, the Bridging Infix surgical procedure was performed prior to anatomical dissection. Two incisions for the lateral windows were made extending from the ASIS 40 mm along the crest bilaterally and a third incision for the medial window approximately 10 mm superior to the pubic symphysis extending 60 mm – 80 mm. A Cobb elevator and blunt dissection were used to create a subcutaneous tunnel traversing between the medial and lateral windows. To pull the rod through the subcutaneous tunnel, Kocher forceps were used.

In both samples, visualisation was used to determine if the construct was adequately contoured as no imaging was available. A set of standard cortical screws (50 mm, 45 mm and 40 mm) were used on both sides for definitive fixation. A 5 mm connector rod was used with rod-to-rod connectors to connect each plate-rod (Figure 6.2).

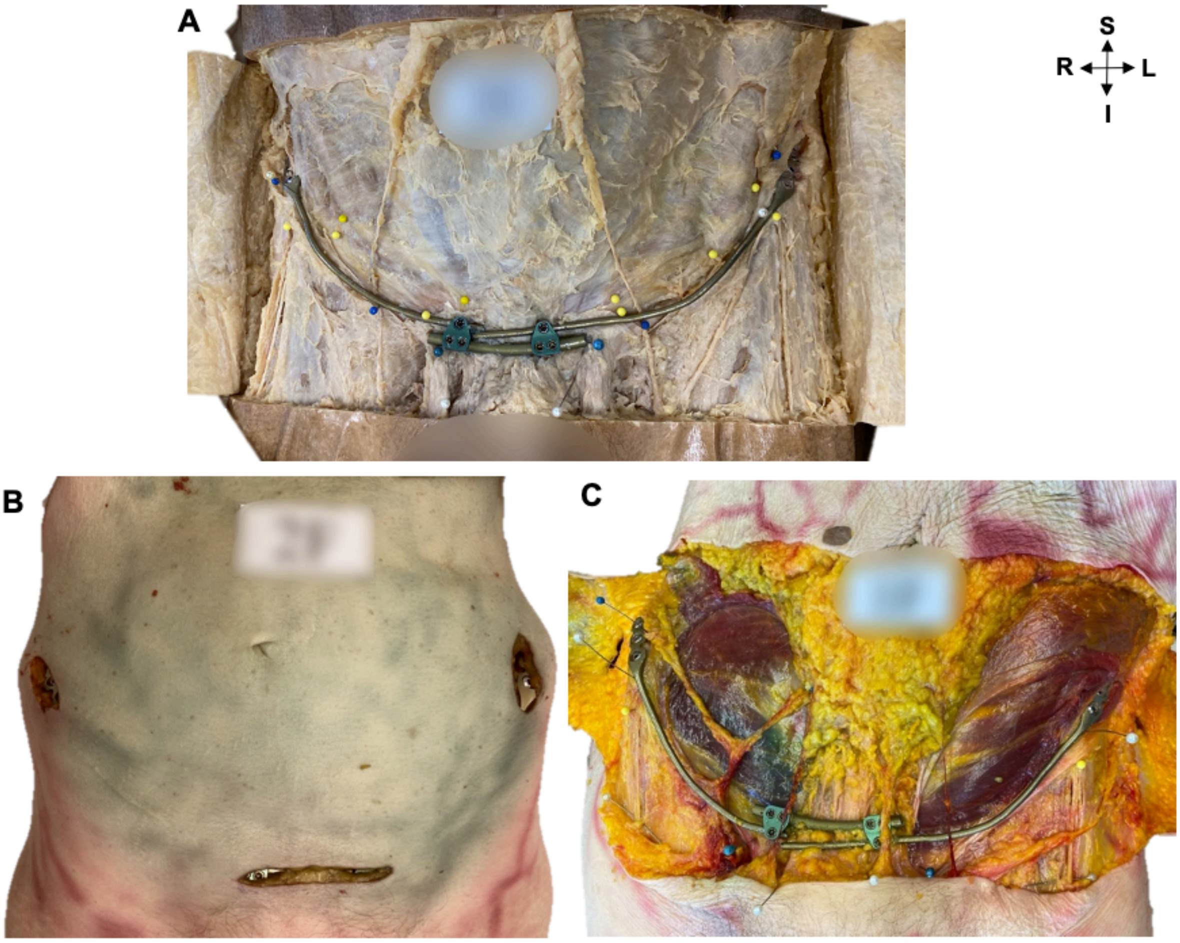

Figure 6.2: Bridging Infix implanted between the iliac crests and pubic symphysis
A: Bridging Infix implanted in a formalin fixed cadaver; B: Bridging Infix implanted in a fresh frozen cadaver prior to dissection; C: Bridging Infix implanted in a fresh frozen cadaver shown after dissection.
Key: I- Inferior, L- Left, R- Right, S- Superior.

6.3.3 Superficial measurements

In both cadaveric samples, measurements were taken using a sliding mechanical calliper of 0.1 mm accuracy. Each measurement originated at either a specific point of the implant (midpoint of the 40 mm cortical screw head or the midpoint of the implant rod-to-rod connector single screw) or at a specific bony landmark (ASIS or PT). Each measurement ended at a specific point of an anatomical structure coursing along (or in relation to) the implant.

Firstly, measurements were taken of the distance from the midpoint of the 40 mm cortical screw head to the closest point of IHN emergence from the internal oblique muscle (number 1), IIN emergence from the internal oblique muscle (number 3), SCIV course (number 4) and spermatic cord emergence from the inguinal canal (number 2) (Figure 6.3A). These measurements were repeated from the ASIS to each of the structures with the addition of the distance to the most prominent point of the pubic tubercle (number 5) (Figure 6.3A).

Secondly, the midpoint of the implant rod-to-rod connector single screw to the closest point of the IHN (number 1), IIN (number 3), SCIV at the ASIS (number 4), SEV as they pass superior to the Bridging Infix rod (number 6) and the spermatic cord emergence from the inguinal canal (number 2) (Figure 6.3B). These measurements were repeated from the most prominent point of the pubic tubercle to all of the above-mentioned structures with an additional measurement to the midpoint of the implant rod-to-rod connector single screw (number 7) (Figure 6.3B).

An osteological measurement from ASIS to ASIS was also taken to assist the surgeons with the implant procedure as well as to aid in determining a safe zone. In some cadavers, a few structures were damaged, cut or not found in the dissection procedure and therefore could not be measured.

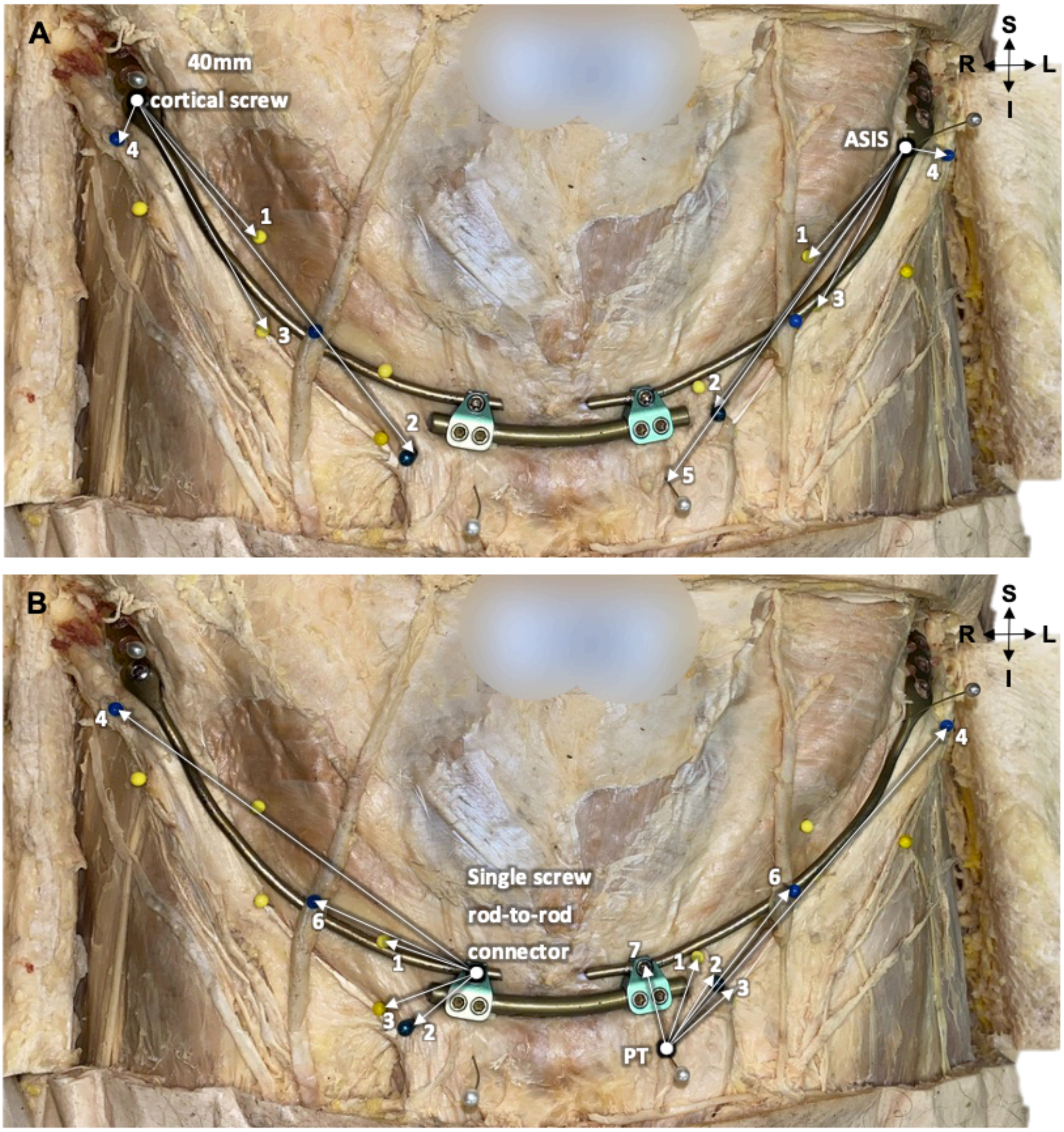

Figure 6.3: Formalin fixed cadavers indicating the superficial measurements conducted on the anterior abdominal wall

(A) Measurements originating laterally from either the ASIS or 40mm screw head; (B) Measurements originating medially from either the single rod-to-rod screw head or PT.

(1) IHN; (2) Spermatic cord; (3) IIN; (4) SCIV; (5) PT; (6) SEV; (7) Rod-to-rod connector single screw

Key: I- Inferior, L- Left, R- Right, S- Superior, ASIS- Anterior Superior Iliac Spine, PT- Pubic Tubercle, IHN- Iliohypogastric nerve, IIN- Ilioinguinal nerve, SCIV- Superficial Circumflex Iliac Vessels, SEV- Superficial Epigastric Vessels.

6.3.4 Deep dissection

All coverings of the femoral neurovascular structures were carefully removed to expose the femoral vein (FV), femoral artery (FA) and femoral nerve (FN) from their emergence below the inguinal ligament.

6.3.5 Deep measurements

After the deep dissections were completed, the following measurements were conducted. The measurements originated from one of the same four origins as the superficial structures, to the closest point of either the FV, FA or FN as they emerge deep to the inguinal ligament (Figure 6.4).

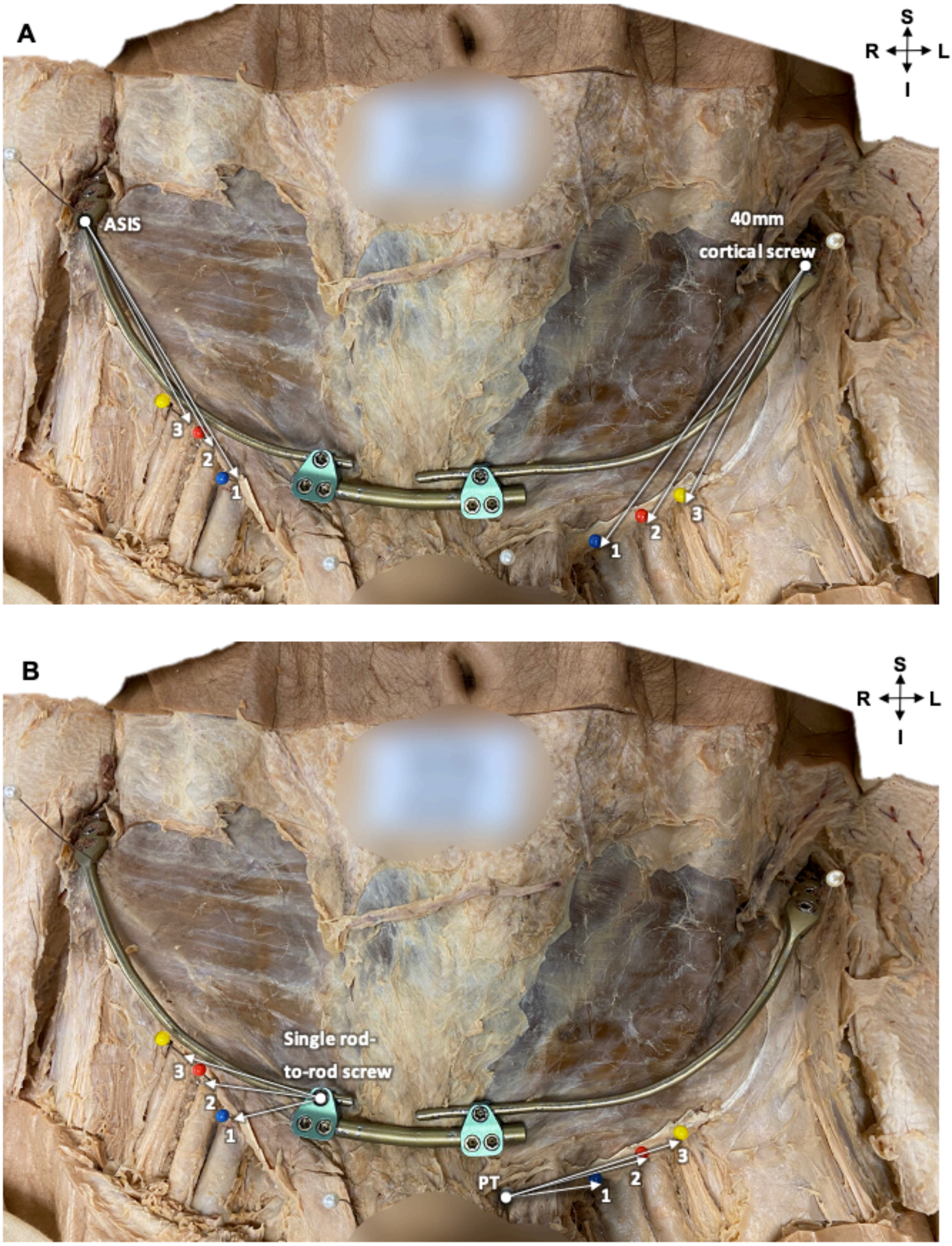

Figure 6.4: Formalin fixed cadavers indicating the deep measurements conducted on the anterior abdominal wall

(A) Measurements originating laterally from either the ASIS or 40 mm screw head; (B) Measurements originating medially from either the single rod-to-rod screw head or PT.

(1) FV; (2) FA; (3) FN.

Key: I- Inferior, L- Left, R- Right, S- Superior, ASIS- Anterior Superior Iliac Spine, PT- Pubic Tubercle, FV- Femoral Vein, FA- Femoral Artery, FN- Femoral Nerve.

6.3.5 Effect of flexion

To determine if flexion of the hips influences the measurements taken, the hips were flexed with a range of 69.30° - 71.33°. Hip flexion was performed one side at a time. Measurements were taken from the midpoint of the 40 mm cortical screw head and the midpoint of the implant rod-to-rod connector single screw to the two most important intermediate structures, IHN and IIN. Only the fresh frozen cadavers were included in the investigation as the formalin fixed cadavers were too rigid to easily flex the joints.

6.3.5 Statistical analysis

The data was evaluated for normality by using the Shapiro-Wilk test. Descriptive statistics were reported. Data was processed and compared using paired t-tests or either a Wilcoxon Signed Rank test or Mann Whitney-U test for non-parametric data. Data analysis was limited to the formalin fixed sample. A statistically significant difference was reported for p-values < 0.05. The *SPSS IBM Statistics* version 27 software was used to perform the data analysis.
To ensure the accuracy and repeatability of the results obtained from the study, intraclass correlation coefficients (ICC) were determined for 10% of the samples using an independent observer.

6.4 RESULTS

The anatomical structures surrounding the Bridging Infix were unaffected in all specimens. The femoral neurovascular structures were found in all specimens, but the IHN, IIN, SCIV or SEV were absent in a few. The spermatic cord was found in all male specimens. The SCIV were found to be the closest structures to the most proximal cortical screw (40 mm) with a minimum distance of 6.74 mm (mean: 20.31 ± 7.06 mm). The closest structure to the single screw of the rod-to-rod connectors was the IHN; approximately 5.40 mm and 3.14 mm on the left and right, respectively. Similarly, in the fresh frozen sample, the SCIV were closest in proximity to the 40 mm cortical screw on the right with 12.54 mm away (mean: 18.17 ± 7.95 mm) and the IHN on the left with 20.56 mm (mean: 26.56 ± 8.75 mm). In the fresh frozen sample, the SEV was found to be the shortest distance from the single screw of the implant rod-to-rod connector with a distance of 7.52 mm and 12.79 mm on the left and right, respectively. Both the IIN and spermatic cord were occasionally found directly coursing over the pubic tubercle in the formalin fixed specimens. Descriptive statistics for the formalin fixed and fresh frozen samples are reported in Table 6.1 and Table 6.2 respectively.

All measurements were tested for normality prior to statistical analysis. For further testing, non-parametric tests were used for the skewed measurements.

To assess whether a difference exists between equivalent measurements taken on the left and right side of the cadaver, a paired t-test or Wilcoxon signed rank test for skewed data was performed. A significant difference was found for all measurements originating from the implant single screw of the rod-to-rod connector, with the exception of the measurement to the pubic tubercle, indicating that the left and right-side measurements were different. Furthermore, a difference between left and right sides was detected for the measurement from the most proximal cortical screw to the IHN. No other statistically significant differences were detected. The results are indicated in Table 6.1 below.

Due to the small sample size of the fresh frozen specimens, statistical analysis regarding the normality of the sample could not be accurately determined. The specimens' demographic data, including age, weight and height were unavailable. Furthermore, due to the limited sample size, potential differences associated between sex and sides of the specimen's statistical analysis could also not be determined. The vast difference in the sample sizes of the formalin fixed and fresh frozen specimens resulted in no statistical analysis being reliable to determine if a difference exists between equivalent measurements taken on the different samples.

Table 6.1: Descriptive statistics and test of difference between left and right of the formalin fixed sample

Measurement Origin	Measurement To	Side	n	Mean	SD	Min	Max	99% CI Lower	99% CI Upper	Sig. [2-tailed]
Implant 40mm screw head	IHN	L	49	44.29	14.42	19.62	81.08	38.76	49.81	0.023
		R	48	38.14	15.71	10.86	81.25	32.05	44.23	
	IIN	L	50	61.96	21.05	23.99	97.62	53.98	69.94	
		R	48	57.20	19.68	16.60	90.02	49.58	64.83	0.140
		Total	98	59.63	20.43	16.60	97.62	54.21	65.05	
	SCIV	L	39	20.94	7.40	8.52	37.36	17.73	24.15	
		R	37	19.64	6.74	6.74	34.16	16.63	22.65	0.780
		Total	76	20.31	7.06	6.74	37.36	18.16	22.45	
	SC	L	31	120.45	12.23	86.89	141.92	114.41	126.49	
		R	30	122.47	11.04	98.11	142.79	116.92	128.02	0.604
		Total	61	120.50	11.96	86.89	141.92	116.46	124.54	
	FV	L	50	104.03	8.95	89.54	124.76	100.64	107.42	
		R	50	104.09	9.79	72.28	129.79	100.38	107.80	0.959
		Total	100	104.06	9.33	72.28	129.79	101.61	106.51	
	FA	L	50	90.77	9.77	73.03	116.29	87.06	94.47	
		R	50	90.85	8.25	63.40	114.20	87.72	93.98	0.490
		Total	100	90.81	9.00	63.40	116.29	88.44	93.17	
	FN	L	50	78.78	8.27	59.41	100.40	75.64	81.91	
		R	50	80.12	8.10	47.22	96.46	77.05	83.19	0.131
		Total	100	79.45	8.17	47.22	100.40	77.30	81.59	
ASIS	IHN	L	49	33.32	14.36	7.42	59.14	27.81	38.82	
		R	48	29.74	14.46	10.34	72.89	24.14	35.35	0.259
		Total	97	31.55	14.45	7.42	72.89	27.69	35.40	
	IIN	L	50	50.32	21.53	10.21	85.26	42.16	58.48	
		R	48	47.54	19.83	10.42	84.61	39.86	55.23	0.276
		Total	98	48.96	20.65	10.21	85.26	43.48	54.44	
	SCIV	L	40	21.26	8.32	2.45	43.08	17.70	24.82	
		R	37	20.53	7.48	4.16	35.96	17.19	23.87	0.970
		Total	77	20.91	7.88	2.45	43.08	18.54	23.28	
	SC	L	31	109.67	13.71	74.46	131.84	102.90	116.45	
		R	30	111.96	11.60	82.99	131.91	106.13	117.80	0.562
		Total	61	110.80	12.66	74.46	131.91	106.49	115.11	
	FV	L	50	93.02	10.25	76.28	119.61	89.13	96.90	
		R	50	92.36	10.16	58.46	116.02	88.51	96.22	0.618
		Total	100	92.69	10.16	58.46	119.61	90.02	95.36	
	FA	L	50	78.93	9.05	62.82	99.00	75.50	82.36	
		R	50	79.58	9.10	49.63	102.54	76.14	83.03	0.619
		Total	100	79.26	9.03	49.63	102.54	76.88	81.63	
	FN	L	50	67.93	8.77	51.18	89.18	64.61	71.26	
		R	50	68.78	8.47	35.74	84.20	65.57	71.99	0.503
		Total	100	68.36	8.59	35.74	89.18	66.10	70.61	
	ASIS	-	50	254.39	32.58	176.84	379.66	242.05	266.74	-
Implant single screw of rod-to-rod connector	IHN	L	49	19.48	8.90	5.40	44.82	16.07	22.89	0.000
		R	49	14.38	6.66	3.14	29.87	11.83	16.94	
	IIN	L	50	29.94	10.49	12.36	55.96	25.97	33.92	0.000
		R	50	20.08	7.56	7.12	37.38	17.22	22.95	
	SCIV	L	42	132.76	19.61	103.07	178.10	124.59	140.94	0.001
		R	40	123.54	18.87	92.64	166.51	115.46	131.61	
	SC	L	35	27.36	8.61	15.29	47.19	23.38	31.33	0.000
		R	35	19.88	5.38	10.23	35.97	17.40	22.36	
	SEV	L	38	37.31	14.64	7.55	65.20	30.86	43.75	0.032
		R	33	31.36	10.41	9.32	48.86	26.39	36.32	
	FV	L	50	47.07	10.22	27.57	66.47	43.20	50.95	0.000
		R	50	36.75	6.50	22.06	51.17	33.28	38.21	
	FA	L	50	57.35	10.73	36.09	77.41	53.29	61.42	0.000
		R	50	45.52	7.03	27.30	60.90	42.86	48.19	
	FN	L	50	68.57	11.32	45.98	93.90	64.28	72.86	0.000
		R	50	56.54	7.65	40.02	72.86	53.64	59.44	
	PT	L	50	29.95	8.34	14.67	50.63	26.79	33.11	
		R	50	31.24	10.15	5.78	53.28	27.39	35.08	0.111
		Total	100	30.59	9.26	5.78	53.28	28.16	33.03	
PT	IHN	L	49	39.86	11.21	15.46	65.50	35.56	44.15	
		R	49	39.34	11.87	12.58	61.52	34.79	43.89	0.931
		Total	98	39.60	11.48	12.58	65.50	36.55	42.65	
	IIN	L	50	33.30	11.34	13.83	60.64	29.01	37.60	
		R	50	35.57	11.47	0.00	51.75	28.22	36.92	0.608
		Total	100	32.94	11.35	0.00	60.64	29.96	35.92	
	SCIV	L	42	141.82	13.05	119.80	180.54	136.38	147.26	
		R	40	141.77	13.79	103.27	172.73	135.87	147.67	0.806
		Total	82	141.80	13.33	103.27	180.54	137.91	145.68	
	SC	L	34	27.67	8.06	16.51	46.43	23.89	31.44	
		R	33	25.93	13.65	0.00	56.49	19.42	32.43	0.214
		Total	67	26.81	11.11	0.00	56.49	23.21	30.41	
	SEV	L	38	50.84	14.96	20.42	76.64	44.25	57.43	
		R	35	53.24	15.41	8.01	74.36	46.13	60.35	0.279
		Total	73	51.99	15.12	8.01	76.64	47.31	56.67	
	FV	L	50	47.67	7.53	32.82	62.26	44.81	50.52	
		R	50	47.41	9.36	26.40	71.96	43.86	50.96	0.822
		Total	100	47.54	8.45	26.40	71.96	45.32	49.76	
	FA	L	50	61.00	8.98	44.36	78.92	57.60	64.40	
		R	50	60.72	10.07	37.46	85.30	56.90	64.54	0.811
		Total	100	60.86	9.49	37.46	85.30	58.37	63.35	
	FN	L	50	74.01	9.51	53.02	92.65	70.40	77.62	
		R	50	73.49	10.56	48.69	101.96	69.48	77.49	0.655
		Total	100	73.75	10.00	48.69	101.96	71.12	76.38	
	ASIS	L	50	135.07	12.87	104.06	161.80	130.19	139.95	
		R	50	135.63	12.63	106.92	162.58	130.85	140.42	0.231
		Total	100	135.35	12.69	104.06	162.58	132.02	138.68	

where n = sample size, L = left, R = right, SD = standard deviation, Min = minimum value, Max = maximum value, CI = confidence interval; significant differences (p ≤ 0.05) between groups are highlighted in grey.

Table 6.2: Descriptive statistics of the fresh frozen sample

Measurement Origin	Measurement To	Side	n	Mean	SD
Implant 40mm screw head	IHN	L	2	26.56	8.75
		R	2	52.76	18.53
	IIN	L	2	70.91	2.29
		R	2	50.80	6.70
	SCIV	L	1	32.56	-
		R	2	18.17	7.95
	SC	L	1	112.92	-
		R	1	115.45	-
	FV	L	2	106.38	2.92
		R	2	99.28	11.11
	FA	L	2	94.57	0.66
		R	2	89.28	7.16
	FN	L	2	85.86	7.45
		R	2	81.75	6.39
ASIS	IHN	L	2	38.30	31.76
		R	2	44.66	23.13
	IIN	L	2	66.76	8.24
		R	2	40.44	7.47
	SCIV	L	1	38.00	-
		R	2	29.30	2.60
	SC	L	1	110.70	-
		R	1	106.95	-
	FV	L	2	100.42	6.05
		R	2	87.64	11.90
	FA	L	2	90.58	5.18
		R	2	78.57	7.98
	FN	L	2	79.22	12.31
		R	2	70.57	6.94
	ASIS	-	2	219.83	18.79
Implant single screw of rod-to-rod connector	IHN	L	2	21.20	3.54
		R	2	22.66	6.93
	IIN	L	2	18.16	3.54
		R	2	25.82	13.99
	SCIV	L	1	136.48	-
		R	2	128.44	2.15
	SC	L	1	23.44	-
		R	1	17.33	-
	SEV	L	2	21.48	19.74
		R	2	14.36	2.22
	FV	L	2	41.43	3.01
		R	2	36.24	10.67
	FA	L	2	45.89	2.53
		R	2	43.96	4.11
	FN	L	2	53.63	8.84
		R	2	50.45	3.30
	PT	L	2	18.09	4.36
		R	2	23.00	3.76
PT	IHN	L	2	31.30	10.09
		R	2	44.45	5.54
	IIN	L	2	27.69	8.03
		R	2	38.99	9.98
	SCIV	L	1	49.04	-
		R	2	146.41	4.94
	SC	L	1	28.06	-
		R	1	26.18	-
	SEV	L	2	41.68	10.09
		R	2	34.93	5.25
	FV	L	2	39.17	8.22
		R	2	34.99	0.88
	FA	L	2	47.31	8.93
		R	2	44.23	2.41
	FN	L	2	53.15	15.77
		R	2	53.25	6.02
	ASIS	L	2	121.89	5.01
		R	2	124.77	9.13

where n = sample size, L = left, R = right.

To determine if sex had an influence on the measurements taken, a t-test for equality of means was performed for the normally distributed data. If data was skewed, a Mann Whitney-U test was conducted. For the pooled measurements, all measurements from the IIN and measurements from the 40 mm screw head – FV and ASIS to all femoral neurovasculature were found to be significantly different between males and females, with males having larger values. Furthermore, no distances on the right and the measurement on the left between the implant rod-to-rod single connecting screw to the IIN followed a normal distribution.

The cadaver sample was further divided into three different BMI categories, namely underweight (BMI < 18.5 kg/m^2), healthy (18.5 kg/m^2 ≥ BMI < 25 kg/m^2) and overweight (BMI

≥ 25 kg/m^2). For six cadavers (n = 6), BMI was unavailable, thus those cadavers were excluded from this analysis. A Kruskal-Wallis test was performed to determine if BMI influences the measurements taken. In general, the overweight category was found to have larger distances with 59.46% and 72.97% of all measurements on the left and right, respectively. On the left side, statistically significant influences were found for the implant rod-to-rod connector to the IIN, spermatic cord, SEV, FV, FA and FN. In contrast, on the right side no significant influences were found. For the pooled measurements, a significant difference was found for the measurements from the pubic tubercle to IIN, FA and FN as well as the ASIS – ASIS distance. Furthermore, overall for the significantly different measurements, the overweight category had the most influence.

A Mann Whitney-U test was run to establish whether hip position, either straight (180°) or flexed (> 45°) influences the distance measurements of the important nerves to the implant. As the formalin fixed specimens were too rigid, flexion could only be carried out with the fresh frozen cadaver specimens (n = 2). No statistically significant differences were found; however, the sample size was limited (n = 2).

Intra- and inter- observer reliability were determined with the use of interclass correlation coefficients (ICC). The ICCs were determined for 10% of each sample using an independent observer to ensure accuracy. It was found that the majority of all the ICCs were greater than 0.9 (90.54%), therefore a favourable reliability can be concluded.

6.5 DISCUSSION

The novel Bridging Infix approach aimed to have the benefits of both established methods, the INFIX and pelvic bridge, whilst reducing the risks associated with either. This study investigated the Bridging Infix relation to neighbouring anatomical structures and prominent bony landmarks in the area. The procedure did not put any of the neighbouring structures investigated in this study at risk. With observation, it was noted that no structures located deep to the Bridging Infix were compressed, however quantitative measurements are required. Therefore, the surgical technique can be considered a low risk if the musculature close to the fixation point is fully retracted away from the iliac crest and layer by layer dissection techniques are followed. It should be noted that the surgeons need knowledge of the course and relationship of the surrounding anatomical structures to the implant but also should be familiar with the distances to palpable bony landmarks in the vicinity.

The IHN and IIN were found emerging from the internal oblique muscle on the anterior abdominal wall 31.55 ± 14.45 mm and 48.96 ± 20.65 mm from the ASIS, respectively. Rahn *et al*. (2010) found the IHN 25 mm (range: 0 mm - 46 mm) and the IIN 25 mm (range: 11 mm

- 51 mm) medial to the ASIS, respectively. Another study conducted by Whiteside *et al*. (2003) reported the emergence of the IHN to be 21 ± 18 mm (range: -16 mm – 50 mm) and the IIN 31 ± 15 mm (range: 9 mm – 63 mm) medial to the ASIS. Mandelkov *et al*. (1988) presented similar results with the IHN (25.9 ± 7.3 mm) and IIN (30.8 ± 11.8 mm) in proximity to the ASIS, however described that the IIN penetrates the internal oblique muscle 40 to 50 mm medial to the ASIS which is similar to the findings of the current study. Moreover, consistent with the findings of the current study, Nahabedian & Dellon, (1997) reported the emergence of the IHN as approximately 30 mm medial to the ASIS. Part of the discrepancy in the distances may be attributed to the precise location on the ASIS where the measurements originated as also reasoned by Rahn *et al*. (2010).

The IHN and IIN are generally protected by the anterior abdominal musculature. As described in the literature, the IHN and IIN were only found once the external oblique muscle was reflected. Although, after dissection of a fresh frozen specimen, the primary investigator noted injury to the external oblique muscle, which occurred during surgical dissection. No other anatomical structures were injured; however, it should be emphasized that the surgeon should fully retract the musculature during the soft tissue dissection down to the iliac crest. It should be noted that injury to these nerves is unlikely as the Bridging Infix is placed subcutaneously and no musculature should be injured during the procedure. The IHN was found to be 23.86 mm from the midpoint of the 40 mm cortical screw, therefore, could be at risk of being severed if not fully retracted (Figure 6.5).

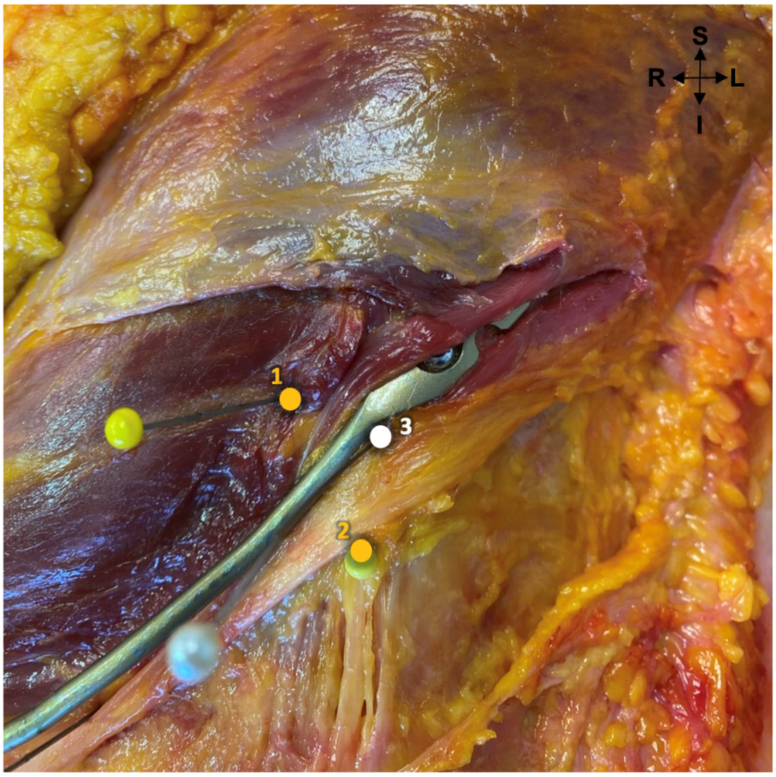

Figure 6.5: Fresh frozen cadaver indicating surgical dissection through the musculature over the iliac crest on the left
(1) IHN; (2) LFCN; (3) ASIS.
Key: I- Inferior, L- Left, R- Right, S- Superior, IHN- Iliohypogastric nerve, LFCN- Lateral Femoral Cutaneous Nerve, ASIS- Anterior Superior Iliac Spine.

To the authors knowledge, no previous publications have assessed the proximity of the SEV to the pubic tubercle as presented in the current study. A possible reason for this is that it is widely stated that the superficial epigastric artery can be easily located via transillumination for laparoscopic surgeries where it is most at risk (Rahn *et al*., 2010). Previous studies have defined the location of the superficial epigastric artery to the midline at the level of the symphysis pubis bilaterally; generally, between 40 mm – 80 mm from the midline where it is usually furthest from the midline at the pubis (Saber *et al*., 2004).

The SCIV is comprised of an artery which usually runs with its venae comitans. The artery gives off multiple branches, which includes bone branch to the a iliac crest and transverse branch. The bone branch to the iliac crest is usually very small and hard to find. In the current study, the transverse branch was measured to be 20.91 ± 7.88 mm (range: 2.45 – 43.08 mm) on average from the ASIS. Similarly, in a publication, this distance was found to be 25.5 ± 13.0 mm (range: 5 – 50 mm) (Yoshimatsu *et al*., 2019). Furthermore, Yoshimatsu *et al*., (2019) also measured the distance between the PT – ASIS, which was on average 122.0 ± 7.7 mm which is lower than that of the current study of 135.35 ± 12.69 mm. This divergence may be explained by the smaller sample size used by the other study or possibly the higher average age of their sample.

The closest structure to the ASIS on average was the SCIV both the left and right of the formalin fixed cadavers; with a minimum distance of 2.45 mm. However, if these vessels are encountered during the surgical procedure, the vessels are small enough to easily cauterize with no substantial risks.

Various surgical risks as a result of minimally invasive surgery have been reported, which include femoral nerve injury and compression concerns of the spermatic cord and femoral canal (Vaidya *et al*., 2012; Hesse *et al*., 2015; Dahill *et al*., 2017; Reichel *et al*., 2018). In the current study, the FN was a substantial distance from the implant with an average distance of 79.45 mm from the most proximal cortical screw (40 mm) as well as a minimum distance of 45.98 mm (left) and 40.02 mm (right) from the rod-to-rod connector. With observation, the spermatic cord (mean: 23.62 mm; range: 10.23 mm – 47.19 mm) was not seen compressed by the rod-to-rod connectors nor the connecting rod. However, quantitative measurements would need to be conducted to confirm the lack of compression. These results coincide with those of the anterior pelvic internal fixation reported by Moazzam *et al*., (2012) where the spermatic cord was easily visualized, thus avoided, with a range of 0 mm – 20 mm from the plate.

Osterhoff *et al*., (2017), concluded that the femoral neurovascular structures were always safe from both compression and impingement when the INFIX was applied. Similarly with the Bridging Infix, the femoral neurovascular structures were always a safe distance away from injury with the FV being closest to the implant rod-to-rod connector (left: 27.57 mm; right: 22.06 mm) and the FN (35.74 mm) to the proximal cortical screw. The femoral neurovascular structures are found deep to the inguinal ligament, thus if the Bridging Infix closely follows the ligament and adds no pressure to it, compression should be avoided. Therefore, it can be noted that it is unlikely to injure the femoral neurovasculature during the Bridging Infix procedure.

Previous studies measuring the distance between the spermatic cord's emergence from the inguinal ligament to the pubic tubercle are scarce. Published studies mainly measure the distance between the pubic tubercle to medial aspect of the spermatic cord (Collinge & Beltran, 2015; Hörlesberger *et al*., 2021). As different points of the spermatic cord were measured from the pubic tubercle, measurements were not comparable to the present results. However, a reference distance was reported, where the spermatic cord is within less than one finger breadth from the pubic tubercle (Hörlesberger *et al*., 2021). This is substantiated by the current study in that the minimum distance found between the spermatic cord to the pubic tubercle was 0.00 mm in three cases. The spermatic cord was always inferolateral to the implant rod-to-rod connecting rod with a minimum distance of 10.23 mm on the left and 15.29 mm on the right. This further shows that the spermatic cord is at minimal risk with the patient in a supine position.

6.6 CONCLUSION

The anatomical investigation lends support to the use of the new modified minimally invasive technique, the Bridging Infix, for anterior pelvic fixation. Particularly given that neurovascular structures were injured during the procedure conducted on the specimens. The importance of strictly following the technique guide should be emphasized to ensure that the surgeons employ layer by layer dissection as well as retract the abdominal musculature fully to avoid potentially injuring the IHN and IIN. None of the investigated anatomical structures, such as the spermatic cord and femoral neurovasculature were observed to be compressed but further quantitative analysis should be conducted.

6.7 LIMITATIONS

Several limitations present in the current study must be acknowledged. Foremost, the majority of cadavers used in the study were embalmed, therefore rigid and the blood vessels collapsed which could have reduced the actual distances. This does not reflect the tissue of the patients who would undergo the surgical procedure as measured distances may vary. This is due to only stable undisrupted pelvi being dissected with no oedema and injury, which may affect the safety margins and should be considered. The results from a small sample of dissections does not reflect the range of anatomical variations that can be encountered operatively. Further clinical studies should be conducted to test the true safety margins.

6.8 REFERENCES

Cole, P.A., Gauger, E.M., Anavian, J., Ly, T.V., Morgan, R.A. & Heddings, A.A. 2012. Anterior pelvic external fixator versus subcutaneous internal fixator in the treatment of anterior ring pelvic fractures. *J Orthop Trauma*, 26(5): 269-277.

Cole, P.A., Hesse, D.K., Dugarte, A.J. & Dyskin, E. 2017. The Pelvic Bridge: A subcutaneous approach for anterior pelvic fixation. *JBJS Essent Surg Tech*, 9(3): 1-9.

Collinge, C.A. & Beltran, M.J. 2015. Anatomic relationship between the spermatic cord and pubic tubercle: are our clamps injuring the cord during symphyseal repair? *J Orthop Trauma*, 29: 290-294.

Dahill, M,., McAuthur, J., Roberts, G.L., Acharya, M.R., Ward, A.J. & Chesser, T.J.S. 2017. The use of an anterior pelvic internal fixator to treat disruptions of the anterior pelvic ring: a report of technique, indications and complications. *Bone Joint J*, 99-B(9): 1232-1236.

Hesse, D., Kandmir, U., Solberg, B., Stroh, A., Osgood, G., Sems, S.A. & Collinge, C.A. 2015. Femoral nerve palsy after pelvic fracture treated with infix: a case series. *J Orthop Trauma*, 29(3): 138-143.

Hiesterman, T., Hill, B. & Cole, P. 2012. Surgical technique: A percutaneous method of subcutaneous fixation for the anterior pelvic ring: The Pelvic Bridge. *Clin Orthop Relat Res*, 470(8): 2116-2123.

Hörlesberger, N., Hohenberger, G., Grechenig, P., Schwarz, A., Grechenig, C., Ornig, M., Tackner, E. & Gänsslen, A. 2021. Danger zone – the spermatic cord during anterior plating of the symphysis pubis. Injury, 6(15): e1-4. doi: doi.org/10.1016/j/injury.2021.09.045.

Moazzam, C., Heddings, A.A., Moodie, P. & Cole, P.A. 2012. Anterior Pelvic Subcutaneous Internal Fixator Application: An Anatomic Study. *J Orthop Trauma*, 26(5): 263-268.

Nahabedian, M.Y. & Dellon, A.L. 1997. Outcome of the operative management of nerve injuries in the ilioinguinal region. *J Am Coll Surg*, 184: 265-268.

Osterhoff, G., Aichner, E.V., Scherer, J., Simmen, H., Werner, C.M.I. & Feigl, G.C. 2017. Anterior subcutaneous internal fixation of the pelvis – what rod-to-bone distance is anatomically optimal. *Injury*, 48: 2162-2168.

Rahn, D.D., Phelan, J.N., Roshanravan, S.M., White, A.B. & Corton, M.M. 2010. Anterior abdominal wall nerve and vessel anatomy: clinical implications for gynecologic surgery. *Am J Obstet Gynecol*, 202: 234e1-5.

Reichel, L.M., MacCormick, L.M., Dugarte, A.J., Rizkala, A.R., Graves, S.C. & Cole, P.A. 2018. Minimally invasive anterior pelvic internal fixation: An anatomic study comparing Pelvic Bridge to INFIX. *Injury*, 49: 309-314.

Rommens, P.M., Wagner, D. & Hofmann, A. 2017. Minimal invasive surgical treatment of fragility fractures of the pelvis. *Chirurgia*, 112: 524-537.

Saber, A.A., Meslemani, A.M., Davis., R. & Pimentel, R.P. 2004. Safety zones for anterior abdominal wall entry during laparoscopy. *Ann Surg*, 239(2): 181-185.

Scheyerer, M.J., Zimmermann, S.M., Osterhoff, G., Tiziani, S., Simmen, H., Wanner, G.A. & Werner, C.M.L. 2014. Anterior subcutaneous internal fixation for treatment of unstable pelvic fractures. *BMC Res Notes*, 7(133): 1-10.

Steer, R., Balendra, G., Matthews, J., Wullschleger, M. & Reidy, J. 2019. The use of anterior subcutaneous internal fixation (INFIX) for treatment of pelvic ring injuries in major trauma patients, complications and outcomes. *SICOT J*, 5: 22.

Strydom, S. & Snyckers, C.H. 2021. Minimally invasive subcutaneous anterior fixation of pelvic fractures in the elderly: Case report and literature review. *S Afr Orthop J*, 20(4): 240-245.

Strydom, S. & Snyckers, C.H. 2022. The Bridging Infix: A modified, minimally invasive subcutaneous anterior fixation technique. [Awaiting submission to Journal].

Vaidya, R., Colen, R., Vigdorchik, J., Tonnos, F. & Sethi, A. 2012. Treatment of unstable pelvic ring injuries with an internal anterior fixator and posterior fixation: initial clinical series. *J Orthop Trauma*, 26(1): 1-8.

Vaidya, R., Woodbury, D. & Nasr, K. 2018. Anterior subcutaneous internal pelvic fixation/INFIX: A systemic review. *J Orthop Trauma*, 32(S6): S24-30.

Whiteside, J.L., Barber, M.D., Walters, M.D. & Falcone, T. 2003. Anatomy of ilioinguinal and iliohypogastric nerves in relation to trocar placement and low transverse incisions. *Am J Obstet Gynecol*, 189: 1574-1578.

Yoshimatsu, H., Yamamoto, T., Hayashi, A., Fuse, Y., Karakawa, R., Iida, T., Narushima, M., Tanakura, K., Weninger, W.J. & Tzou, C.H.J. 2019. Use of the transverse branch of the superficial circumflex iliac artery as a landmark facilitating identification and dissection of the deep branch of the superficial circumflex iliac artery for free flap pedicle: Anatomical study and clinical applications. *Microsurgery*, 39: 721-729.

CHAPTER 7: MANUSCRIPT 3

TITLE: The unusual appearance of the superficial external pudendal vein at the saphenofemoral junction in a cadaver: A case report

7.1 ABSTRACT

It is known that anatomical variations are more prevalent in veins than in arteries. Furthermore, the great saphenous vein is known to have numerous variations relating to its tributaries. Common tributaries of the great saphenous vein include the superficial epigastric vein, superficial external pudendal vein (SEPV), and the superficial circumflex iliac vein. During routine dissection of the lower abdominal region, an unusual appearance of the SEPV relating to its course, shape, and size was noted in both lower extremities of a sixty-two-year-old, white male cadaver. The SEPV was seen coursing in a tortuous manner over the anterior abdominal wall and proximal thigh. The SEPV drained into the great saphenous vein on the right and directly into the saphenofemoral junction on the left. No tributaries of the SEPV were noted in the thigh or in the lower abdominal wall. The saphenofemoral junction constituents varied on both sides. It is important to note anatomical variations, especially in the position where this one was found, as it can lead to excessive bleeding during surgical approaches of the anterior abdominal wall. This type of variation would affect gynaecologic and obstetric, general surgical and internal pelvic and especially laparoscopic procedures.

KEYWORDS: Superficial external pudendal vein, femoral vein, variation, lower limb, great saphenous vein, saphenofemoral junction

7.2 INTRODUCTION

The SEPV is a vein that together with the deep external pudendal vein drains into the great saphenous vein (Drake *et al*., 2020). The external pudendal veins drain the anterior parts of the labia majora in females and scrotum in males as well as some overlap with the area of the internal pudendal veins (Drake *et al*., 2020). The superficial dorsal vein of the penis drains directly into the SEPV (Moore *et al*., 2015; Detton & Tank, 2017; Brennan *et al*., 2020). It has been reported in literature, that the external pudendal veins can be a single vein or multiple veins (Castro *et al*., 1998).

The great saphenous vein is known as the largest superficial vein of the lower limb (Eldho & Ushadevi, 2019). It runs superiorly on the medial border of the tibia to the posteromedial aspect of the knee where it ascends anteriorly over the thigh to ultimately drain into the femoral vein (FV) through the saphenous opening (Eldho & Ushadevi, 2019). Typical tributaries of the greater saphenous vein include the SEPV, superficial epigastric vein and superficial circumflex iliac vein (Detton & Tank, 2017; Baggish & Karram, 2021). However, it has also been reported that these tributaries may drain into the femoral vein instead (Chun *et al*., 1992).

The saphenofemoral junction is where the femoral vein and great saphenous vein join (Drake *et al*., 2020). The saphenofemoral junction is a structure which encompasses the great saphenous vein arch, tributaries and terminal and pre-terminal valves (Eldho & Ushadevi, 2019). Several venous variations of the great saphenous vein and tributaries as well as saphenofemoral junction are known to exist (Elzawawy & Khanfour, 2018). Furthermore, Donnelly *et al*. (2005) found that these veins have no definite pattern as they are so variable. Among the variations of the lower limb, the variations at the saphenofemoral junction are considered the most important. A thorough knowledge of the anatomical variations at this junction is crucial for surgical procedures such as varicose vein ligation (Eldho & Ushadevi, 2019). Within the femoral triangle, the great saphenous vein tributaries at the saphenofemoral junction have normal variations (Kim *et al*., 2017). One consistency however, is that the great saphenous vein usually drains into the common femoral vein in the femoral triangle (Kim *et al*., 2017).

7.3 CASE REPORT

The SEPV in the present report was deemed unusual due to the course, shape, and size of the vessels (Figure 7.1 – number 2). The unusual SEPV was found in a sixty-two-year-old male cadaver during anatomical research dissection in the Department of Anatomy, University of Pretoria. All subcutaneous tissue and fascia were removed to fully expose the course of the SEPV. No weight or height information was available. The specimen had no recorded medical history that would explain the size and variation of the vessels seen.

The SEPV was observed medial to the common femoral vein and lateral to the spermatic cord bilaterally. On both sides, the SEPV anastomosed on the midline, 41.90 mm superior to the pubic symphysis. The SEPV coursed in a inferolateral direction from their midline anastomosis, over the emergence of the spermatic cord from the inguinal canal. The SEPV can been seen to be rather tortuous along its course on the anterior abdominal wall and proximal thigh.

Figure 7.1: Dissected anterior abdominal wall and proximal thigh indicating the SEPV anastomosis and origin
(1) Common femoral vein; (2) SEPV; (3) Great saphenous vein.
Key: I- Inferior, L- Left, R- Right, S- Superior, SEPV- Superficial External Pudendal Vein, SC-Spermatic Cord, PS- Pubic Symphysis, SFJ- Saphenofemoral Junction.

The SEPV was seen as a tributary of the great saphenous vein on the right, 15.22 mm from the saphenofemoral junction (Figure 7.2A). On the right, the saphenofemoral junction was comprised of the common femoral vein (Figure 7.2A – number 1), great saphenous vein (Figure 7.2A – number 3), anterolateral vein (Figure 7.2A – number 2) and a common trunk for the superficial circumflex iliac vein (Figure 7.2A – number 6) and superficial epigastric vein (Figure 7.2A – number 7).

However, on the left side, the SEPV drained directly into the saphenofemoral junction which connects with the common femoral vein (Figure 7.2B – number 1), great saphenous vein (Figure 7.2B – number 3), anterolateral vein (Figure 7.2B – number 2), superficial circumflex iliac vein (Figure 7.2B – number 6) and superficial epigastric vein (Figure 7.2B – number 7).

Figure 7.2: Dissected formalin fixed cadaver indicating the venous formations in the anterior abdominal wall and proximal thigh
A: Right side showing the SEPV drain into the great saphenous vein; B: Left side showing the SEPV drain into the saphenofemoral junction.
(1) Common femoral vein; (2) Anterolateral vein; (3) Great saphenous vein; (4) Great saphenous vein; (5) Posteromedial vein; (6) superficial circumflex iliac vein; (7) Superficial epigastric vein; (8) SEPV.
Key: I- Inferior, L- Left, R- Right, S- Superior, FV- Common Femoral Vein, SEPV- Superficial External Pudendal Vein.

The SEPV measured 5.08 mm at its junction with the great saphenous vein on the right and 6.33 mm at its junction with the saphenofemoral junction on the left. Overall, the greatest diameter of the SEPV was 7.75 mm and the smallest diameter was 3.91 mm.

Moreover, the SEPV was 2.97 mm from the spermatic cord on the right and coursed directly over the spermatic cord on the left.

7.4 DISCUSSION

It is common knowledge that anatomical variations are more commonly found in veins than arteries (Udhaya *et al*., 2011; Eldho & Ushadevi, 2019). Variations of the great saphenous vein (Elzawawy & Khanfour, 2018) are also found more frequently in the superior segment of the great saphenous vein, in its tributaries, at the saphenofemoral junction where it enters the femoral vein (Udhaya *et al*., 2011; Eldho Ushadevi, 2019).

Chun *et al*., (1992) concluded that the tributaries of the great saphenous vein are inconsistent. Udhaya *et al.* (2011) reported that in 21 of their specimens (30%), a normal pattern of the superficial circumflex iliac vein, superficial epigastric veins and SEPV were found directly draining into the saphenofemoral junction. Similarly, in the present study, this pattern was found on the left side. The SEPV draining into either the great saphenous vein or femoral vein have been reported in past studies. In the cadaver case, it was noted that the SEPV drained into the great saphenous vein on the right. In a study by Chun *et al*. (1992) if was reported that the SEPV drained into the great saphenous vein in 95.2% of cases and into the femoral vein directly or with other saphenous tributaries in 4.8%. Moreover, Mühlberger *et al*. (2009) found the SEPV joining the great saphenous vein in 90.3% of cases, 16.9 mm distal to the saphenofemoral junction. This was the case on the right side of the specimen with a distance of 14.82 mm.

Eldho & Ushadevi (2019) also published findings regarding the drainage pattern of the saphenofemoral junction tributaries. Interestingly, the drainage pattern seen in the case specimen of the superficial epigastric veins and superficial circumflex iliac veins forming a common trunk that drained directly into the saphenofemoral junction was found in 11.3% of their sample.

In another study, using twenty dissected cadavers, the diameter of the external pudendal veins ranged between 1.56 mm – 3.70 mm with a mean of 2.99 mm for a single vein (Castro *et al*., 1998). In contrast though, in the current study, the diameter of the SEPV ranged between 3.91 mm - 7.75 mm which overall is greater than their maximum diameter. This further emphasizes that the current vein is a notable variation.

The anomalous course of the SEPV in the current study seems to be a unique finding as no other similar variation has been published to the authors knowledge. A previous case report published in 1998 (Ozan & Önderoglu, 1998) reported another rare variation of the external pudendal vein where it coursed through the inguinal canal. Although this is not the same as the current variation; this further emphasizes the idea that the external pudendal vein has reported variations which should be considered prior to surgical procedures. The superficial epigastric veins and SEPV may be encountered when incising the skin during numerous surgical procedures such as hernia repair. However, Detton & Tank (2017) describes that both veins should either be ligated or cauterized in these circumstances.

Although the variation of the SEPV currently reported is unique and has not been previously published to the authors knowledge, this type of anomaly could be encountered during surgical procedures of the anterior abdominal wall or proximal thigh. Variations such as the one presented in the current study should be kept in mind by surgeons who routinely dissect this area during procedures to avoid possible complications.

7.5 REFERENCES

Baggish, M.S. & Karram, M.M. 2021. *Atlas of Pelvic Anatomy and Gynecologic Surgery*, Fifth ed, Elsevier: Philadelphia, PA.

Brennan, PA., Standring, S. & Wiseman, S.M. 2020. *Gray's Surgical Anatomy*, Elsevier: London.

Castro, M., Brenda, E., Marques, A. & Pereira, M.D. 1998. Anatomic study of the external pudendal vessels to the anterior scrotal region. *Eur J Plast Surg*, 21: 86-90.

Chun, M., Han, S., Chung, J., Cho, S.S., Ko, J., Chung, I.H., Ching, G., Lee, M.S., Kang, H.S., Park, S.S. 1992. Anatomical observation on draining patterns of saphenous tributaries in Korean adults. *J Korean Med Sci*, 7(1): 25-33.

Detton, A.J. & Tank, P.W. 2017. *Grant's dissector*. Sixteenth ed, Wolters Kluwer: Philadelphia, PA.

Donnelly, M., Tierney, S. & Feeley, T.M. 2005. Anatomical variation at the saphenofemoral junction. *Br J Surg*, 92: 322-325.

Drake, R.L., Vogl, W., Michell, A.W.M. & Gray, H. 2020. *Gray's Anatomy for Student,* Fourth ed, Elsevier: Philadelphia, PA.

Eldho, J.T. & Ushadevi, K.B. 2019. Study of great saphenous vein and its tributaries at the saphenofemoral junction and its variations. *J Evolution Med Dent Sci*, 8(47): 3521-3525.

Elzawawy, E.M. & Khanfour, A.A. 2018. Saphenofemoral complex: anatomical variations and clinical significance. *Int J Clin Dev Anat*, 4(1): 32-39.

Kim, D.S., Kim, S.W., Lee, H.S., Byun, K.H. & Choe, M.S. 2017. Rare vascular anomalies in the femoral triangle during varicose vein surgery. *Korean J Thorac Cardiovasc Surg*, 50: 99-104.

Moore, K.L., Agur, A.M.R. & Dalley, A.F. 2015. *Essential Clinical Anatomy*, Fifth ed, international ed, Walters Kluwer Health: Philadelphia, PA.

Mühlberger, D., Morandini, L. & Brenner, E. 2009. Venous valves and major superficial tributary veins near the saphenofemoral junction. *J Vasc Surg*, 49(6): 1562-1569.

Ozan, H. & Önderoglu, S. 1998. An unusual content of the inguinal canal: the external pudendal vein. *Hernia*, 2: 41-43.

Udhaya, K., Rajendran, M., Sridhar, J. 2011. Variations in the tributaries of great saphenous vein at the saphenofemoral junction and its clinical implication. *Natl J Basic Med Sci*, 1(4): 190-193.

CHAPTER 8: SYNOPSIS AND CONCLUSION

The Bridging Infix was proposed as a novel minimally invasive technique for anterior pelvic fixation. The novel method was proposed with the objective of reducing known complications of the established INFIX or Pelvic Bridge techniques. The complications encompass lateral femoral cutaneous nerve (LFCN) impingement, femoral nerve palsy, spermatic cord compression, heterotopic ossification, and patient discomfort leading to explant and neuropraxia. With regard to the placement of the Bridging Infix, it was hypothesized that structures in the vicinity of the ASIS would be at risk and therefore were considered in the current study. Additional and more pertinent distances to the implant were also needed in order to establish the safety of the Bridging Infix in this reference sample.

Currently the LFCN is the most prevalent structure of concern mentioned in publications relating to anterior pelvic fixation. A common pathology related to the LFCN is meralgia paresthetica, which can be avoided with knowledge of the anatomy and known variations in this region. When comparing the Bridging Infix to the established techniques, it was found that the LFCN can be considered to be a safe distance from the cortical screws when they are directly inserted into the iliac crest. No variations were found in this sample where the LFCN course over the anterior superior iliac spine (ASIS). If the layer-by-layer dissection procedure, as described in the technique guide is adhered to, the surgeon should visualize the LFCN if it happens to cross over the ASIS.

The LFCN was found to be a minimum distance of 18.40 mm medial to the most proximal cortical screw. Finger breadth measurements are an easy mechanism for surgeons to use operatively to estimate the location of the LFCN or other pertinent or relevant structures. It has been previously suggested that the LFCN courses two finger breadths medial to the ASIS, however the results of the current study suggest that a three finger breadth, or 40 mm estimation, may be a better approximation to avoid any injury to this structure. Furthermore, it was determined that the LFCN lies roughly one fifth of the distance between the ASIS-pubic tubercle along the inguinal ligament.

In the current study, no other surrounding anatomical structure, namely the iliohypogastric nerve (IHN), ilioinguinal nerve (IIN), superficial epigastric vessels, superficial circumflex iliac vessels, femoral vein (FV), femoral artery (FA), femoral nerve (FN) or spermatic cord were found to be injured as a result of the implant procedure.

The IHN and IIN are protected by the external oblique and rectus abdominis muscles anteriorly. The IHN was an average distance of 44.29 mm and 38.14 mm from the most proximal cortical screw on the left and right, respectively. However, it was observed that the nerves lie in close proximity to the lateral window surgical dissection site and are at risk if the musculature is not fully retracted. Therefore, care should be taken when retracting and dissecting the lateral windows to ensure that the musculature is not injured when creating a bare area on the iliac crest for fixation. The IHN and IIN lie in close vicinity, medial to the ASIS; thus, they are at risk of injury if the full technique is not carefully followed.

The superficial epigastric and superficial circumflex iliac vessels have variable courses and were found to course within the dissection field of the medial and lateral windows, respectively. The superficial circumflex iliac vessels were found to be the closest structure to the ASIS with a distance of 2.45 mm. However, the vessels were mostly small, and could be cauterized if inadvertently encountered during surgery.

Literature has described various surgical risks associated with subcutaneous anterior fixation; which include compression concerns and injury to both the LFCN and FN. The femoral neurovasculature lie deep to the subcutaneous tunnel and inguinal ligament and are therefore at minimal risk of injury. The closest distance of the FN to the ASIS was 35.74 mm on the right of one specimen. Furthermore, the FN was a substantial average distance of 79.45 mm from the most proximal cortical screw for definitive fixation and 23.62 mm from the implant single rod-to-rod connector screw. Observations regarding no compression of the spermatic cord were recorded as the spermatic cord can easily be visualized.

Referring to the most prominent point of the palpable bony landmarks for the distances measured in the study, allows the surgeon to better estimate the safe zones during implantation. These distances aren't only relevant to the Bridging Infix procedure, but also any surgery within the field.

Anatomical venous variations are known to have a high prevalence and thus are widely reported. During dissection, a unique variation, relating to the course, size, and shape of the superficial external pudendal vein (SEPV) was noted. The SEPV anastomosed on the midline of the anterior abdominal wall and coursed in a tortuous manner across the anterior abdominal wall to the proximal thigh. The diameter of the vessel ranged between 3.01 mm – 7.75 mm which is much larger than reported in literature. Although the variation of the SEPV is an anomaly, surgeons should still be mindful of this during surgical procedures involving the anterior abdominal wall to circumvent bleeding complications.

In conclusion, the Bridging Infix procedure can be considered safe if layer by layer dissection is employed, the screws are directly inserted on the iliac crest, and the musculature is properly retracted during the lateral window dissection, with no pressure being applied within three finger breadths medial to the ASIS. These results are of interest to orthopaedic surgeons operating to reduce pelvic fractures using a minimally invasive technique. These results could assist in reducing post-operative complications following anterior pelvic fixation.

CHAPTER 9: LIMITATIONS AND FUTURE DIRECTION

9.1 LIMITATIONS

During the course of the study, numerous limitations were encountered as specified below:

- A modified technique had to be used to accommodate the hardened nature of formalin fixed cadaveric tissue in order to ease the procedure of placing the implant subcutaneously. The modified technique used was on only the formalin fixed cadavers where anatomical dissection preceded the implantation of the Bridging Infix.
- No imaging guidance was available thus the surgical technique had to be altered to only make use of palpable bony anatomic landmarks and naked eye visualisation. To completely simulate the *in-vivo* use of the implant, x-rays are needed to bend the constructs pre-operatively. In the current study, a set of dry articulated pelvic bones were used to bend the constructs externally as imaging was not available.
- The majority of the sample was comprised of formalin fixed specimens. The embalming process results in the cadaver being rigid and blood vessels collapsing which could have affected some of the distances measured. Due to the rigidity of formalin fixed cadavers, attempting to simulate the correct clinical position of a patient was not always possible and at times proved difficult to reproduce. As far as possible, all cadavers were placed in the same supine position before any measurements were taken.
- The study documented some incomplete data sets for cadavers because of either the cadaver demographics being unavailable or structures missing or being damaged. The incomplete data can be attributed to human error, possible prior surgical procedures that weren't detected (which would have resulted in the exclusion of the specimens) or circumstances beyond the investigators control. Due to limited cadaver availability, those cadavers were still included in the study.
- Only fifty (n = 50) cadaveric specimens were utilized due to availability within the department of anatomy as a consequence of the COVID-19 pandemic, which limited cadaver intake and reduced available donors. Of the fifty cadavers, only four (n = 4) were of black ancestry. Thus, statistical tests investigating the effect of ancestry could not be conducted. Furthermore, due to the small sample size, few anatomical variations which could be present clinically were seen, which could affect the safety zones.
- Additionally, only two sets of constructs (4 mm plate-rod construct with a straight rod and two rod-to-rod clamps) could be sponsored by DePuy Synthes. The sets are originally described for use in occipito-cervical fusion. As one needs to take the structural integrity of the implants into consideration, they usually cannot be used for

more procedures. However, in the current study the same set was reused on all the specimens by bending the construct to the cadaver specifications.

- Due to financial limitations, only two (n = 2) fresh frozen cadaver specimens could be utilized for the clinical simulation. Furthermore, hip flexion could only be done in these specimens. As a result of the small sample, no statistical analysis could be conducted.
- The rod-to-rod connectors could be placed with either with the single screw or double screw side facing superiorly (n = 7) if the rods could not be contoured enough to sit well, approximately ± 10 mm above the pubic symphysis. This could have affected the implant single rod-to-rod connecting screw mean and measured distances.
- The removal of the skin and subcutaneous tissue to locate, identify and measure structures, could have resulted in the movement of some structures, especially during hip flexion.

9.2 FUTURE DIRECTION

In future studies, the following can be taken into consideration:

- Future studies will explore the possible movement between pelvic anatomical structures while the patient's hip is either straight, flexed or extended which could affect the patients comfort with the subcutaneous implant post-operatively. In the current study, no influence was found; however, another study with a larger sample size would be more reliable. To the author's current knowledge, no studies like this have been performed.
- Future studies will investigate the height of the implant from the anatomical structures by measuring the distance from the implant to the various anatomical structures. The measurements will assist in determining the risk of compression on structures such as the lateral femoral cutaneous nerve (LFCN), iliohypogastric nerve (IHN), ilioinguinal nerve (IIN), and spermatic cord.
- A direct comparison anatomical study between the INFIX, Pelvic Bridge and Bridging Infix could be performed to directly determine which implant is considered safer from neighbouring structures.
- As suggested by Osterhoff *et al*. (2017), large sample morphometric measurements using either magnetic resonance imaging (MRI) or computed tomography (CT) scans, would allow the investigators to determine if flexion does affect the anatomic surrounding structures and if any structure is compressed post-operatively in large samples.

REFERENCES: CHAPTER 1,2,3,9

Al-dabbagh, A.K.R. 2002. Anatomical variations of the inguinal nerves and risks of injury in 110 hernia repairs. *Surg Radiol Anat*, 24: 102-107.

Anloague, P.A. & Huijbregts, P. 2009. Anatomical variations of the lumbar plexus: a descriptive anatomy study with proposed clinical implications. *J Manual Manip Ther*, 17(4): e107-e114.

Apaydin, N. 2015. Variations of the lumbar and sacral plexuses and their branches. In: Tubbs, R.S., Rizk, E., Shoja, M.M., Loukas, M., Barbaro, N., Spinner, R.J., eds. Nerves and Nerve Injuries. Vol 1. San Diego: Elsevier: 614-617.

Arvieux, C., Thony, F., Broux, C. Ageron, F.-X., Rancurel, E., Abba, J., Faucheron, J.-L., Rambeaud, J.-J. & Tonetti, J. 2012. Current management of severe pelvic and perineal trauma. *J Visc Surg*, 149, e227-e238.

Ashkal, A., Kong, V.Y., Blodgett, J.M., Smith, M.T.D., Bekker, W., Bruce, J.L., Laing, G.L. & Clarke, D.L. 2021. A Review of blunt pelvic injuries at a major trauma centre in South Africa. *S Afr J Surg*, 59(1): 26a-26e.

Aszmann, O.C., Dellon, E.S. & Dellon, A.L. 1997. Anatomical course of the lateral femoral cutaneous nerve and its susceptibility to compression and injury. *Plast Reconstr Surg*, 100: 600-604.

Avsar, F.M., Sahin, M., Arikan, A.F., Demirci, S. & Elhan, A. 2002. The possibility of nervus ilioinguinalis and nervus iliohypogastricus injury in lower abdominal incisions and effects on hernia formation. *J Surg Res*, 107(2): 179-185.

Banierink, K., ten Duis, K., de Vries, R., Wendt, K., Heineman, E., Reininga, I. & Ijpma, F. 2019. Pelvic ring injury in the elderly: Fragile patients with substantial mortality rates and long-term physical impairment. *PLoS ONE*, 14(5): e0216809.

Coccolini, F., Stahel, P., Montori, G., Biffl, W., Horer, T., Catena, F., Kluger, Y., Moore, E., Peitzman, A., Ivatury, R., Coimbra, R., Fraga, G., Pereira, B., Rizoli, S., Kirkpatrick, A., Leppaniemi, A., Manfredi, R., Magnone, S., Chiara, O., Solaini, L., Ceresoli, M., Allievi, N., Arvieux, C., Velmahos, G., Balogh, Z., Naidoo, N., Weber, D., Abu-Zidan, F., Sartelli, M. and Ansaloni, L., 2017. Pelvic trauma: WSES classification and guidelines. *World J Emerg Surg*, 12(1): 1-18.

Cole, P.A., Gauger, E.M., Anavian, J., Ly, T.V., Morgan, R.A. & Heddings, A.A. 2012. Anterior pelvic external fixator versus subcutaneous internal fixator in the treatment of anterior ring pelvic fractures. *J Orthop Trauma*, 26(5): 269-277.

Cole, P.A., Hesse, D.K., Dugarte, A.J. & Dyskin, E. 2017. The Pelvic Bridge: A subcutaneous approach for anterior pelvic fixation. *JBJS Essent Surg Tech*, 9(3): 1-9.

Collinge, C.A. & Beltran, M.J. 2015. Anatomic relationship between the spermatic cord and pubic tubercle: are our clamps injuring the cord during symphyseal repair? *J Orthop Trauma*, 29: 290-294.

Costantini, T., Coimbra, R., Holcomb, J., Podbielski, J., Catalano, R., Blackburn, A., Scalea, T., Stein, D., Williams, L., Conflitti, J., Keeney, S., Suleiman, G., Zhou, T., Sperry, J., Skiada, D., Inaba, K., Williams, B., Minei, J., Privette, A., Mackersie, R., Robinson, B. & Moore, F. 2015. Current management of haemorrhage from severe pelvic fractures. J*ournal Trauma Acute Care Surg*, 80(5): 717-725. doi: 10.1097/TA.0000000000001034.

Court-Brown, C.M. & Caesar, B. 2006. Epidemiology of Adult Fractures: A Review. *Injury*, 37(8): 691–697. doi: 10.1016/j.injury.2006.04.130.

Cox, S.L. 2021. A geometric morphometric assessment of shape variation in adult pelvic morphology. *Am J Phys Anthropol*, 176: 652-671.

Dahill, M,., McAuthur, J., Roberts, G.L., Acharya, M.R., Ward, A.J. & Chesser, T.J.S. 2017. The use of an anterior pelvic internal fixator to treat disruptions of the anterior pelvic ring: a report of technique, indications and complications. *Bone Joint J*, 99-B(9): 1232-1236.

de Ridder, V.A., de Lange, S. & Popta, J.V. 1999. Anatomical variations of the lateral femoral cutaneous nerve and the consequences for surgery. *J Orthop Trauma*, 13(3): 207-211.

de Rosnay, P., Chandiramani, M., Usman, S. & Owen, E. 2011. Injury of epigastric vessels in laparoscopy: diagnosis and management. *Gynecol Surg*, 8: 353-356.

Doklamyai, P., Agthong, S., Chentanez, V., Huanmanop, T., Amarase, C., Surunchupakorn, P. & Yotnuengnit, P. 2008. Anatomy of the lateral femoral cutaneous nerve related to inguinal ligament, adjacent bony landmarks and femoral artery. *Clin Anat*, 21: 769-774.

Drake, R.L., Vogl, A.W. & Mitchell, A.W.M. 2015. Gray's Anatomy for Students. 3rd ed. Philadelphia: Churchill Livingstone Elsevier, 398-401.

Dyer, G.S. & Vrahas, M.S. 2006. Review of the pathophysiology and acute management haemorrhage in pelvic fracture. *Injury*, 37: 602-613.

Ellis H. 2010. The femoral triangle and superficial veins of the leg. *Anaesth Intensive Care Med*, 11(1):21-24. doi:10.1016/j.mpaic.2009.10.006

Grewal., I.S. & Starr, A.J. 2020. What's new in percutaneous pelvis fracture surgery?. *Orthop Clin North Am*, 51(3): 317-324.

Gustafson, K.J., Pinault, G.C. Neville, J.J. 2009. Fascicular anatomy of human femoral nerve: implications for neural prostheses using nerve cuff electrodes. *J Rehabil Res Dev*, 46(7): 973-984.

Hesse, D., Kandmir, U., Solberg, B., Stroh, A., Osgood, G., Sems, S.A. & Collinge, C.A. 2015. Femoral nerve palsy after pelvic fracture treated with infix: a case series. *J Orthop Trauma*, 29(3): 138-143.

Hiesterman, T., Hill, B. & Cole, P. 2012. Surgical technique: A percutaneous method of subcutaneous fixation for the anterior pelvic ring: The Pelvic Bridge. *Clin Orthop Relat Res*, 470(8): 2116-2123.

Hung, C., Wu, J., Li, Y., Cheng, Y., Wu, C., Shen, H. & Yeh, T. 2018. Minimally Invasive Treatment for Anterior Pelvic Ring Injuries with Modified Pedicle Screw-Rod Fixation: A Retrospective Study. *J Orthop Surg Res*, 13(1):1–8. doi: 10.1186/s13018-018-0945-4.

Karakas, H.M., Harma, A. & Alicioglu, B. 2013. The subpubic angle in sex determination: Anthropometric measurements and analyses on Anatolian Caucasians using multidetector computed tomography datasets. *J Forensic Leg Med*, 20: 1004-1009.

Klaassen, Z., Marshall, E., Tubbs, R.S., Louis Jr, R.G. & Wartmann, C.T., Loukas, M. 2011. Anatomy of the ilioinguinal and iliohypogastric nerves with observations of their spinal nerve contributions. *Clin Anat*, 24(4): 454-461.

Küper, M.A., Trulson, A., Stuby, F.M. & Stöckle, U. 2019. Pelvic ring fractures in the elderly. EFORT Open Rev, 4: 313-320. doi: 10.1302/2058-5241.4.180062.

Maier, G.S., Kolbow, K., Lazovic, D., Horas, K., Roth, K.E., Seeger, J.B. & Maus, U. 2016. Risk factors for pelvic insufficiency fractures and outcome after conservative therapy. *Arch Gerontol Geriat*, 67: 80-85.

Martin, J.G., Kassin, M., Park, P., Ermentrout, M. & Dariushnia, S. 2017. Evaluation and treatment of blunt pelvic trauma. *Tech Vasc Interventional Rad*, 20: 237-242.

Mason, W.T.M., Khan, S.N., James, C.L., Chesser, T.J.S. & Ward, A.J. 2005. Complications of temporary and definitive external fixation of pelvic ring injuries. *Injury*, 36: 599-604.

Mischkowski, R.A., Selbach, I., Neugebauer, J., Koebke, J. & Zöller, J.E. 2006. Lateral femoral cutaneous nerve and iliac crest bone grafts- anatomical and clinical considerations. *Int J Oral Maxillofac Surg*, 35: 366-372.

Moazzam, C., Heddings, A.A., Moodie, P. & Cole, P.A. 2012. Anterior Pelvic Subcutaneous Internal Fixator Application: An Anatomic Study. *J Orthop Trauma*, 26(5): 263-268.

Moore, K.L., Dalley, A.F. & Aguir, A.M.R. 2014. Moore Clinically Orientated Anatomy. 7th ed. Philadelphia: Lippincott Williams & Wilkins, 186.

Mosheiff, R. & Leibergall, M. 2002. Maneuvering the retrograde medullary screw in pubic ramus fractures. *J Orthop Trauma*, 16(8): 594-596.

Ndiaye, A., Diop, M., Ndoye, J.M., Konaté, I., Ndiaye, A.Ï., Mané, L., Nazarian, S. & Dia, A. 2007. Anatomical basis of neuropathies and damage to the ilioinguinal nerve during repairs of the groin hernias (about 100 dissections). *Surg Radiol Anat*, 29: 675-681.

Niola, R., Pinto, A., Sparano, A., Ignarra, R., Romano, L. & Maglione, F. 2012. Arterial bleeding in pelvic trauma: priorities in angiographic embolization. *Curr Probl Diagn Radiol*, 41: 93-101.

Oberkircher, L., Ruchholtz, S., Rommens, P.M., Hofmann, A., Bücking, B. & Krüger, A. 2018. Osteoporotic Pelvic Fractures. *Dtsch Arztebl Int*, 115(5): 70-80.

Ogami, K., Murata, H., Sakai, A., Sato, S., Saiki, K., Okamoto, K., Manabe, Y., Hara, T. & Tsurumoto, T. 2017. Deep and superficial circumflex iliac arteries and their relationship to the ultrasound-guided femoral nerve block procedure: a cadaver study. *Clinl Anat*, 30: 413-420.

Ogeng'o, J., Misiani, M., Waisiko, B., Olabu, B.O. & Maranga, E. 2015. Variant branching of the common femoral artery in a black Kenyan population: trifurcation is common. *Anat J Afr*, 4(1): 528-533.

Osterhoff, G., Aichner, E.V., Scherer, J., Simmen, H., Werner, C.M.I. & Feigl, G.C. 2017. Anterior subcutaneous internal fixation of the pelvis – what rod-to-bone distance is anatomically optimal. *Injury*, 48: 2162-2168.

Patriquin, M.L., Loth, S.R. & Steyn, M. 2003. Sexually dimorphic pelvic morphology in South African whites and blacks. *Homo*, 53(3): 255-262.

Ray, B., D'Souza, A.S. Kumar, B., Marx, C., Ghosh, B., Gupta, N. & Marx, A. 2010. Variations in the course and microanatomical study of the lateral femoral cutaneous nerve and its clinical significance. *Clin Anat*, 23(8): 978-984.

Reichel, L.M., MacCormick, L.M., Dugarte, A.J., Rizkala, A.R., Graves, S.C. & Cole, P.A. 2018. Minimally invasive anterior pelvic internal fixation: An anatomic study comparing Pelvic Bridge to INFIX. *Injury*, 49: 309-314.

Reinpold, W., Schroeder, M., Berger, C., Rohr, M. & Wehrenberg, U. 2015. Retroperitoneal anatomy of the iliohypogastric, ilioinguinal, genitofemoral and lateral femoral cutaneous nerve: consequences for prevention and treatment of chronic inguinodynia. *Hernia*, 19(4): 539-548.

Rommens, P.M., Wagner, D. & Hofmann, A. 2017. Minimal Invasive Surgical Treatment of Fragility Fractures of the Pelvis. *Chirurgia*, 112(5): 524–537. doi: 10.21614/chirurgia.112.5.524.

Scheyerer, M.J., Zimmermann, S.M., Osterhoff, G., Tiziani, S., Simmen, H., Wanner, G.A. & Werner, C.M.L. 2014. Anterior Subcutaneous Internal Fixation for Treatment of Unstable Pelvic Fractures. BMC Res Notes, 7(1): 133–133. doi: 10.1186/1756-0500-7-133.

Starr, A., Nakatani, T., Reinert, C. & Cederberg, K. 2008. Superior pubic ramus fractures fixed with percutaneous screws: What predicts fixation failure?. *J Orthop Trauma*, 22(2): 81-87.

Steer, R., Balendra, G., Matthews, J., Wullschleger, M. & Reidy, J. 2019. The use of anterior subcutaneous internal fixation (INFIX) for treatment of pelvic ring injuries in major trauma patients, complications and outcomes. *SICOT J*, 5: 22.

Strydom, S. & Snyckers, C.H. 2021. Minimally invasive subcutaneous anterior fixation of pelvic fractures in the elderly: Case report and literature review. *S Afr Orthop J*, 20(4): 240-245.

Strydom, S. & Snyckers, C.H. 2022. The Bridging Infix: A modified, minimally invasive subcutaneous anterior fixation technique. [Awaiting acceptance by Journal].

Taghavi, K., Geneta, V.O. & Mirjalili, S.A. 2016. The pediatric inguinal canal: Systematic review of the embryology and surface anatomy. *Clin Anat*, 29: 204-210.

Tubbs, R.S., Loukas, M., & Hanna, A.S. 2018. Surgical Anatomy of the Lumbar Plexus. Thieme Medical Publishers, Incorporated, New York. Available from: ProQuest Ebook Central. [17 February 2021].

Vaidya, R., Colen, R., Vigdorchik, J., Tonnos, F. & Sethi, A. 2012a. Treatment of unstable pelvic ring injuries with an internal anterior fixator and posterior fixation: initial clinical series. *J Orthop Trauma*, 26(1): 1-8.

Vaidya, R., Kubiak, E., Bergin, P., Dombroski, D., Critchlow, R., Sethi, A. 2012b. Complications of anterior subcutaneous internal fixation for unstable pelvis fractures: A multicenter study. *Clin Orthop Relat Res*, 470(8): 2124-2131.

Vaidya, R., Woodbury, D. & Nasr, K. 2018. Anterior subcutaneous internal pelvic fixation/INFIX: A systemic review. *J Orthop Trauma*, 32(S6): S24-30.

Yin, Y., Luo, J., Zhang, R., Li, S., Jiao, Z., Zhang, Y. & Hou, Z. 2019. Anterior subcutaneous internal fixator (INFIX) versus plate fixation for pelvic anterior ring fracture. *Sci Rep*, 9(1): 2578-2578.

Yu, K., Hong, J., Sun, Y., Shi, C., Guo, X. & Zhou, D. 2015. Anatomical measurement and finite element study on screw channel parameter in percutaneous fixation of canulated screw for symphyseolysis. *Cell Biochem Biophys*, 71(2): 1243-1248. doi:10.1007/s12013-014-0335-4

ANNEXURES

ANNEXURE 1: ETHICAL CLEARANCE CERTIFICATE

UNIVERSITEIT VAN PRETORIA
UNIVERSITY OF PRETORIA
YUNIBESITHI YA PRETORIA

Faculty of Health Sciences

Institution: The Research Ethics Committee, Faculty Health Sciences, University of Pretoria complies with ICH-GCP guidelines and has US Federal wide Assurance.

- FWA 00002567, Approved dd 22 May 2002 and Expires 03/20/2022.
- IORG #: IORG0001762 OMB No. 0990-0279 Approved for use through February 28, 2022 and Expires: 03/04/2023.

15 April 2021

Approval Certificate
New Application

Ethics Reference No.: 182/2021
Title: Establishing the safe use of the bridging infix method for anterior pelvic fixation in a South African sample

Dear Miss J van Schalkwyk

The **New Application** as supported by documents received between 2021-03-29 and 2021-04-14 for your research, was approved by the Faculty of Health Sciences Research Ethics Committee on 2021-04-14 as resolved by its quorate meeting.

Please note the following about your ethics approval:

- Ethics Approval is valid for 1 year and needs to be renewed annually by 2022-04-15.
- Please remember to use your protocol number (182/2021) on any documents or correspondence with the Research Ethics Committee regarding your research.
- Please note that the Research Ethics Committee may ask further questions, seek additional information, require further modification, monitor the conduct of your research, or suspend or withdraw ethics approval.

Ethics approval is subject to the following:

- The ethics approval is conditional on the research being conducted as stipulated by the details of all documents submitted to the Committee. In the event that a further need arises to change who the investigators are, the methods or any other aspect, such changes must be submitted as an Amendment for approval by the Committee.

We wish you the best with your research.

Yours sincerely

Professor Werdie (CW) Van Staden
MBChB MMed(Psych) MD FCPsych(SA) FTCL UPLM
***Chairperson**: Faculty of Health Sciences Research Ethics Committee*

The Faculty of Health Sciences Research Ethics Committee complies with the SA National Act 61 of 2003 as it pertains to health research and the United States Code of Federal Regulations Title 45 and 46. This committee abides by the ethical norms and principles for research, established by the Declaration of Helsinki, the South African Medical Research Council Guidelines as well as the Guidelines for Ethical Research: Principles Structures and Processes, Second Edition 2015 (Department of Health)

Research Ethics Committee
Room 4-60, Level 4, Tswelopele Building
University of Pretoria, Private Bag x323
Gezina 0031, South Africa
Tel +27 (0)12 356 3084
Email: deepeka.behari@up.ac.za
www.up.ac.za

Fakulteit Gesondheidswetenskappe
Lefapha la Disaense tša Maphelo

ANNEXURE 2: DATA SHEET

Due to size, the raw data capturing sheet is available on request.